



The research described in this thesis was performed at the Laboratory of Physiopharmacology (Antwerp) and the laboratory of Experimental Cardiology (Leiden). This work was supported by a Geconcentreerde onderzoeksactie grant (GOA, PID36444) of the University of Antwerp; by a Senior Clinical Investigator fellowship (to VFS) and research grants of the Fund for Scientific Research Flanders (Application numbers 1842219N, G021019N, and G021420N); VLIR/iBOF Grant 20-VLIR-iBOF-027 (to HH, VFS, HLR, and GWDK). Salubris Biotherapeutics supplied the drug JK07, used within this research.



**Universiteit  
Antwerpen**

**Faculteit Farmaceutische, Biomedische en Diergeneeskundige  
wetenschappen**  
Departement Farmaceutische wetenschappen

**ACTIVATION OF ERBB4 ATTENUATES ATRIAL  
FIBRILLATION IN MICE**

**ACTIVATIE VAN ERBB4 VERMINDERT VOORKAMER-  
FIBRILLATIE IN MUIZEN**

Proefschrift voorgelegd tot het behalen van de graad van Doctor in de  
Farmaceutische wetenschappen aan de Universiteit Antwerpen te verdedigen  
door

**Jens VAN FRAEYENHOVE**

Promotoren: Prof. Dr. Gilles W De Keulenaer en Prof. Guido Y De Meyer

Antwerpen, 2024

**Cover and chapter front design:** Jens Van fraeyenhove (inspired by Alessandra Greco)

**Printed by:** Universitas

Disclaimer

©Jens Van fraeyenhove, 2024.

The author allows to consult and copy parts of this work for personal use. Further reproduction or transmission in any form or by any means, without the prior permission of the author is strictly forbidden.

## **MEMBERS OF THE JURY**

Prof. Pieter Van Der Veken, PharmD PhD (Chair of the jury)  
*Laboratory of Medicinal Chemistry – University of Antwerp, Belgium*

Prof. Karin Sipido, MD PhD (Member)  
*Laboratory of Experimental Cardiology – KU Leuven, Belgium*

Prof. Yves De Greef, MD PhD (Member)  
*Department of Cardiology – ZNA Middelheim, Belgium*

Prof. Ingrid De Meester, PharmD PhD (Chair of the individual doctoral committee)  
*Laboratory of Medical Biochemistry – University of Antwerp, Belgium*

Prof. Emeline Van Craenenbroeck, MD PhD (Member of the individual doctoral committee)  
*Research group Cardiovascular Diseases, GENCOR Department – University of Antwerp, Belgium*

Prof. Guido Y De Meyer, PharmD PhD (Promotor)  
*Laboratory of Physiopharmacology – University of Antwerp, Belgium*

Prof. Gilles W De Keulenaer, MD PhD (Promotor)  
*Laboratory of Physiopharmacology – University of Antwerp, Belgium*



## TABLE OF CONTENT

NON-STANDARD ABBREVIATIONS AND ACRONYMS	9
<b>CHAPTER 1 GENERAL INTRODUCTION</b>	<b>15</b>
<b>CHAPTER 2 HYPOTHESES AND AIMS OF THE STUDY</b>	<b>41</b>
<b>CHAPTER 3 MATERIALS AND METHODS</b>	<b>47</b>
<b>CHAPTER 4 EFFECTS OF JK07 <i>IN VITRO</i></b>	<b>67</b>
<b>CHAPTER 5 EFFECTS OF NRG1 AND JK07 ON ATRIAL FIBRILLATION IN TNF1.6 MICE</b>	<b>79</b>
<b>CHAPTER 6 JK07 MITIGATES AF INDUCIBILITY AND DURATION IN MICE</b>	<b>91</b>
<b>CHAPTER 7 JK07 MITIGATES REENTRY INDUCIBILITY IN CULTURED ATRIAL CARDIOMYOCYTES</b>	<b>111</b>
<b>CHAPTER 8 SUMMARY, GENERAL DISCUSSION AND FUTURE PERSPECTIVES</b>	<b>117</b>
<b>CHAPTER 9 NEDERLANDSTALIGE SAMENVATTING EN CONCLUSIES</b>	<b>139</b>
SCIENTIFIC CURRICULUM VITAE	149
ACKNOWLEDGEMENT – DANKWOORD	153





## NON-STANDARD ABBREVIATIONS AND ACRONYMS

<b>AAD</b>	Antiarrhythmic drug
<b>Actb</b>	Beta-actin
<b>AERP</b>	Atrial effective refractory period
<b>AF</b>	Atrial fibrillation
<b>Akt</b>	Protein kinase B
<b>ANEPS</b>	Amino Naphthyl Ethenyl Pyridinium
<b>Ang II</b>	Angiotensin-II
<b>ANOVA</b>	Analysis of the variance
<b>AP</b>	Action potential
<b>APD</b>	Action potential duration
<b>APD<sub>80</sub></b>	Action potential duration at 80% repolarization
<b>AUC</b>	Area under the curve
<b>BMI</b>	Body mass index
<b>BPM</b>	Beats per minute
<b>BSA</b>	Bovine serum albumin
<b>Ca<sup>2+</sup></b>	Calcium
<b>CL</b>	Cycle length
<b>Col1a1</b>	Collagen type 1
<b>Col3a1</b>	Collagen type 3
<b>CV</b>	Conduction velocity
<b>CX</b>	Connexin
<b>DAD</b>	Delayed afterdepolarization
<b>DMEM</b>	Dulbecco's modified eagle medium
<b>DNA</b>	Deoxyribonucleic acid
<b>DOAC</b>	Direct oral anticoagulants
<b>EAD</b>	Early afterdepolarization
<b>EAST</b>	Early treatment of atrial fibrillation for stroke prevention
<b>EAT</b>	Epicardial adipose tissue
<b>EC</b>	Endothelial cell
<b>ECD</b>	Extracellular domain
<b>ECG</b>	Electrocardiogram
<b>ECM</b>	Extracellular matrix
<b>EC50</b>	Half maximal concentration
<b>EF</b>	Ejection fraction
<b>EGF</b>	Epidermal growth factor
<b>EGFR</b>	Epidermal growth factor receptor
<b>EP</b>	Electrophysiology
<b>ERBB</b>	Erythroblastic leukemia viral oncogene homolog
<b>ERK1/2</b>	Extracellular signal-related kinases 1/2
<b>ESC</b>	European society of cardiology
<b>FBS</b>	Fetal bovine serum
<b>FC</b>	Fold change
<b>FVB</b>	Friend leukemia virus B strain

<b>Gapdh</b>	Glyceraldehyde-3-phosphate dehydrogenase
<b>HER</b>	Human epidermal growth factor receptor
<b>HF</b>	Heart failure
<b>HFD</b>	High fat diet
<b>hiAM</b>	Human conditional immortalized atrial myocyte
<b>iAM</b>	Conditional immortalized rat atrial myocyte
<b><math>I_{Ca}</math></b>	L-type calcium current
<b><math>I_{kur}</math></b>	Ultra-rapid delayed rectifier current
<b><math>I_{Na}</math></b>	Cardiac sodium current
<b>I.P.</b>	Intraperitoneal
<b><math>I_{to}</math></b>	Cardiac transient outward potassium current
<b>I.V.</b>	Intravenous
<b>ICD</b>	Intracellular domain
<b>INR</b>	International normalized ratio
<b>IVSd</b>	Interventricular septum thickness in diastole
<b><math>K^+</math></b>	Kalium
<b>KDa</b>	Kilodalton
<b>LA</b>	Left atrium
<b>LPS</b>	Lipopolysaccharide
<b>LV</b>	Left ventricle
<b>LVPWd</b>	Left ventricular posterior wall thickness in diastole
<b>mAb</b>	Monoclonal antibody
<b>MAPK</b>	Mitogen-activated protein kinase
<b>MHC</b>	Murine $\alpha$ -myosin heavy chain
<b>MMP</b>	Matrix metalloproteinase
<b>mTOR</b>	Mammalian target of rapamycin
<b>mV</b>	Millivolt
<b>Mye-KO</b>	Myeloid knock out
<b>NCX</b>	Sodium calcium exchanger channel
<b>NDCC</b>	Non-dihydropyridines calcium channel blockers
<b>Nm</b>	Nanometer
<b>NOAC</b>	Non-vitamin K antagonist oral anticoagulants
<b>NRG1</b>	Neuregulin-1
<b><math>O_2</math></b>	Oxygen
<b>Padj</b>	Adjusted p-value
<b>PES</b>	Programmed electrical stimulation
<b>PI3K/Akt</b>	Phosphatidylinositol-3 kinase / protein kinase B
<b>PTK</b>	Protein tyrosine kinase
<b>PV</b>	Pulmonary vein
<b>RA</b>	Right atrium
<b>RAAS</b>	Renin-angiotensin-aldosterone system
<b>RACE</b>	Race Control Efficacy in Permanent Atrial Fibrillation
<b>RLU</b>	Relative light units
<b>RNA</b>	Ribonucleic acid
<b>RP</b>	Refractory period

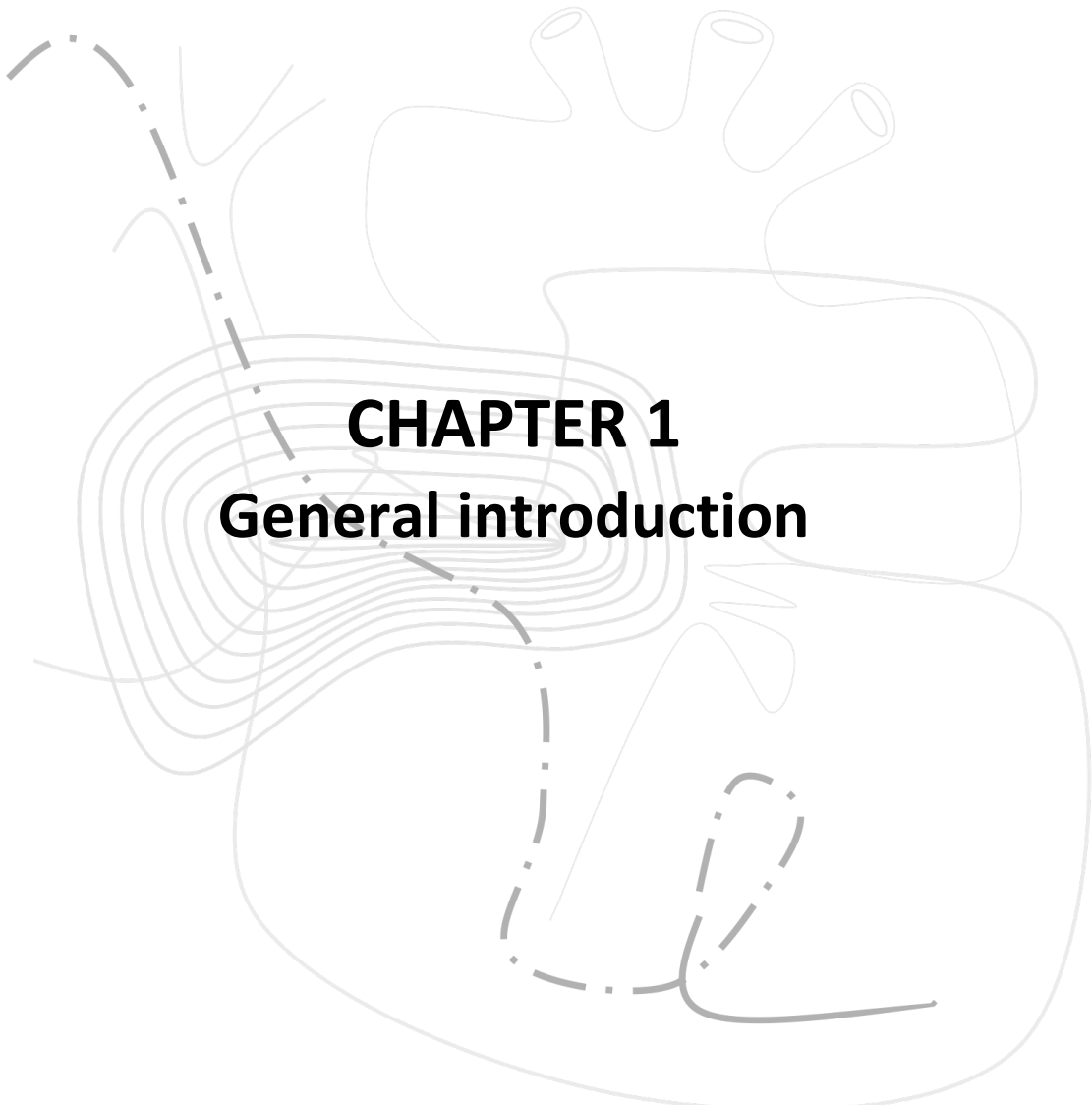
<b>RTK</b>	Receptor tyrosine kinase
<b>RT-qPCR</b>	Real-time quantitative polymerase chain reaction
<b>RV</b>	Right ventricle
<b>S.C.</b>	subcutaneous
<b>SD</b>	Standard deviation
<b>SEM</b>	Standard error of the mean
<b>SER</b>	Serine
<b>SNRT</b>	Sinus node recovery time
<b>TGF-<math>\beta</math></b>	Transforming growth factor – beta
<b>TM</b>	Transmembrane
<b>TP</b>	Threshold potential
<b>T3</b>	Triiodo-L-thyronine
<b>VSMC</b>	Vascular smooth muscle cells
<b>VKA</b>	Vitamin K antagonist



## Preface

Atrial fibrillation is an important health problem, with increasing incidence and prevalence worldwide. It is the most common cardiac arrhythmia, and exposes patients to severe symptoms and to an increased risk for death, heart failure, hospitalization and thromboembolic events. Despite important progress over the past decades, medical treatment remains incomplete, and in many cases unsatisfactory. When I started this project on AF, four years ago, I soon realized that it was both a blessing and a curse. It was a blessing because as a just-graduated pharmacist, I received an exciting opportunity to test a new drug candidate for an important health problem. It was also a curse, because I realized that AF is a complex disorder, with a complex pathophysiology, and that I would be faced by numerous challenges. For instance, we needed a reliable animal model, which was not present in the lab at the time I started this project. At the start, we anticipated to have access to a small-animal model that developed spontaneous AF, which would be relevant because it would mimic the clinical course of AF in humans. For this reason we selected a transgenic mouse model that had previously been described in the literature and that overexpressed tumor necrosis alpha in the myocardium. We obtained this model in our laboratory and with full enthusiasm, I quickly learned how to handle small laboratory animals. I spent months practicing how to implant tele-transmitter devices and built a full operational room dedicated for our expensive telemetry recording setup to monitor these mice in a longitudinal fashion. Unfortunately, despite intense monitoring, we observed that the transgenic mice developed far less spontaneous AF as anticipated, and also had severe heart failure, which made them unsuitable to test our hypotheses. Halfway through my PhD, while dealing with a pandemic, I had to start over and search for a new animal model. Despite this setback, I was more determined than ever. We switched to other clinically relevant models, now based on a chronic exposure to the most important risk factors of AF in humans. The disadvantage of these models was that they did not develop spontaneous AF, and that I had to learn how to perform intracardiac catheterizations and electrophysiology studies in mice, which was a challenging but most rewarding part of my project. After countless EP studies we obtained promising results, in part confirming but also diverging from our original hypotheses, hence opening new avenues for discoveries. What follows in this thesis is the result of an extensive study in which a new drug candidate has been tested as a potential therapy for AF in different mouse models.





**CHAPTER 1**  
**General introduction**





## GENERAL INTRODUCTION

### Atrial fibrillation

AF is defined as a supraventricular tachyarrhythmia with uncoordinated atrial electrical activation and consequently ineffective atrial contraction (Figure 1) (1). AF consists of a complex interplay between triggers, risk factors and substrates. With a life time risk of one in three individuals, it is the most common arrhythmia (1, 2). AF is associated with substantial morbidity and mortality and is therefore a burden for patients, social health and the economy. Globally, the incidence and prevalence of AF are expected to increase 2.3-fold by 2050, mostly due to an increase in life span of the population (2, 3).

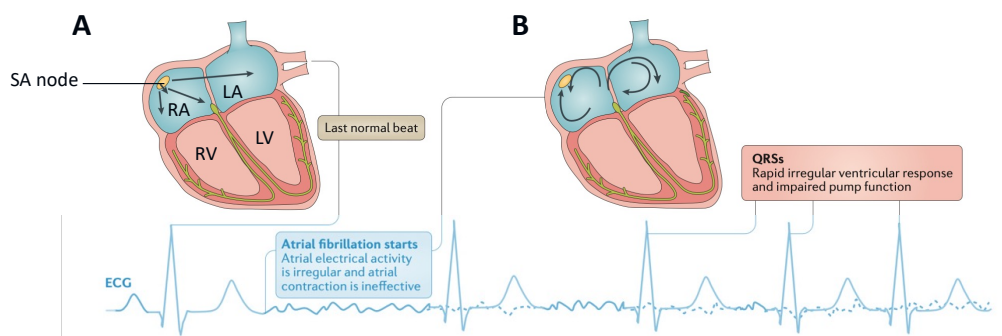


**Figure 1. Schematic overview of normal sinus rhythm compared to atrial fibrillation.** Adapted from S. Nattel (4). **(A)** The last normal beat before the onset of AF. **(B)** Initiation of AF, characterized by rapid and uncoordinated atrial activity, followed by ineffective atrial contractions. SA node indicates sinoatrial node; RA, right atrium; RV, right ventricle; LA, left atrium; LV, left ventricle.

### Risk factors of AF

Numerous risk factors have been uncovered to play a role in initiating and maintaining AF, and driving its underlying mechanisms (Figure 2). Some of the most common risk factors are hypertension, obesity, aging, obstructive sleep apnea, oxidative stress, and hemodynamic overload. Management of these risk factors should always be evaluated and optimized where possible (1, 5, 6). Hypertension (22%) is the most important risk factor, followed by obesity (13%) (6). For this reason, hypertension and obesity will be discussed in more detail.

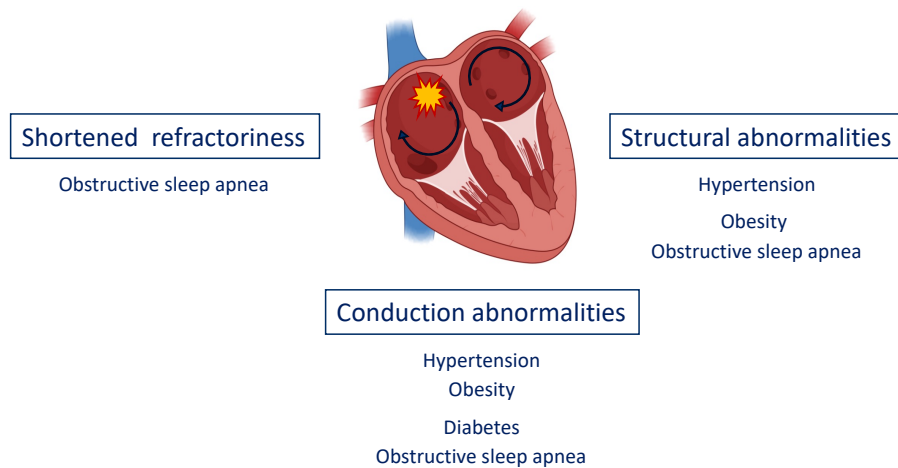


**Figure 2. Schematic overview of AF risk factors and their mechanisms.** After Lau *et al.* *Circulation*, 2017 (6). Correlation between AF risk factors and their causal mechanism of AF-related arrhythmia.

## Hypertension

Hypertension is an important, independent, and modifiable risk factor of AF. The pathophysiological link with AF is mainly through structural changes as a result of hemodynamic alterations in response to increased blood pressure. Chronic hypertension leads to left ventricular hypertrophy, and eventually left atrial remodeling (enlarged size and stretch). Hypertension is directly associated with dysregulation of RAAS, which facilitates the fibrotic process (7). The link and underlying mechanism between hypertension and AF has been demonstrated in humans and in different experimental models. Moreover, human data indicate that increased serum levels of Ang II are linked to AF and that counteracting these pharmacologically protects against atrial remodeling. Similarly, mouse models of Ang II-induced hypertension, showed remodeling of the atria and increased AF susceptibility. Elevated levels of Ang II cause extensive structural and electrical remodeling of the atria. Electrical remodeling can be observed by alterations in AP morphology, and an increase in APD predominantly in the left atrium. Furthermore, a reduction in atrial  $I_{Na}$  was seen, resulting in a reduction in AP upstroke velocity. Additionally, atrial fibrosis and stretch result in disruption of cardiomyocytes and reduces the atrial conduction. These structural and electrical changes combined, increase the likelihood of early afterdepolarizations and reentry, and hence AF (7-9).

## **Obesity**

The relationship between AF and obesity is more complex and dynamic as already short-lasting (5 years) increases in BMI ( $>25 \text{ kg/m}^2$ ) increase the risk for AF (10). Moreover, the Framingham Heart study determined that every unit increase in BMI is correlated with a 4–5% increase in AF risk (11). The second most common risk factor for AF is obesity (12). Until now, the pathophysiology of AF in obesity is not completely elucidated and likely contains multiple mechanisms. These mechanisms consist of hemodynamic alterations induced by left ventricular hypertrophy and diastolic dysfunction, atrial dilation/remodeling, increased (systemic) pro-inflammatory state and atrial fibrosis due to EAT. EAT is located between the visceral pericardium and the epicardial layer of the myocardium and covers 80% of the heart surface, spanning both the atria and ventricles. Epicardial fat is metabolically active and shares its blood supply with the coronary vessels of the myocardium leading to paracrine signaling. Cross sectional imaging shows that EAT volume, particularly left atrial EAT, correlates with increased AF risk (13, 14). EAT produces a range of pro-inflammatory adipocytokines (e.g. activin A, a member of the TGF- $\beta$  superfamily), linking the relationship between obesity and AF directly to inflammation and subsequent fibrosis (13, 15). Moreover, direct fatty infiltration of the myocardium might play a role in both structural and electrical remodeling in the atria. All these underlying consequences of obesity increase the risk of AF by altering the conduction heterogeneity and changing the CV (13, 14).

## **AF classification**

AF arises in different patterns and can be classified based on its presentation, duration, and spontaneous termination of episodes. Based on these characteristics, AF is defined as paroxysmal or non-sustained when it terminates spontaneously or after intervention within seven days. However, when AF lasts longer than seven days it is categorized as persistent. AF that lasts longer than one year, even after therapeutic intervention, is defined as permanent. Additionally, AF can be defined as long-standing persistent when it continuous for more than one year and patients are adopted to a rhythm control strategy. Transition of subclinical to clinical AF or paroxysmal to persistent AF or persistent to permanent AF is often accompanied by progressive atrial remodeling (1).

### Mechanisms of AF initiation and sustainability

AF is triggered by rapidly discharging foci (focal activity) and afterdepolarizations which are the result of enhanced automaticity and triggered activity outside the sinus node (16). These triggers typically consist of focal spontaneous firing, often originating around the PVs.

AF can be initiated due to alterations in sinus rate or by shift in the site of impulse initiation and is referred to as 'abnormal automaticity'. Abnormal automaticity eventually leads to the formation of focal ectopic stimulations within the heart, meaning that electrical signals arise from areas that are not the sinus node (Figure 3A). Variations in sinus rate can be accompanied by alterations in the origin of the dominant pacemaker (16, 17).

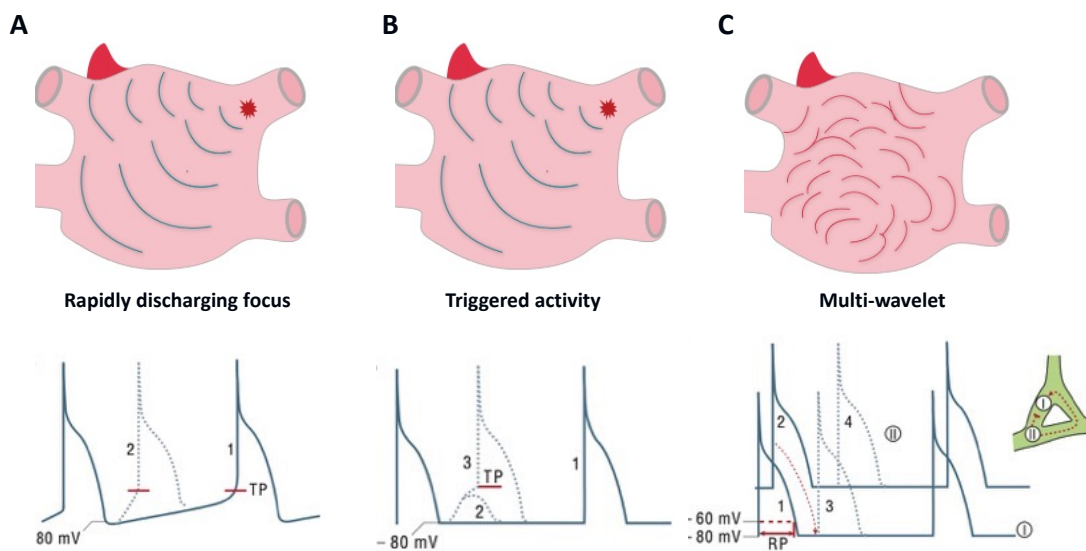


**Figure 3. Basic mechanisms of AF.** adapted from S. Nattel. Nature, Jan 2002 (18). **(A)** Abnormal automaticity occurs when cells reach their potential threshold (A2) before the normal automaticity action potential (A1) takes place and results in focal ectopic activity. **(B)** Afterdepolarizations arise when inward currents are increased, eventually reaching threshold potentials (B2) and depolarizing the cell. This results in premature (B3) ectopic action potentials. **(C)** Reentry occurs when different cardiac tissue zones (I and II) re-activate each other by sending electrical impulses through alternative pathways to each other, circumventing their refractory period. zone II (C2) acts as an ectopic complex during the refractory period (C1) in zone I. The electrical impulse from this ectopic complex propagates through an alternative path (red arrow) to reactivate zone I (C3) after its refractory period. Zone I (C3) then reactivates on its turn zone II (C4) if there is sufficient time and space, avoiding its refractory period. Zones I and II can repetitively reactivate each other resulting in a persistent reentrant activity. TP indicates threshold potential; RP, refractory period; mV, millivolt.

Alternatively, AF manifests through 'triggered activity', which involves the development of abnormal depolarizations during or following the cardiac AP plateau, also known as afterdepolarizations. These spontaneous APs reaching the threshold potential occur spontaneously due to  $\text{Ca}^{2+}$  abundance, resulting in increased NCX current and creating a higher vulnerability for afterdepolarizations (4, 18). Afterdepolarizations are dependent on the preceding transmembrane activity and can be divided in two subtypes, EAD and DAD. EADs arise during repolarization phase 2 and/or phase 3, while DADs occur after complete repolarization of the ventricles, as seen in Figure 3B (16).

Finally, a different type of mechanism known to initiate and mostly sustain AF is 'reentry'. Reentry emerges in a single circuit or multiple unstable reentry circuits at the same time (multi-wavelet, Figure 3C), producing even more irregular (fibrillatory) activity. The refractory period and conduction velocity play an essential role during reentry. Reentry exists when its circuits are longer than the longest refractory period and is thus favored by short refractory periods or slowing of conduction velocity (16, 17). Once AF is induced, reentry plays a key role in its sustainability. Reentry develops around a vulnerable substrate such as fibrosis (anatomical reentry) or in absence of a substrate (functional reentry), and makes the atria prone to maintain AF. Multiple reentry circuits can co-exist at the same time containing their individual initiating and sustaining factors, which is often seen in well-established (persistent or permanent) AF (19).

Anatomical reentry is characterized by a wave propagating in a fixed ring-like path with an excitable gap separating the wavefront from the wavetail (Figure 4A). In contrast, functional reentry does not require an anatomical obstacle and there is no excitable gap as the circulating excitation wavefront invades its tail. During functional reentry, cardiac tissue inside the reentry wave is considered to receive a centripetal excitation wavefront, which renders it continuously refractory. This refractory tissue then acts as a functional barrier that sustains reentry, similar to a fixed anatomic barrier (Figure 4B) (20, 21). This latter form of reentry is often referred to as the 'leading circle' model.

Apart from functional reentry, a more complicated concept was discovered. Rotors, which are spiral waves instead of circular waves, arise due to heterogeneity in tissue conduction and refractory period. Spiral waves are connected by a curved wavefront (depolarized region) and meet their wavetail (repolarizing region) at a focal point, called a phase singularity (Figure 4C). Leading up to the phase singularity, the wavefront curvature is so high and the conduction velocity so slow that the continuing wavefront is not able to penetrate and excite a core of tissue in the center of the rotor. This core forms an area of functional block, similar to the center of the leading circle circuit, however, tissue at the core is not truly refractory in rotors. Because of this, rotors are able to meander as they rotate around unexcited but highly excitable tissue.

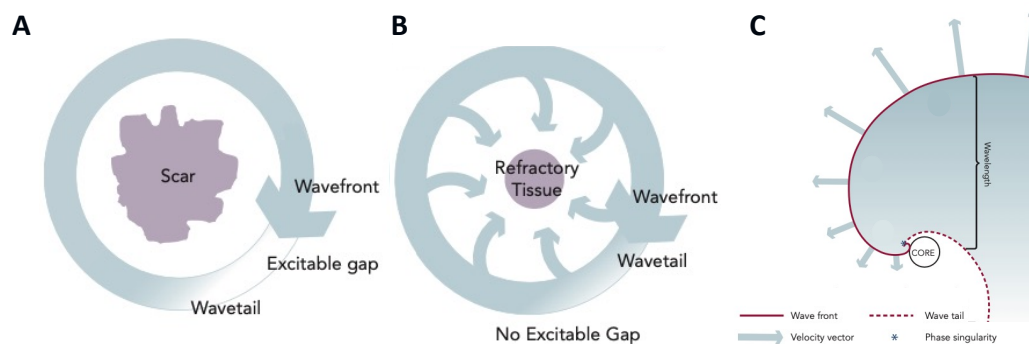


**Figure 4. Mechanisms sustaining AF.** Adapted from Waks *et al.* (21) and Xu *et al.* (22) **(A)** Reentry circuit around an anatomic substrate (fibrosis). The wavefront (blue arrow) and wavetail are separated by an excitable gap excitable gap (white). **(B)** Leading circle reentry, without an excitable gap and a continuous wavefront invading its wavetail. The centripetal activation of the circuit center renders it refractory, making it possible for reentry to exist without anatomic substrate. **(C)** Rotor-induced spiral wave with characteristic decrease in conduction velocity and increase in wavefront curvature near the core of the rotor. The point of phase singularity is where wavefront and wavetail meet each other.

### Atrial myopathy

AF is the result of a more substantial condition called atrial myopathy. The term “atrial myopathy” was first described by Zipes *et al.* (23). The relationship between AF and atrial myopathy is more complex than initially thought, as atrial myopathy does not always coincides with AF, but can facilitate the development of AF (24). Atrial myopathy is characterized by different types of remodeling: electrical, structural and autonomic remodeling. The development of atrial myopathy is complicated and there are multiple contributing factors to it. For the purpose of this thesis and

in order to not lose focus on the performed research, structural and electrical remodeling and their link with AF is briefly described.

### **Atrial structural remodeling**

Structural remodeling manifests itself in different ways and is probably the most obvious change in the atria (25). Structural changes affect tissue properties, atrial size, and cellular structure. An important aspect of atrial structural remodeling is interstitial fibrosis formation which directly increases conduction heterogeneity within the atria and forms an important substrate for reentry and rotor formation, resulting in AF and its sustainability (24). Different underlying factors can contribute to increased atrial fibrosis, such as aging (24), oxidative stress (24), and inflammation (26). Fibrosis is characterized by fibroblast proliferation and differentiation which plays a key role in ECM deposition. TGF- $\beta$ 1 signaling is an essential mediator in fibrogenesis and is (upstream) activated by different triggers, such as an increase in Ang II levels, mechanical stretch, etc., resulting in canonical TGF- $\beta$ 1/Smad activation. The resulting fibrotic substrate interferes with electrical conduction by altering cardiomyocyte coupling, which is normally regulated by connexins. Changes in connexin expression, distribution, and intracellular orientation has profound effects and eventually reduces conduction velocity and increases APD dispersion, promoting reentry. The mRNA and protein expression of the most important connexins in atrial tissue (Cx40 and Cx43) is known to be altered in patients with AF (19, 27, 28).

### **Atrial electrical remodeling**

Electrical remodeling of the atria is driven by alterations in Ca<sup>2+</sup>-handling, ion channels, and gap junctions. The action potential is regulated by different inward and outward currents. Specifically, the balance between inward and outward currents during the repolarization phase determines the APD. Following this, increasing the inward current prolongs the APD, and increased outward current shortens the APD. Therefore, the resulting ionic current balance regulates also the refractory period and thus the likelihood of reentry. Shortening in APD or thus decrease of the refractory period favors reentry and sustains AF. Increase in atrial rate (up to ten fold) caused by atrial tachycardia or already existing AF is a primary stimulus for electrical remodeling. As a result, more Ca<sup>2+</sup> enters the cells through the  $I_{Ca,L}$  within every AP. These alterations in Ca<sup>2+</sup>-handling

eventually result in  $\text{Ca}^{2+}$  overload, promoting triggered activity, afterdepolarizations and apoptosis. As a response, cardiomyocytes will alter their expression of  $I_{\text{Ca,L}}$  to reduce the cellular amounts of  $\text{Ca}^{2+}$ . Since  $I_{\text{Ca,L}}$  is a key mediator in the AP plateau, a decrease in its expression will also result in a decrease of APD, and shorten the effective refractory period. This does not only promote but also maintain reentry cycling. Additionally, downregulation of  $I_{\text{Ca,L}}$ , results in decreased systolic  $\text{Ca}^{2+}$  release as well as intracellular  $\text{Ca}^{2+}$ -handling proteins. Furthermore, other ion channel alterations take place during electrical remodeling of the atria. As seen in atrial myocytes from patients in AF,  $I_{\text{to}}$ , and  $I_{\text{kur}}$  are altered which accelerates the repolarization of atrial cells, additionally shortening the refractory period (4, 24). Changes in atrial ion channels expression and function increases electrical conduction heterogeneity, and eventually alters CV, APD and effective refractory period (18, 24, 29).

### **Symptoms, clinical presentation and diagnosis**

Symptoms of AF range from shortness of breath to fatigue, palpitation, dizziness, etc., but are frequently absent and non-specific resulting in patients not noticing any discomfort. This makes it often more difficult to make the diagnosis based on symptoms alone and therefore often happens incidentally. Since AF can present itself in a paroxysmal way, its diagnosis can be overlooked or missed. To diagnose AF, an ECG examination is required showing irregularly irregular RR-intervals (in absence of atrioventricular conduction impairment), absence of distinct P-waves, and irregular atrial activity in the baseline. By convention, an episode lasting at least 30 s is diagnostic for clinical AF. Once AF is documented, an echocardiography should be performed to screen for underlying structural heart disease, and assess atrial size and cardiac function, as well as laboratory tests to screen for underlying conditions. With current advancing technologies such as oscillometry and photoplethysmography implemented in phones and wearables, screening for AF becomes more cost effective and can be done in earlier stages (30).

### **Therapy**

AF therapy has seen numerous changes and advancements since the first proposed patient management strategy. However, there are many underlying mechanisms leading to AF, and the current available therapies only target one branch (rate and rhythm control) in this system, leading



to insufficient therapies in clinical practice. This results in a high and unmet medical need for a treatment targeting the structural remodeling associated with AF. The following section outlines the current therapies for AF and is based on the latest guidelines (2020) of the ESC (1). Current treatment strategies implement both pharmacological and non-pharmacological therapies. Pharmacological therapies include rhythm and rate control, and anti-coagulation. These are all non-invasive of nature compared to non-pharmacological therapies, such as cardioversion and ablation. Recent research showed that ablation therapy is more successful (less AF recurrence) when performed within 36 months after AF diagnosis (31). Depending on the AF type (paroxysmal vs. permanent) different approaches of treatment can be followed, but will not be discussed in detail in this thesis.

### **Anti-coagulation**

Patients with AF have a five-fold increased risk to develop stroke (32). Therefore anticoagulation is of high importance and needs to be closely monitored and controlled. Several factors need to be taken into account to determine the actual risk of developing stroke and thus varies highly between patients. All patients need to be accurately evaluated based on their lifestyle and comorbidities in order to provide the most accurate treatment. To assess the risk of non-anticoagulated patients with (non-valvular) AF developing a stroke, clinicians make use of the clinical risk-factor-based CHA<sub>2</sub>DS<sub>2</sub>-VASc score (33). The CHA<sub>2</sub>DS<sub>2</sub>-VASc score is a point based score system including various risk factors: congestive heart failure, hypertension, age  $\geq$  75 years, diabetes mellitus, stroke, vascular disease, age 65—74 years, and sex. Current strategies for stroke prevention include oral-anticoagulation and antiplatelet therapy. Oral-anticoagulation can consist of VKAs, such as warfarin. A downside of VKAs is that they are limited by a narrow therapeutic window, requiring intense monitoring of the INR. NOACs (such as, apixaban, dabigatran, edoxaban, and rivaroxaban) show similar results in stroke prevention compared to VKAs, however NOACs are associated with reduced all-cause mortality and are less associated with major bleeding when INR is poorly controlled.

## **Rate control**

To improve quality of life and additionally reduce AF symptoms, patients require heart rate management. Rate control forms an integral part of AF management. There is no fixed heart-rate target for AF patients, however, the RACE II clinical trial showed that there was no difference between the strict (target heart rate < 80 bpm) and the lenient (target heart rate < 110 bpm) group in the prevention of major cardiovascular events (34). This means that initially a lenient rate controlling approach is sufficient unless symptoms or patient's condition requires for a more strict rate control. There are different pharmacological ways in which rate control can be achieved. This choice depends on symptoms, potential adverse effects, and comorbidities of the patient and need to be individually assessed for each patient. First line choice for (acute) rate control are beta-blockers, followed by NDCC therapy. NDCCs are known for improvement of AF-related symptoms and moderate rate control. Digoxin and amiodarone are less frequently used as rate controlling therapy, however they can be used in patients where heart rate is more difficult to control with combination therapy or patients not qualified for non-pharmacological rate control. If pharmacological intervention does not succeed, controlling ventricular rate, ablation of the atrioventricular node and pacemaker implantation can be performed.

## **Rhythm control**

In order to restore and maintain patients in sinus rhythm, a rhythm control strategy is applied. The EAST (2020) trial, showed that starting rhythm-control therapy in early AF patients was associated with a lower risk of death from cardiovascular causes, stroke, or hospitalization for heart failure or acute coronary syndrome (35). Rhythm control can be obtained by different approaches or a combination of such. Cardioversion from AF to normal sinus rhythm might be reached by electrical (defibrillator) and/or pharmacological cardioversion (AADs). AADs can be classified into categories by their mode of action: Na<sup>+</sup> channel blockers (class I), β-blockers (class II), multichannel blockers (class III), Ca<sup>2+</sup> channel blockers (class IV). Specific choices of a drug is based on the type and severity of associated heart disease, and the onset of AF. After cardioversion, chronic rhythm control with AADs can be used to prevent recurrence of AF.

## **Animal models to study AF**

When choosing an animal model to study cardiac arrhythmias, it is important to consider the research question and the type of arrhythmia investigated. Important considerations for this decision include anatomy (heart size and macrostructure) and species specific differences (heart rate, ion currents, autonomic regulation). No animal model completely replicates human cardiac anatomy, electrophysiology, and hemodynamic parameters. For example, K<sup>+</sup> currents underlying cardiac repolarization are different in mice compared to humans, resulting in a distinct AP morphology. Moreover, interspecies differences exist in arrhythmia susceptibility. Large animals, for example, are more prone to ventricular arrhythmias and sudden death. Over the last decades, the number of small animal models to study cardiac arrhythmias significantly increased and played an important role in the understanding of arrhythmia mechanisms and arrhythmogenesis. Nevertheless, translation of this knowledge from small animals to humans has always been a limiting factor and encourages to also perform studies in large animals. Despite being more costly and labor-intensive, large animals are competent for arrhythmia assessment and their tissue substrates, and increase translational value (36). In line with this rationale, studies similar to the ones described in this thesis were conducted in parallel but independently from my project by another PhD student, in which a pig model of AF was used to evaluate the effects of the same drug candidate for AF. Importantly, the results of these pig studies turned out to highly resemble the results in this thesis. This should be considered when interpreting the results of this thesis and their translational value. Notwithstanding the importance of large animal models, all *in vivo* experiments in this thesis were performed in mice. They often remain the preferred animal model due to the availability of transgenic lines, lower costs, shorter life extents, and mainly their ease of use. These factors play an important role in animal studies with multiple testing groups and distinct models, and deepen translational value of the hypothesis by using transgenic mice (36). For a detailed overview of different animal models to study AF, I refer to the review paper mentioned in reference (37). Despite all the improvements and results obtained from animal models, no major breakthrough in the treatment of AF in humans has been made recently, illustrating both the complexity of AF and/or the limitations of using small animal models to study new and effective treatments for humans.

## NRG1 and its role in structural remodeling (fibrosis)

Tissue fibrosis is the result of a complex cascade of cellular and molecular responses, triggered by disease-related injury in any organ. As shown in Figure 5, both acute and chronic inflammation upon injury results in an increased release of inflammatory mediators and leads to recruitment of a variety of inflammatory mediator cells (mainly neutrophils and macrophages), eventually triggering fibrosis. (Myo)fibroblasts are identified as key effector cells for the synthesis and secretion of ECM proteins in numerous organs. These matrix proteins are highly conserved across distinct tissues and mainly consist of interstitial collagens (type I and III are most abundant), fibronectin, laminin and other smaller proteins. Normally, ECM deposition and resorption (organ repair) are in a homeostatic equilibrium. However, during chronic injury, effector cells are in a state of continuous activation, leading to excessive ECM deposition and eventually organ damage. Therefore, fibrosis is seen as a dynamic process that involves the deposition and resorption of ECM. The latter includes the elimination of effector cells and a shift in balance of matrix synthesis and degradation. Because fibrosis is such a dynamic process, resulting in adverse effects in all organs, it has become an attractive therapeutic target. Anti-fibrotic treatments are widely investigated, with most research being performed in fibrotic diseases of lung, kidney, liver and intestines.

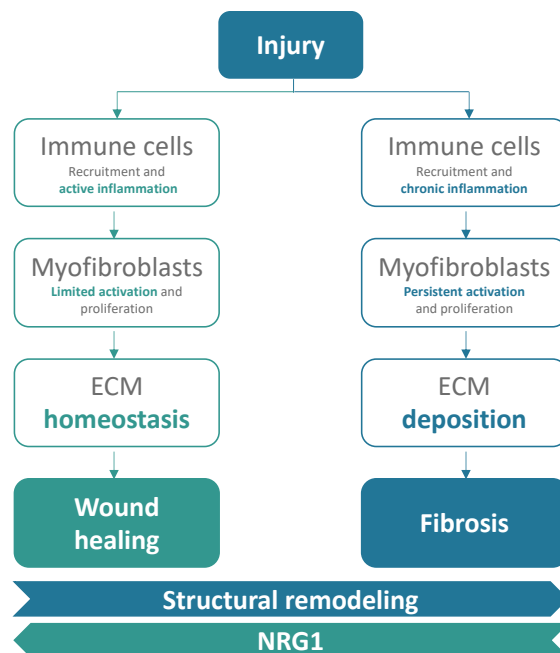


Figure 5. Schematic overview of the interplay between tissue fibrosis and NRG1. A series of complex cellular and

molecular responses regulate wound healing, after tissue injury. Different immune cells are recruited during acute inflammation. This is followed by limited fibroblast activation and differentiation to myofibroblasts. Finally, ECM synthesis and deposition takes place in a controlled manner leading to wound healing. During disease and chronic inflammation, myofibroblasts are continuously activated, resulting in excessive ECM deposition and organ remodeling through fibrosis.

Previous research has shown that ERBB4 activation by its endogenous ligand NRG1 plays an indispensable role in cardiac development, physiology, and adaptation during pathophysiologic changes. Several recent observations from our own and other groups has shown that NRG1 has anti-fibrotic and anti-inflammatory effects in various organs (including heart, kidneys, lung, and skin) and different disease models, comprising heart failure, lung and skin fibrosis, and diabetic nephropathy. First, using a model of diabetic nephropathy our group reported that NRG1 reduces albuminuria, glomerular sclerosis, and the production of collagen by mesangial cells (38). Secondly, NRG1 reduced dermal thickness and collagen accumulation, in a model of bleomycin-induced skin fibrosis. Finally, in mice with Ang II-induced arterial hypertension, NRG1 treatment prevented the development of myocardial fibrosis in the ventricles (39).

Thus, the NRG1/ERBB4 system emerges as a key modulator of tissue remodeling, and activation of this system embodies a new way to counteract tissue remodeling. A central hypothesis of this thesis is that this potentially includes atrial remodeling, a process strongly related with AF. ERBB4 is widely expressed in various cell types, including fibroblasts and macrophages (40, 41). Moreover, our group has built substantial evidence and knowledge for the NRG1/ERBB4 system in cardiac remodeling and fibrosis (38, 39).

Apart from effects on fibrosis, NRG1 also influences inflammatory responses, as shown in heart, lung, skin, and colon. In a DNA microarray experiment of isolated dermal fibroblasts, Vermeulen *et al.* observed that NRG1 induced significant upregulation of 510 genes and downregulation of 450 other genes. Ingenuity pathway analysis confirmed that NRG1 significantly modified pathways of connective tissue development (fibrogenesis) and inflammatory processes (regulation of different cytokines, cytokine receptors and transcription factors of cytokine signaling) (40).

## **NRG1**

NRGs belong to the EGF family and emerge as cell-cell signaling proteins known to participate in cell proliferation, differentiation, and survival in different tissues, including the cardiovascular system, lung, kidney, skeletal muscle, nervous system and breast (42-44). Out of the four structurally related transmembrane proteins (NRG1—4), NRG1 is the most studied member (42). Conserved over the different NRG isoforms is their 'EGF-like domain', which facilitates receptor binding. At the C-terminal region of the EGF-like domain, two variants ( $\alpha$  and  $\beta$ ) are found. Although, the NRG1 $\alpha$  isoform is more expressed, NRG1 $\beta$  has been shown to be 10—100 times more potent at receptor phosphorylation and intracellular signaling compared to NRG1 $\alpha$  (43-45).

## **ERBB family of receptor tyrosine kinase signaling**

RTKs have the ability to phosphorylate tyrosine residues on substrate proteins, and therefore, transduce biological signals (such as polypeptides of the EGF family) from the extracellular to the intracellular compartment (46, 47). Accordingly, RTKs regulate a diverse array of cellular functions, maintaining cellular homeostasis or regulating changes in cellular function. These RTK mediated functions are activated in response to specific polypeptide ligand binding. A total of 55 RTKs are identified containing 19 subfamilies, and they all emerge as key regulators of critical cellular processes, such as proliferation and differentiation, cell survival, cell migration, metabolism and cell cycle control (48-50). RTKs are activated upon binding of a ligand, leading to receptor homo- and heterodimerization, kinase domain activation, and subsequent phosphorylation of tyrosine residues. Phosphorylated tyrosines serve as docking sites for a variety of intracellular adaptors and effector enzymes that transmit signals to the cytoplasm and nucleus, resulting in changes in cell function. Many regulatory cellular processes and also developmental functions are regulated by RTKs. This also means that abnormalities in structure or activity of the RTKs can lead to human diseases (49, 50).

The ERBB subfamily of the RTKs was first discovered half a century ago by Das *et al.* (51), identifying the EGFR, now also known as ERBB1/HER1, as the receptor for the growth factor EGF. Later, discovery of ERBB2/HER2, ERBB3/HER3, and ERBB4/HER4 completed the ERBB receptor family (50). All four ERBB receptors are structurally homologues and have a molecular weight

around 180 KDa. They consist of three functional domains: a glycosylated ECD, the single TM region, and an ICD which contains the PTK sub-domain. This PTK sub-domain is a bilobed structure that becomes phosphorylated upon ligand binding and possesses a regulatory role in downstream signaling (46).

Ligands of ERBB1 include EGF, transforming growth factor alpha (TGF $\alpha$ ), heparin-binding EGF-like growth factor, betacellulin, epiregulin, and epigen which are all EGF-like ligands. Whereas NRG1 – 4 are ligands for ERBB3 and ERBB4 (Figure 6). Additionally, TGF $\alpha$  and EGF can bind to ERBB3, and HB-EGF, betacellulin and epiregulin are other ligands to ERBB4. The ERBB2 receptor is known to be an “orphan” receptor since it has no known ligands binding to its ECD. Since the tyrosine kinase domain of ERBB2 is catalytically active, it serves as a co-receptor that can heterodimerize with the other ERBB receptor members to initiate signal transduction (46, 47).

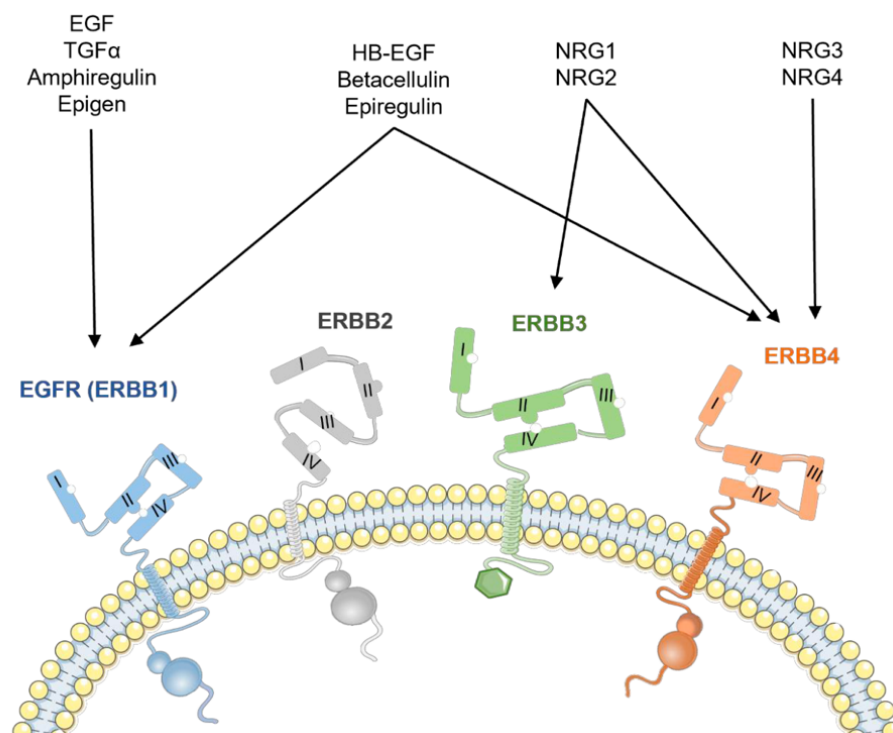


**Figure 6. ERBB receptor family and their ligands.** Modified after Segers VFM *et al.*, Cellular oncology, 2020 (52). ERBB1 has multiple EGF-like ligands. ERBB2 has no known ligands because of a defective ligand binding domain, where the ERBB3 receptor lacks tyrosine kinase domain functionality. Therefore ERBB2 and ERBB3 receptors both require heterodimerization for transphosphorylation of the tyrosine kinase domain.

ERBB4 can be activated by all NRGs. EGF indicates epidermal growth factor; ERBB, V-erb-b avian erythroblastic leukemia viral oncogene homolog; NRG, Neuregulin. HB-EGF, heparin-binding EGF-like growth factor; TGF $\alpha$ , Transforming growth factor alpha.

ERBB receptors naturally exist as inactive monomers with its ECD folded in such a way that it prevents dimerization. Binding of a ligand to the glycosylated ECD, initiates conformational rearrangement which exposes the dimerization domain and promotes either homo- (between the same receptors) or heterodimerization (between two different receptors). Receptor dimerization results in transactivation of the cytoplasmatic tyrosine kinase domain, and transphosphorylation of intracellular tyrosine residues (Figure 7B). Transphosphorylation then allows for recruitment of signaling proteins and activation of a broad range of downstream signaling pathways (46, 49, 53). In summary, ERBB receptors undergo conformational changes upon ligand binding. This is essential and allows the receptors to dimerize with subsequent intracellular signaling through a complex and tightly controlled network of signaling pathways that drive and regulate many cellular functions.

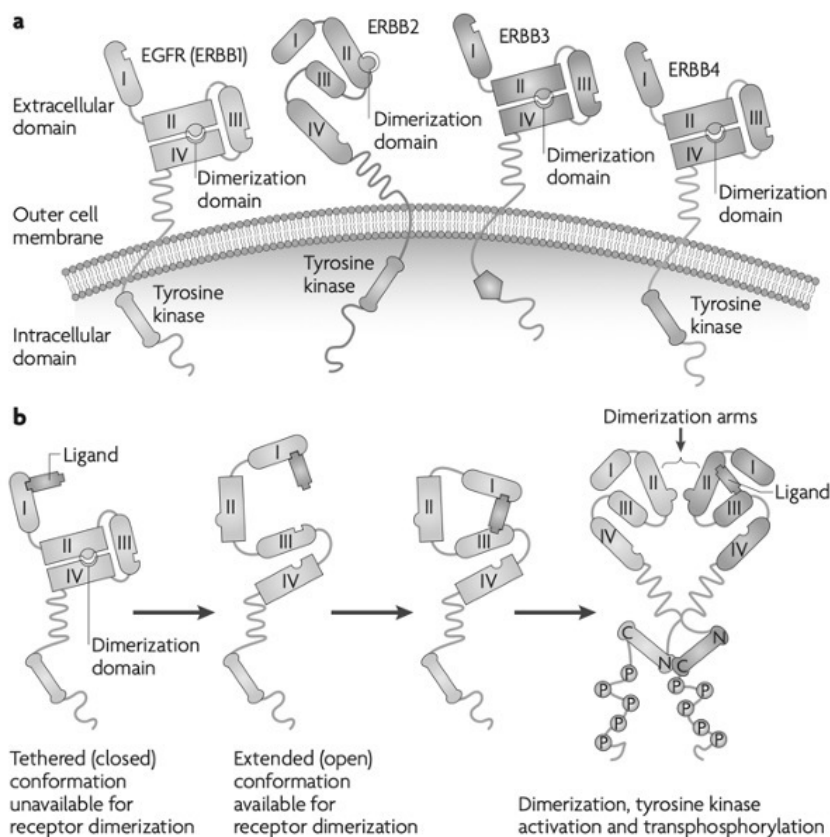


**Figure 7 ERBB receptor family activation - overview.** Modified after Baselga J. *et al.* Nat Rev Cancer, 2009 (53).



**(A)** The ERBB family contains four closely related tyrosine kinase receptors, including ERBB1 or EGFR, ERBB2, ERBB3, and ERBB4. They are composed of three functional domains: an extracellular domain responsible for ligand binding, an intracellular protein tyrosine kinase domain to mediate interactions with intracellular signaling molecules, and a transmembrane segment to connect the ECD with the ICD. The ECD contains four sub-domains of which I and III are leucine-rich ligand binding domains and II and IV are cysteine-rich domains. **(B)** Conformational rearrangement of ERBB receptor upon ligand binding to initiate receptor dimerization and subsequent functional activation. ERBB indicates V-erb-b avian erythroblastic leukemia viral oncogene homolog; EGFR, EGF receptor; ECD, extracellular domain; ICD, intracellular domain.

## **NRG1/ERBB pathway in the heart**

### **Effects of NRG1 in distinct cardiac cells**

Numerous studies have shown that NRG1 acts as an adaptive growth factor following cardiac injury and that it slows cardiac remodeling. Although the precise pathways through which NRG1 transmits its disease mitigating effects remain poorly defined. NRG1 emerges as a pleiotropic substance with the ability to modulate various biological processes by acting on all the different cell types in the heart. Not only cardiomyocytes respond to NRG1, also endothelial cells, smooth muscle cells, macrophages, and fibroblasts play their part (40).

NRG1 has both structural and functional effects on **cardiomyocytes**. NRG1 modulates the viability of cardiomyocytes, primarily through ERBB4, by inhibiting apoptosis both *in vitro* and *in vivo*. This effect is mediated by PI3K/Akt signaling (40). Furthermore, NRG1 plays an important role in the regenerative capacity of the heart, more specifically on cardiomyocytes. Different studies showed protein synthesis and hypertrophy of isolated cardiomyocytes after stimulation with NRG1. These effects are mediated by activation of ERK1/2 and Akt/ mTOR pathway and were seen in different models (39, 54-56). NRG1 induces cardiac repair through a combination of cardiomyogenic stem cell activation and by stimulating cardiomyocyte cell cycle in an ERBB4-dependent manner (40, 57). However, ERBB4-dependent stimulation of cardiomyocyte proliferation is limited to a short postnatal window. As shown by D'Uva *et al.* (58), also ERBB2 receptors play a crucial role in cardiomyocyte proliferation. ERBB2 expression is decreased within the first week after birth, together with cardiomyocyte proliferation. Genetically induced constitutive expression of ERBB2 results in extensive cardiomyocyte hypertrophy, dedifferentiation, and proliferation.

Transient induction of ERBB2, after myocardial infarction, stimulated cardiomyocyte dedifferentiation and proliferation with subsequent redifferentiation and regeneration (58).

NRG1 controls survival and cytokine release in **macrophages** and thus contributes to the protective and regenerative effects in pathophysiological conditions, including the heart. Mice with a specific deletion of the ERBB4 receptor in macrophages, subjected to distinct triggers of inflammation and fibrosis showed significantly more tissue fibrosis compared to wild type mice (39). This proves that NRG1 has a regulatory role in macrophages, and more specifically through ERBB4 signaling. Pro-inflammatory activation of macrophages increases ERBB4 expression and induces macrophage apoptosis. Thus, ERBB4 activation attenuates pro-inflammatory cytokine release from macrophages (39, 40).

Human **fibroblasts** are known to express ERBB2, ERBB3, and ERBB4 receptors. Preventive NRG1 treatment reduced fibrosis in different tissues and organs, such as the development of myocardial fibrosis in the ventricles of an Ang II-induced arterial hypertension mouse model (39). Moreover, anti-fibrotic effects were seen in a model of diabetic nephropathy where collagen production by mesangial cells was reduced (38), and in bleomycin-induced skin and lung fibrosis models, where dermal thickness and collagen accumulation was significantly reduced by preventive NRG1 treatment (39). In a DNA microarray analysis on primary mouse fibroblasts from adult hearts, NRG1 differentially expressed 960 genes. NRG1 thus promotes upregulation of pro-reparative factors and the downregulation of fibrogenesis-related signaling pathways in fibroblasts (40).

**Endothelial cells** act as a main source of NRG1. NRG1 mediates endothelial cell proliferation, function, and role in angiogenesis and is therefore part of an autocrine communication loop in endothelial cells. Genetic deletion of NRG1 or its receptors in ECs results in aborted development (ventricular trabeculae and cardiac cushion) (40). Endothelial cell stimulation with NRG1 leads to increased growth of vascular endothelial cells and increased myocardial capillary density. This means that NRG1/ERBB signaling mediates myocardial recovery by increasing its angiogenic potential through endothelial stimulation (40, 41, 59).

ERBB receptors, mainly ERBB4, are also expressed by **vascular smooth muscle cells**. rhNRG1 administration in a rat model decreased formation of neointima and platelet-derived growth factor-induced proliferation of vascular smooth muscle cells. Furthermore, NRG1 attenuates stress-induced vascular smooth muscle cells senescence in cultured conditions and *in vivo* in a model of diabetes mellitus. On top, smooth muscle cell-specific *ErbB4*-deficient mice show early vascular senescence and increased mortality in diabetic conditions. This shows that NRG1 not only serves as a growth-inducing agent, but also behaves as a growth-stabilizing agent (40).

## References

1. Hindricks G, Potpara T, Dagres N, Arbelo E, Bax JJ, Blomström-Lundqvist C, et al. 2020 ESC Guidelines for the diagnosis and management of atrial fibrillation developed in collaboration with the European Association for Cardio-Thoracic Surgery (EACTS): The Task Force for the diagnosis and management of atrial fibrillation of the European Society of Cardiology (ESC) Developed with the special contribution of the European Heart Rhythm Association (EHRA) of the ESC. *European Heart Journal*. 2020;42(5):373-498.
2. Kornej J, Börschel CS, Benjamin EJ, Schnabel RB. Epidemiology of Atrial Fibrillation in the 21st Century: Novel Methods and New Insights. *Circ Res*. 2020;127(1):4-20.
3. Lippi G, Sanchis-Gomar F, Cervellin G. Global epidemiology of atrial fibrillation: An increasing epidemic and public health challenge. *Int J Stroke*. 2021;16(2):217-21.
4. Lip GY, Fauchier L, Freedman SB, Van Gelder I, Natale A, Gianni C, et al. Atrial fibrillation. *Nat Rev Dis Primers*. 2016;2:16016.
5. Goette A, Kalman JM, Aguinaga L, Akar J, Cabrera JA, Chen SA, et al. EHRA/HRS/APHS/SOLAECE expert consensus on Atrial cardiomyopathies: Definition, characterisation, and clinical implication. *J Arrhythm*. 2016;32(4):247-78.
6. Lau DH, Nattel S, Kalman JM, Sanders P. Modifiable Risk Factors and Atrial Fibrillation. *Circulation*. 2017;136(6):583-96.
7. Walker M, Patel P, Kwon O, Koene RJ, Duprez DA, Kwon Y. Atrial Fibrillation and Hypertension: "Quo Vadis". *Curr Hypertens Rev*. 2022;18(1):39-53.
8. Jansen HJ, McRae MD, Mackasey M, Rose RA. Regional and temporal progression of atrial remodeling in angiotensin II mediated atrial fibrillation. *Front Physiol*. 2022;13:1021807.
9. Jansen HJ, Mackasey M, Moghtadaei M, Belke DD, Egom EE, Tuomi JM, et al. Distinct patterns of atrial electrical and structural remodeling in angiotensin II mediated atrial fibrillation. *J Mol Cell Cardiol*. 2018;124:12-25.
10. Tedrow UB, Conen D, Ridker PM, Cook NR, Koplan BA, Manson JE, et al. The long- and short-term impact of elevated body mass index on the risk of new atrial fibrillation the WHS (women's health study). *J Am Coll Cardiol*. 2010;55(21):2319-27.
11. Wang TJ, Parise H, Levy D, D'Agostino RB, Sr., Wolf PA, Vasan RS, et al. Obesity and the risk of new-onset atrial fibrillation. *Jama*. 2004;292(20):2471-7.
12. Huxley RR, Lopez FL, Folsom AR, Agarwal SK, Loehr LR, Soliman EZ, et al. Absolute and attributable risks of atrial fibrillation in relation to optimal and borderline risk factors: the Atherosclerosis Risk in Communities (ARIC) study. *Circulation*. 2011;123(14):1501-8.
13. Vyas V, Lambiase P. Obesity and Atrial Fibrillation: Epidemiology, Pathophysiology and Novel Therapeutic Opportunities. *Arrhythm Electrophysiol Rev*. 2019;8(1):28-36.
14. Javed S, Gupta D, Lip GYH. Obesity and atrial fibrillation: making inroads through fat. *European Heart Journal - Cardiovascular Pharmacotherapy*. 2020;7(1):59-67.
15. Venteclef N, Guglielmi V, Balse E, Gaborit B, Cotillard A, Atassi F, et al. Human epicardial adipose tissue induces fibrosis of the atrial myocardium through the secretion of adipo-fibrokinases. *Eur Heart J*. 2015;36(13):795-805a.
16. Antzelevitch C, Burashnikov A. Overview of Basic Mechanisms of Cardiac Arrhythmia. *Card Electrophysiol Clin*. 2011;3(1):23-45.
17. Brugada J, Katritsis DG, Arbelo E, Arribas F, Bax JJ, Blomström-Lundqvist C, et al. 2019 ESC Guidelines for the management of patients with supraventricular tachycardia The Task Force for

the management of patients with supraventricular tachycardia of the European Society of Cardiology (ESC): Developed in collaboration with the Association for European Paediatric and Congenital Cardiology (AEPC). *European Heart Journal*. 2019;41(5):655-720.

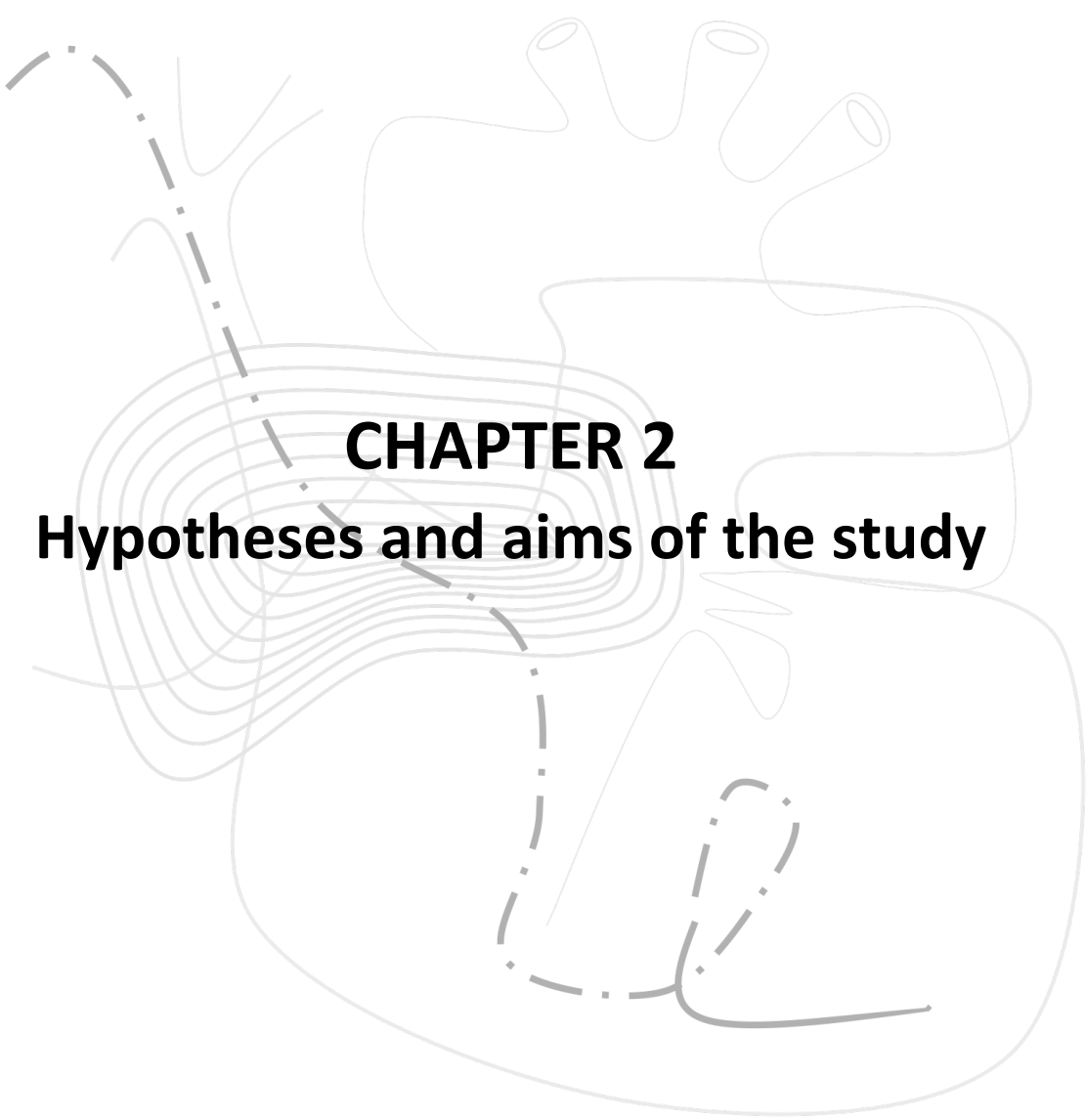
18. Nattel S. New ideas about atrial fibrillation 50 years on. *Nature*. 2002;415(6868):219-26.
19. Steinberg JS, Mittal S. *Electrophysiology: The Basics : a Companion Guide for the Cardiology Fellow During the EP Rotation*: Lippincott Williams & Wilkins/Wolters Kluwer Health; 2010.
20. Pandit SV, Jalife J. Rotors and the Dynamics of Cardiac Fibrillation. *Circulation Research*. 2013;112(5):849-62.
21. Waks JW, Josephson ME. Mechanisms of Atrial Fibrillation - Reentry, Rotors and Reality. *Arrhythm Electrophysiol Rev*. 2014;3(2):90-100.
22. Xu C-H, Xiong F, Jiang W-F, Liu X, Liu T, Qin M. Rotor mechanism and its mapping in atrial fibrillation. *EP Europace*. 2023;25(3):783-92.
23. Zipes DP. Atrial Fibrillation. *Circulation*. 1997;95(3):562-4.
24. Shen MJ, Arora R, Jalife J. Atrial Myopathy. *JACC Basic Transl Sci*. 2019;4(5):640-54.
25. Li M, Ning Y, Tse G, Saguner AM, Wei M, Day JD, et al. Atrial cardiomyopathy: from cell to bedside. *ESC Heart Failure*. 2022;9(6):3768-84.
26. Hu YF, Chen YJ, Lin YJ, Chen SA. Inflammation and the pathogenesis of atrial fibrillation. *Nat Rev Cardiol*. 2015;12(4):230-43.
27. Kato T, Iwasaki Y-k, Nattel S. Connexins and Atrial Fibrillation. *Circulation*. 2012;125(2):203-6.
28. Dobrev D, Carlsson L, Nattel S. Novel molecular targets for atrial fibrillation therapy. *Nature Reviews Drug Discovery*. 2012;11(4):275-91.
29. Gilbert G, Demydenko K, Dries E, Puertas RD, Jin X, Sipido K, et al. Calcium Signaling in Cardiomyocyte Function. *Cold Spring Harb Perspect Biol*. 2020;12(3).
30. Perez MV, Mahaffey KW, Hedlin H, Rumsfeld JS, Garcia A, Ferris T, et al. Large-Scale Assessment of a Smartwatch to Identify Atrial Fibrillation. *N Engl J Med*. 2019;381(20):1909-17.
31. De Greef Y, Bogaerts K, Sofianos D, Buyschaert I. Impact of Diagnosis-to-Ablation Time on AF Recurrence: Pronounced the First 3 Years, Irrelevant Thereafter. *JACC: Clinical Electrophysiology*. 2023;9(11):2263-72.
32. Choi SE, Sagris D, Hill A, Lip GYH, Abdul-Rahim AH. Atrial fibrillation and stroke. *Expert Rev Cardiovasc Ther*. 2023;21(1):35-56.
33. Lip GY, Nieuwlaat R, Pisters R, Lane DA, Crijns HJ. Refining clinical risk stratification for predicting stroke and thromboembolism in atrial fibrillation using a novel risk factor-based approach: the euro heart survey on atrial fibrillation. *Chest*. 2010;137(2):263-72.
34. Van Gelder IC, Groenveld HF, Crijns HJGM, Tuininga YS, Tijssen JGP, Alings AM, et al. Lenient versus Strict Rate Control in Patients with Atrial Fibrillation. *New England Journal of Medicine*. 2010;362(15):1363-73.
35. Kirchhof P, Camm AJ, Goette A, Brandes A, Eckardt L, Elvan A, et al. Early Rhythm-Control Therapy in Patients with Atrial Fibrillation. *New England Journal of Medicine*. 2020;383(14):1305-16.
36. Ripplinger CM, Glukhov AV, Kay MW, Boukens BJ, Chiamvimonvat N, Delisle BP, et al. Guidelines for assessment of cardiac electrophysiology and arrhythmias in small animals. *American Journal of Physiology-Heart and Circulatory Physiology*. 2022;323(6):H1137-H66.

37. Schüttler D, Bapat A, Käab S, Lee K, Tomsits P, Clauss S, et al. Animal Models of Atrial Fibrillation. *Circ Res.* 2020;127(1):91-110.
38. Vandekerckhove L, Vermeulen Z, Liu ZZ, Boimvaser S, Patzak A, Segers VF, et al. Neuregulin-1 attenuates development of nephropathy in a type 1 diabetes mouse model with high cardiovascular risk. *Am J Physiol Endocrinol Metab.* 2016;310(7):E495-504.
39. Vermeulen Z, Hervent AS, Dugaucquier L, Vandekerckhove L, Rombouts M, Beyens M, et al. Inhibitory actions of the NRG-1/ErbB4 pathway in macrophages during tissue fibrosis in the heart, skin, and lung. *Am J Physiol Heart Circ Physiol.* 2017;313(5):H934-h45.
40. De Keulenaer GW, Feyen E, Dugaucquier L, Shakeri H, Shchendrygina A, Belenkov YN, et al. Mechanisms of the Multitasking Endothelial Protein NRG-1 as a Compensatory Factor During Chronic Heart Failure. *Circ Heart Fail.* 2019;12(10):e006288.
41. Geissler A, Ryzhov S, Sawyer DB. Neuregulins: protective and reparative growth factors in multiple forms of cardiovascular disease. *Clin Sci (Lond).* 2020;134(19):2623-43.
42. Falls DL. Neuregulins: functions, forms, and signaling strategies. *Exp Cell Res.* 2003;284(1):14-30.
43. Lemmens K, Doggen K, De Keulenaer GW. Role of neuregulin-1/ErbB signaling in cardiovascular physiology and disease: implications for therapy of heart failure. *Circulation.* 2007;116(8):954-60.
44. Parodi EM, Kuhn B. Signalling between microvascular endothelium and cardiomyocytes through neuregulin. *Cardiovasc Res.* 2014;102(2):194-204.
45. Wang Y, Wei J, Zhang P, Zhang X, Wang Y, Chen W, et al. Neuregulin-1, a potential therapeutic target for cardiac repair. *Front Pharmacol.* 2022;13:945206.
46. Fuller SJ, Sivarajah K, Sugden PH. ErbB receptors, their ligands, and the consequences of their activation and inhibition in the myocardium. *J Mol Cell Cardiol.* 2008;44(5):831-54.
47. Sanchez-Soria P, Camenisch TD. ErbB signaling in cardiac development and disease. *Semin Cell Dev Biol.* 2010;21(9):929-35.
48. Hubbard SR. Structural analysis of receptor tyrosine kinases. *Prog Biophys Mol Biol.* 1999;71(3-4):343-58.
49. Lemmon MA, Schlessinger J. Cell signaling by receptor tyrosine kinases. *Cell.* 2010;141(7):1117-34.
50. Wheeler DL, Yarden Y, SpringerLink. *Receptor Tyrosine Kinases: Family and Subfamilies.* 1st 2015. ed. Cham: Springer International Publishing : Imprint: Springer; 2015.
51. Das M, Miyakawa T, Fox CF, Pruss RM, Aharonov A, Herschman HR. Specific radiolabeling of a cell surface receptor for epidermal growth factor. *Proc Natl Acad Sci U S A.* 1977;74(7):2790-4.
52. Segers VFM, Dugaucquier L, Feyen E, Shakeri H, De Keulenaer GW. The role of ErbB4 in cancer. *Cell Oncol (Dordr).* 2020;43(3):335-52.
53. Baselga J, Swain SM. Novel anticancer targets: revisiting ERBB2 and discovering ERBB3. *Nat Rev Cancer.* 2009;9(7):463-75.
54. Bersell K, Arab S, Haring B, Kühn B. Neuregulin1/ErbB4 signaling induces cardiomyocyte proliferation and repair of heart injury. *Cell.* 2009;138(2):257-70.
55. Polizzotti BD, Ganapathy B, Walsh S, Choudhury S, Ammanamanchi N, Bennett DG, et al. Neuregulin stimulation of cardiomyocyte regeneration in mice and human myocardium reveals a therapeutic window. *Sci Transl Med.* 2015;7(281):281ra45.

56. Chang T, Liu C, Yang H, Lu K, Han Y, Zheng Y, et al. Fibrin-based cardiac patch containing neuregulin-1 for heart repair after myocardial infarction. *Colloids Surf B Biointerfaces*. 2022;220:112936.
57. Santoro F, Sahara M. A specified therapeutic window for neuregulin-1 to regenerate neonatal heart muscle. *Ann Transl Med*. 2015;3(17):249.
58. D'Uva G, Aharonov A, Lauriola M, Kain D, Yahalom-Ronen Y, Carvalho S, et al. ERBB2 triggers mammalian heart regeneration by promoting cardiomyocyte dedifferentiation and proliferation. *Nat Cell Biol*. 2015;17(5):627-38.
59. Dugaucquier L, Feyen E, Mateiu L, Bruyns TAM, De Keulenaer GW, Segers VFM. The role of endothelial autocrine NRG1/ERBB4 signaling in cardiac remodeling. *Am J Physiol Heart Circ Physiol*. 2020;319(2):H443-h55.







**CHAPTER 2**  
**Hypotheses and aims of the study**



## Hypotheses and aims of the study

Because atrial inflammation and fibrosis are important processes in the development of AF and atrial remodeling, and because activation of the ERBB4 receptor mitigates inflammation and fibrosis in several tissues including the heart, we postulate that NRG1 can have preventive and/or therapeutic effects on AF. In support of this hypothesis, circulating NRG1 levels are increased in patients with AF compared to control subjects (1). Advanced atrial fibrosis is associated with more severe forms of AF and with reduced effectiveness of antiarrhythmic drugs and ablation. In this thesis, **we hypothesize that the NRG1/ERBB4 pathway is an inhibitory pathway in the development of atrial inflammation and fibrosis, hence of AF** (Figure 8). Systemic and atrial inflammation is known to participate in the initiation and progression of atrial remodeling and is closely linked with fibrosis. Current therapies of AF are mainly focused on rate or rhythm control using antiarrhythmic drugs or ablation, which insufficiently target the underlying pathophysiology. Therefore, there is an unmet medical need for novel treatments that target atrial inflammation and fibrosis to mitigate atrial remodeling and prevent and/or treat AF.

During this thesis we will extensively test a drug candidate (JK07) as a potential new therapy for AF. In **chapter 4**, we will first validate the selectivity of JK07 on ERBB4 activation and phosphorylation compared to NRG1. Subsequently, we will assess if the effects of selective ERBB4 activation recapitulate the effects of NRG1 *in vitro*. This study will aid to validate and confirm if ERBB4 activation suffices in attenuating inflammatory and fibrotic response.

Following validation of ERBB4 activation by JK07, **chapter 5** continues with the evaluation of the effects of NRG1 and JK07 on AF and atrial remodeling, using a first *in vivo* model. This first model is a transgenic mouse model with cardiac-specific overexpression of TNF- $\alpha$ , leading to atrial inflammation and fibrosis in which we will study spontaneous AF via longitudinal telemetry monitoring.

Additionally, we will evaluate two distinct mouse models exposed to two common risk factors of AF (hypertension and obesity) in **chapter 6**. Here, we will investigate AF inducibility through programmed electrical stimulation. Following the previous observations of Vermeulen *et al.*, we

will also study the hypothesis that **ERBB4 in macrophages contributes to the anti-inflammatory and anti-fibrotic effects in atrial tissue** within this chapter. Therefore, we will use a myeloid-specific *ErbB4* knockout mouse model to study the role of ERBB4 in macrophage-mediated fibrosis during atrial remodeling.

Throughout these studies, results deviating from the original hypothesis led to the discovery of novel effects. More specifically, we found that ERBB4 activation in mice reduced AF inducibility in the absence of effects on structural remodeling. Therefore, a complementary hypothesis will be assessed in **chapter 7**. Here we will test if **ERBB4 signaling attenuates AF by directly acting on cardiomyocytes**. This hypothesis will be explored *in vitro* by testing reentry activity in hiAM monocultures during point stimulation and will be performed in collaboration with the Laboratory of Experimental Cardiology in Leiden, under supervision of Prof. Daniel Pijnappels.

Following extensive assessment of these hypotheses ERBB4 activation, upon NRG1 or JK07 administration, was tested as a potential treatment for AF. Moreover, we studied the underlying mechanisms including effects on atrial inflammation and fibrosis and effects on electrical activity of cardiomyocytes.

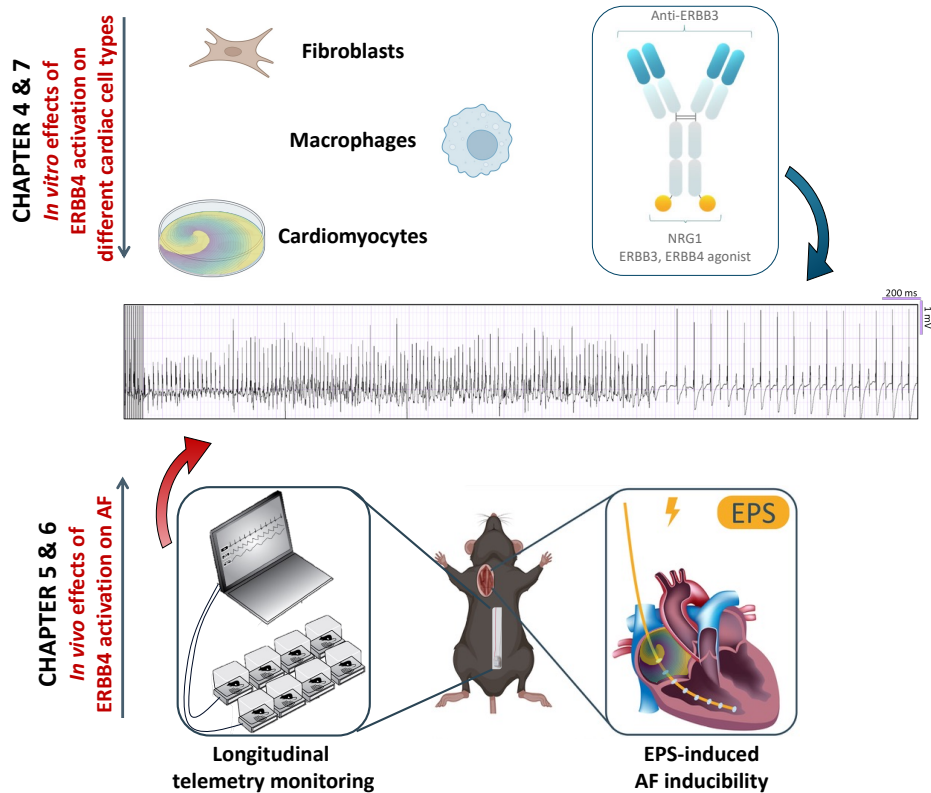
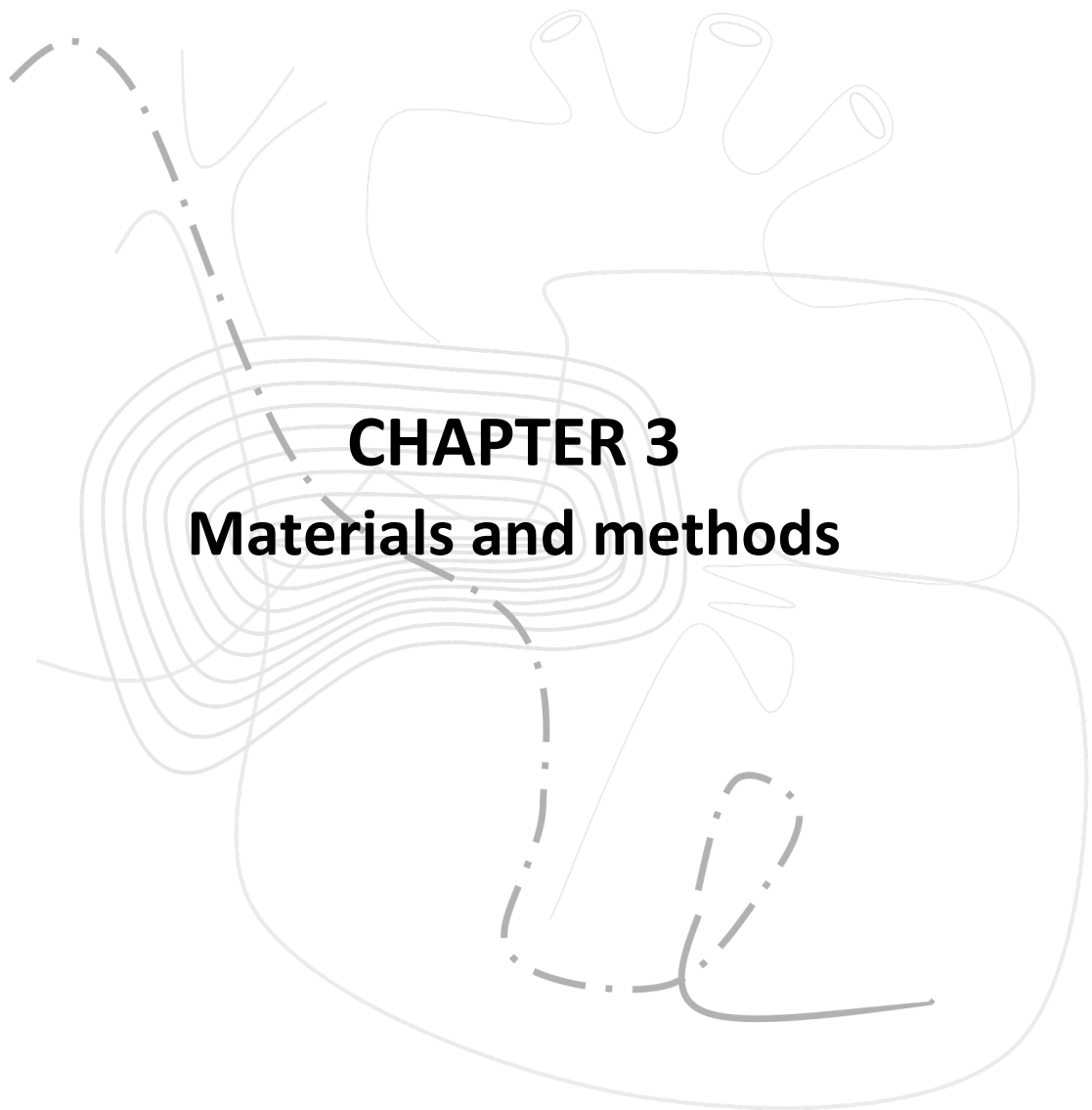


**Figure 8. Overview of aims to test if the NRG1/ERBB4 pathway is an inhibitory pathway in the development of atrial inflammation and fibrosis, and hence of AF.** NRG1 has anti-inflammatory and anti-fibrotic effects in distinct tissues, including the left ventricle. Here, we studied the effects of NRG1/ERBB4 signaling on atrial inflammation and fibrosis, *in vitro* and *in vivo*. Therefore, we used a new drug candidate JK07, a recombinant fusion protein consisting of an anti-ERBB3 immunoglobulin G1 monoclonal antibody and an active polypeptide fragment of human NRG1.

## References

1. Shao Q, Liu H, Ng CY, Xu G, Liu E, Li G, et al. Circulating serum levels of growth differentiation factor-15 and neuregulin-1 in patients with paroxysmal non-valvular atrial fibrillation. *Int J Cardiol.* 2014;172(2):e311-3.



## CHAPTER 3

### Materials and methods

#### ADAPTED FROM

**Jens Van fraeyenhove\***, Kasper Favere\*, Griet Jacobs, Matthias Bosman, Sander Eens, Johan De Sutter, Hielko Miljoen, Pieter-Jan Guns, Gilles W. De Keulenaer, Vincent F.M. Segers, Hein Heidbuchel. Cardiac electrophysiology studies in mice via the transjugular route: a comprehensive practical guide. *Am J Physiol Heart Circ Physiol* 323: H763-H773, 2022. DOI:10.1152/ajpheart.00337.2022





## Ethical approval of study design

All mouse experiments were approved by University of Antwerp Ethical Committee for Animal Testing (file number 2019-09) and were conform with the ARRIVE guidelines, with the guidelines from Directive 2010/63/EU of the European Parliament on the protection of animals used for scientific purposes, with the Belgian Royal Decree of 2013, and with the National Institutes of Health Guide for the Care and Use of Laboratory Animals. All animals were kept on a standard chow (unless otherwise specified) and water *ad libitum* at a constant temperature of 22°C and humidity of 50% in a 12 h controlled light/dark cycle.

## Treatment

Recombinant human NRG1 $\beta$  (NRG1 $\beta$ ; Peprotech) is a polypeptide (7.5 kDa) consisting of only the EGF domain of the NRG1 $\beta$  isoform (65 amino acid residues). It is currently used in different clinical trials and basic research. In our *in vivo* experiment, mice were randomized for treatment with either vehicle (PBS) or NRG1 $\beta$  (20  $\mu$ g/kg/day, I.P., 1x/day; referring to the recombinant version). This dose is based on previous studies from our lab and others. As an alternative to NRG1 $\beta$ , JK07 was used in various experiments. JK07 is a recombinant fusion protein consisting of a fully humanized anti-ERBB3 immunoglobulin G1 monoclonal antibody and an active polypeptide fragment of human NRG1 (as shown in [Chapter 4, Figure 18, p. 71](#)). JK07 was kindly gifted to us by Salubris Biotherapeutics. Due to its composition, JK07 shows a longer half-life compared with NRG1 $\beta$  (1). Mice were randomized for treatment with either vehicle or JK07 (1 mg/kg, I.V., 2x/week). Vehicle solution consists of formulation buffer (25 mM histidine/histidine-HCl, 205 mM sucrose and 0.04% Polysorbate 80) diluted with 0.9% sodium chloride solution for injection to maintain a minimum concentration of formulation buffer of 15% (v/v). Control (CTRL) mice were treated with vehicle.

## Animal models

Distinct mouse models were used to study the effects of NRG1 and JK07 on AF and atrial remodeling. More specifically, two transgenic mouse models and two wild type mouse models exposed to distinct risk factors of AF were used throughout this thesis. All mouse models will be discussed in detail in the next section.

## Tg(Myh6-Tnf)1.6Amf (TNF1.6) transgenic mice

TNF1.6 transgenic mice were obtained from Dr. McTiernan (University of Pittsburgh) and subsequently housed and bred in the central animal care facility of the University of Antwerp. TNF1.6 transgenic mice were originally created, using a transgene construct containing the MHC promoter with cDNA to murine TNF- $\alpha$  (2). TNF1.6 transgenic mice were crossbred with FVB controls to create transgenic and control littermates. Cardiomyocyte overexpression of the TNF- $\alpha$  transgene was monitored by PCR. TNF1.6 transgenic mice were used to study the effect of NRG1 and JK07 on AF and the role of the ERBB4 signaling in atrial remodeling. First, six weeks old male TNF1.6 transgenic mice and their wild type littermates were randomized for treatment with either vehicle or NRG1 (20  $\mu$ g/kg/day, I.P., 1x/day). After six weeks of treatment and four weeks of ECG monitoring, mice were euthanized and hearts were collected (Figure 9).

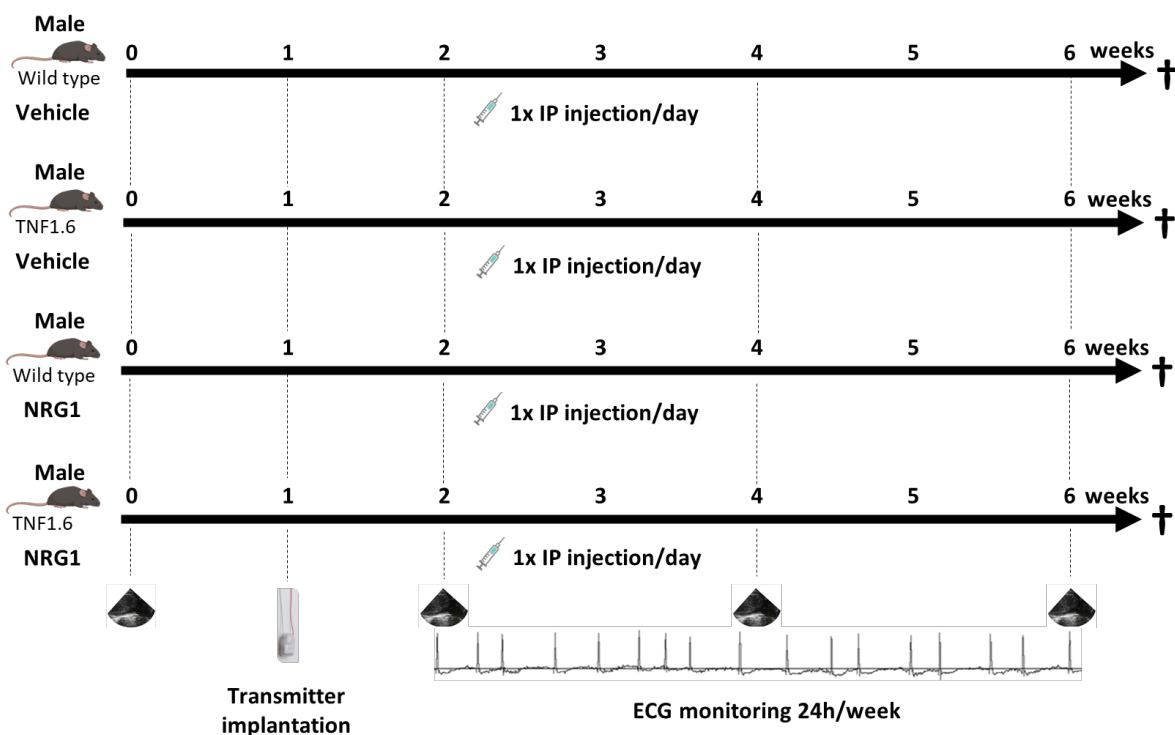


**Figure 9. Overview of time course of TNF1.6 transgenic mice to study the effect of NRG1 on AF and atrial remodeling.** Six weeks old male transgenic mice and wild type littermates were randomized for treatment with either NRG1 (20  $\mu$ g/kg/day, I.P., 1x/day) or vehicle, starting at day zero. After one week, at a weight of  $\pm$  20 g, mice were implanted with a telemetry device and ECGs were monitored following one week of recovery (week 2). Mice were subjected to a two weekly echocardiographic evaluation. After six weeks, mice were euthanized and hearts were collected.

In a second experiment, six weeks old female TNF1.6 transgenic mice and their wild type littermates were randomized for treatment with either vehicle or JK07 (1 mg/kg, I.V., 2x/week; Salubris Biotherapeutics). After five weeks of treatment and three weeks of ECG monitoring, mice were euthanized and hearts were collected (Figure 10).

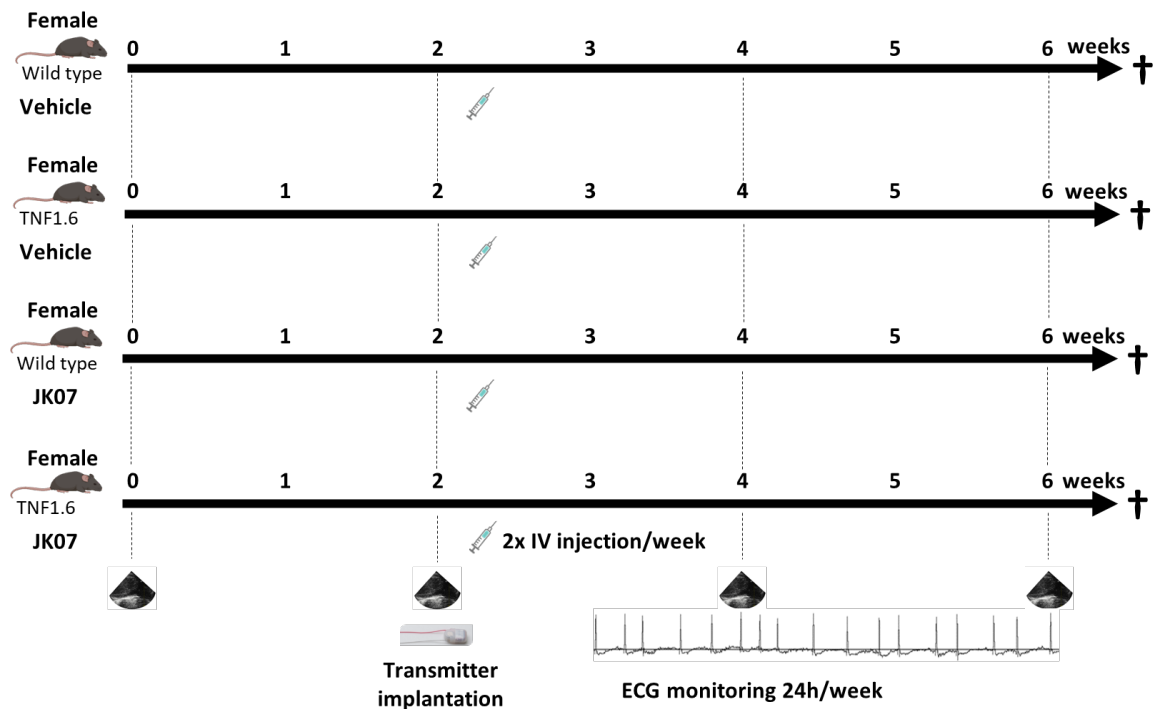


**Figure 10. Overview of time course of TNF1.6 transgenic mice to study the effect of JK07 on AF and atrial remodeling.** Six weeks old female transgenic mice and wild type littermates were randomized for treatment with either JK07 (1 mg/kg, I.V., 2x/week) or vehicle, starting at day zero. After two weeks, at a weight of  $\pm 20$  g, mice were implanted with a telemetry device and ECGs were monitored following one week of recovery (week 3). Mice were subjected to a two weekly echocardiographic follow-up and. After six weeks, mice were euthanized and hearts were collected.

### Ang II-induced hypertension mice

Male C57BL/6N mice (Charles River) at the age of eight weeks, were randomized to sham operation (CTRL) or S.C. implantation of osmotic minipumps (Alzet, model 1004) with Ang II (4.3 mg/kg/day, Abcam) for a treatment of four weeks. Mice were anesthetized with sevoflurane (3% v/v) during both sham operation or osmotic minipump implantations. Ang II-treated mice were randomized for treatment with either vehicle (Ang II group) or JK07 (1 mg/kg, I.V., 2x/week; Ang II + JK07 group). Control mice were treated with vehicle.

Following four weeks Ang II treatment or sham operation, mice were subjected to an EP study, euthanized, and hearts were collected. Two independent experiments were performed. In a first experiment, JK07 treatment was tested in a preventive strategy (Figure 11A). Whereas in a second experiment, JK07 was tested in a therapeutic strategy.

The preventive strategy started at the same day of osmotic minipump implantation (day zero), whereas the therapeutic strategy started three weeks after osmotic minipump implantation (Figure 11B).

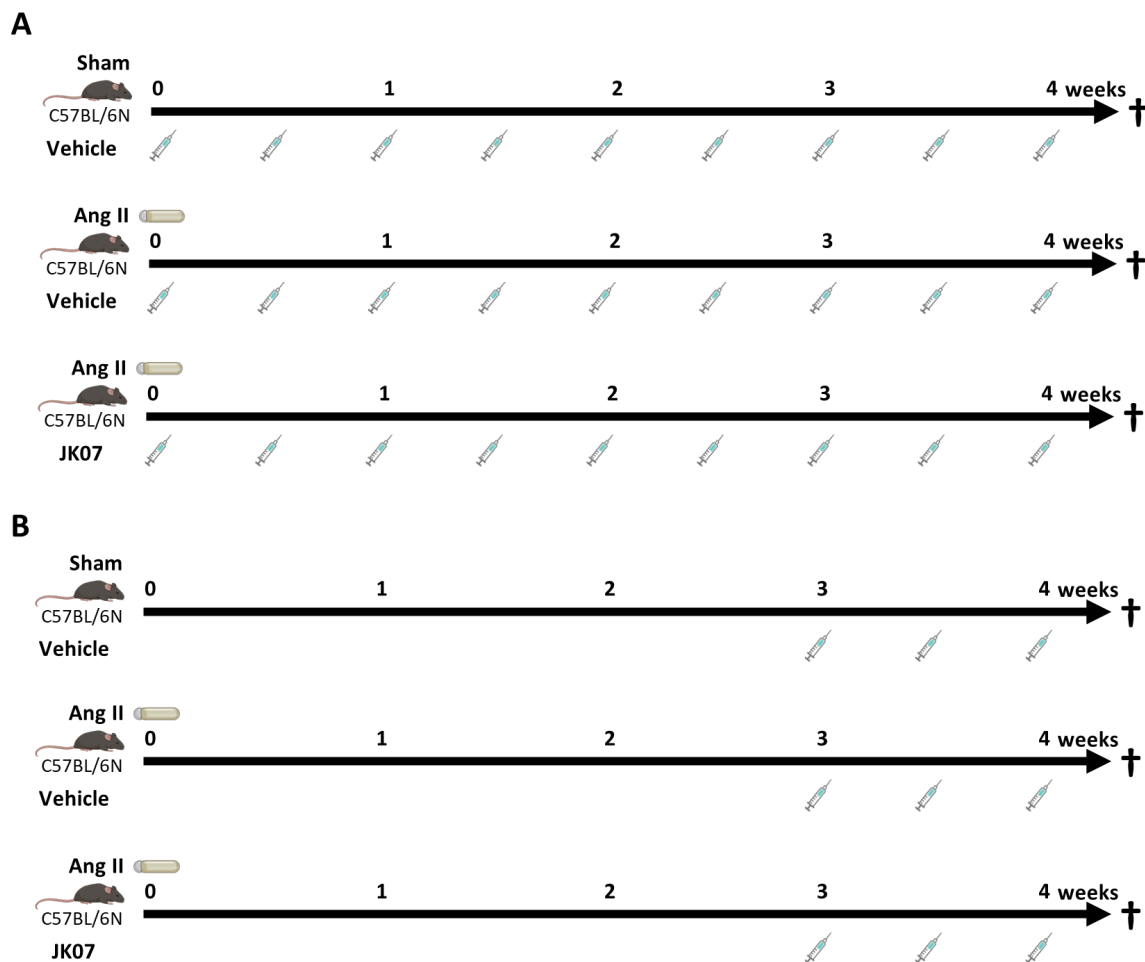


**Figure 11. Overview of time course of Ang II-induced hypertension in mice to study the effects of JK07 on PES-induced AF. (A)** JK07 was tested in a preventive treatment strategy. Mice were sham operated or implanted with osmotic minipumps with Ang II (4.3 mg/kg/day) at day zero. Sham operated mice were treated with vehicle and Ang II-treated mice were randomized for treatment with either JK07 (1 mg/kg, I.V., 2x/week) or vehicle, starting at day zero. Following four weeks of treatment, mice were subjected to an electrophysiology study after which mice were euthanized, and hearts were collected. **(B)** JK07 was tested in a therapeutic treatment strategy. Mice were sham operated or implanted with osmotic minipumps with Ang II (4.3 mg/kg/day) at day zero.

Sham operated mice were treated with vehicle and Ang II-treated mice were randomized for treatment with either JK07 (1 mg/kg, I.V., 2x/week) or vehicle, starting after three weeks of Ang II. Following one week of treatment, mice were subjected to an electrophysiology study after which mice were euthanized, and hearts were collected.

### High fat diet-induced obesity mice

Male C57BL/6N mice (Charles River) at the age of 8 weeks were randomized to be fed with either regular chow (CTRL) or a HFD containing 60% Kcal fat (D12492, Research Diets) for eight weeks. HFD mice were randomized for treatment with either vehicle (HFD group) or JK07 (1 mg/kg, I.V., 2x/week; Salubris Biotherapeutics; HFD + JK07 group). Control mice were treated with vehicle. After 8 weeks of HFD or regular chow, mice were subjected to EP study, euthanized, and hearts were collected. Treatment with JK07 or vehicle in HFD mice was tested in a preventive strategy and started at the same day of the HFD (day zero) (Figure 12).

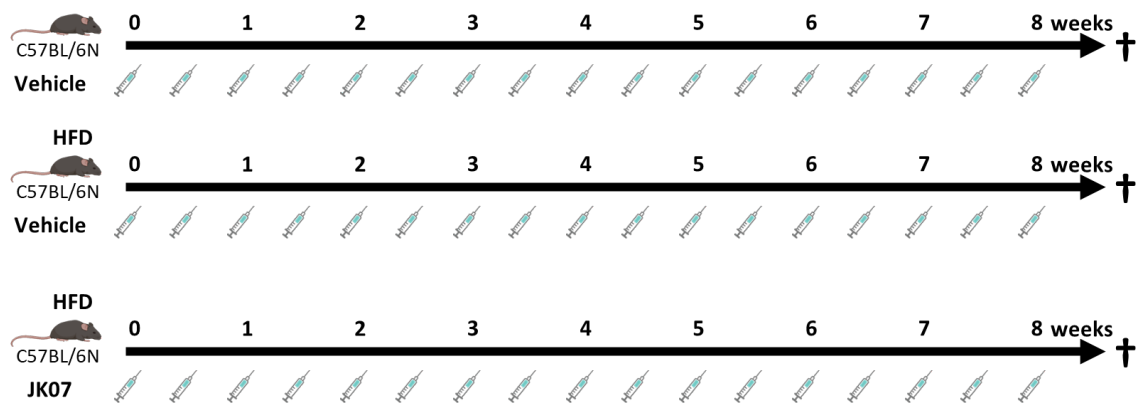


**Figure 12. Overview of time course of HFD-induced obesity mice to study the effects of JK07 on PES-induced AF.** JK07 was tested in a preventive treatment strategy. Mice were fed with regular chow or a HFD starting at day zero. Mice that received a normal diet were treated with vehicle and mice that received a HFD were randomized for treatment with either JK07 (1 mg/kg, I.V., 2x/week) or vehicle, starting at day zero. Following eight weeks of treatment, mice were subjected to an electrophysiology study after which mice were euthanized, and hearts were collected.

### Myeloid-specific *ErbB4* gene deletion

A genetically modified mouse model in which the *ErbB4* gene was deleted in myeloid cells (*ErbB4<sup>F/F</sup>LysM-Cre<sup>+/-</sup>* knockout; Mye-KO), and previously described to develop extensive

ventricular fibrosis in response to Ang II. Male Mye-KO mice and control littermates (*ErbB4<sup>F/F</sup>LysM-Cre<sup>-/-</sup>* control, Mye-CTRL) were generated as previously described (3).

Briefly, Mye-KO mice were created by crossbreeding *LysM-cre<sup>+/+</sup>* (*B6.129P2-Lyz2tm1<sup>(cre)lfo</sup>/J* mice, Jackson laboratories) mice with *C57BL/6-ErbB4<sup>F/F</sup>* mice, carrying LoxP-flanked *ErbB4* alleles (*B6;129-ErbB4tm1Fej/Mmucd*, #010439-UCD, MMRRC) (Figure 13). The *LysM-Cre* knock-in allele has a nuclear-localized Cre-recombinase inserted into the first coding ATG of the *Lyz2*, placing Cre-expression under control of the endogenous *Lyz2* promoter. When crossbred with *C57BL/6-ErbB4<sup>F/F</sup>* mice, Cre-mediated recombination results in deletion of *ErbB4* (*ErbB4<sup>F/F</sup>-LysM-Cre<sup>+/-</sup>* mice) in the myeloid cell lineage, which includes monocytes, macrophages, and granulocytes (4).

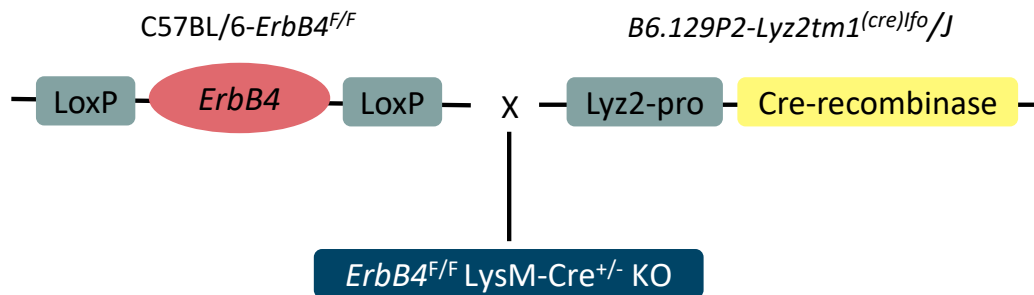


**Figure 13. Myeloid-specific *ErbB4* gene deletion.** Application of the Cre/LoxP system to create cell (myeloid) specific gene (*ErbB4*) deletion resulting in *ErbB4<sup>F/F</sup> LysM-Cre<sup>+/-</sup>* knockout mice (Mye-KO).

Eight weeks old Mye-KO mice and Mye-CTRL were randomized to sham operation or S.C. implantation of osmotic minipumps (Alzet, model 1004) with Ang II (2.9 mg/kg/day, Abcam) for a treatment of four weeks (Figure 14). In these experiments, Ang II concentration in the osmotic minipumps was lower than in previous experiments following observations of a high mortality (67% within a week) of Mye-KO with a dose of 4.3 mg/kg/day.

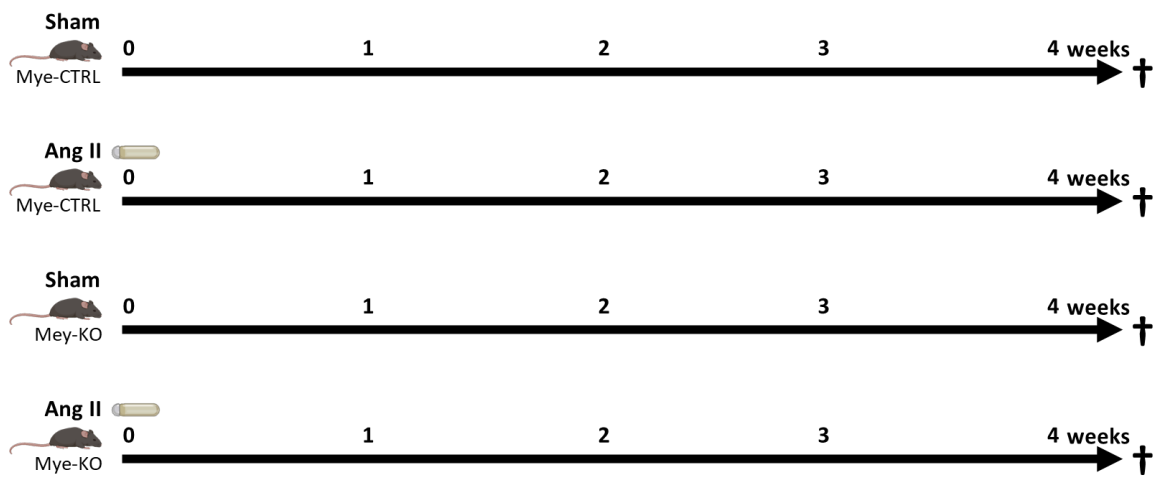


**Figure 14. Overview of time course of myeloid-specific *ErbB4* gene deletion in mice to study the importance of ERBB4 signaling in myeloid cells during atrial fibrosis.** *ErbB4<sup>F/F</sup>LysM-Cre<sup>+/-</sup>* (Mye-KO) and *ErbB4<sup>F/F</sup>LysM-Cre<sup>-/-</sup>* (Mye-CTRL) mice were sham operated or implanted with osmotic minipumps with Ang II (2.9 mg/kg/day) at day zero. Following four weeks of Ang II treatment, mice were euthanized and hearts were collected.

## **Electrophysiology testing in mice**

AF was assessed using two distinct methods. For detection and evaluation of spontaneous occurring AF, longitudinal telemetry monitoring was used. During experiments involving mice exposed to risk factors of AF, PES was used to assess AF inducibility and duration, and other EP parameters as described in detail elsewhere (5).

### **Telemetry monitoring**

To measure ECG signals in free roaming mice, transmitters (PhysioTel<sup>®</sup> transmitter, ETA-F10; DSI) were intraperitoneally implanted, as shown in Figure 15A, B. The surgical implantation of these telemetry transmitters was based on the protocol of Cesarovic *et al.* (6). Briefly, mice were induced with anesthesia of 8% (v/v) sevoflurane and O<sub>2</sub> in a ventilated gas mixture. The toe-pinch reflex was used as reference and anesthesia was maintained with 3% (v/v) sevoflurane and O<sub>2</sub> in a ventilated gas mixture. Subsequently, the surgical area (abdomen) was shaved and disinfected with alcohol. Mice were positioned on a heating pad and temperature was constantly monitored to maintain a core temperature at 37°C ± 0.5°C. Before the surgical procedure was started, the lead wires from the transmitter were adjusted to a length appropriate for the mice. Next, a small incision was made in the skin and peritoneum from the lower thorax along the midline to the abdomen. A transmitter was then positioned in the intraperitoneal cavity and sutured in the peritoneum. The ECG leads were S.C. positioned in a lead II configuration. The negative lead was tunneled towards the right pectoral muscle and the positive lead was positioned 1 cm left from the xyphoid. Following implantation, mice received S.C. injection of analgesic (0.05 mg/kg buprenorphine) and were left for observation and recovery under a heating lamp. Spontaneous AF incidence was then assessed in telemetry-implanted mice by recording their ECGs through a receiver device using Ponemah Physiology platform (version 5.41; DSI) and Labchart8 (ADInstruments) (Figure 15C). All recordings were performed in a noise isolated cabinet with 12 h controlled night/day cycle to limit environmental impact on cardiac rhythm.



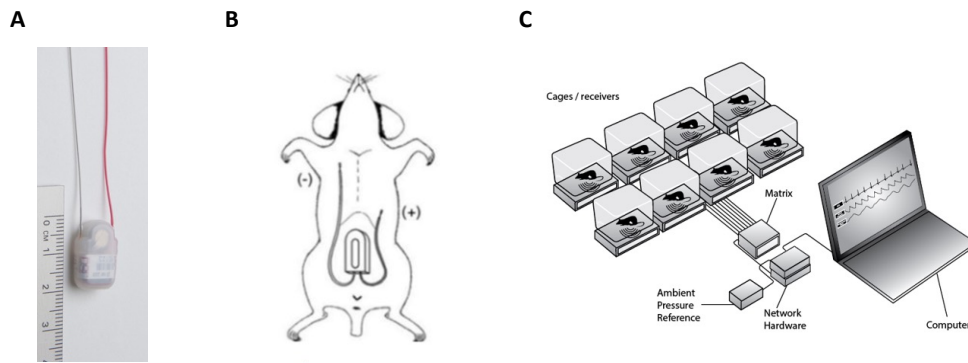


**Figure 15. Electrophysiology assessment via telemetry monitoring. (A)** Representative image of the implantable telemetry device. **(B)** Schematic overview of implanted telemetry device (intraperitoneal) and subcutaneous configuration of positive and negative lead positioning in mice (lead II). **(C)** Schematic overview of ECG recording in free roaming mice.

### ECG analysis

Longitudinal recordings of 24 hours ECG data were analyzed with the Ponemah Physiology platform. Assessment of spontaneous AF episodes was done by specific and custom searches on the recorded ECG data. Custom searches were used to automatically detect possible AF episodes in the recorded ECG data. Subsequently, these possible AF episodes were individually assessed and considered as AF when at least 5 consecutive beats showed an irregularly irregular pattern.

### Programmed electrical stimulation

In some studies, PES was used to evaluate AF inducibility and sustainability. An octapolar catheter (ERP-800, Millar) was positioned, through the jugular vein, in the right atrium and ventricle as described elsewhere (5). Briefly, mice were anesthetized with an intraperitoneal injection of Avertin® (2,2,2-tribromoethanol; 250 mg/kg; Merck). Body temperature was monitored with a rectal temperature probe and kept at  $37^{\circ}\text{C} \pm 0.5^{\circ}\text{C}$  with a heating lamp. Heart rate was monitored using a surface ECG (Lead II). A 0.5 mm transversal opening was made in the jugular vein to insert a 1.1 French octapolar catheter. The catheter was advanced until the electrodes were correctly positioned throughout the right atrium and ventricle, as shown in Figure 16. Next, electrophysiology parameters were assessed using PES (STG3008-FA, Multi Channel Systems). Atrial capture threshold was determined by delivering stimulation trains of rectangular current pulses (8 pulses with a shorter CL than normal sinus rhythm) with decremental intensity until

capture was lost. The lowest stimulation intensity with 1:1 capture was considered to be the capture threshold. AERP was obtained by delivering drive trains of minimal 8 (S1) stimuli at a CL within the 1:1 capture range, followed by delivery of a single extra stimulus (S2). The interval between the S1 train and S2 stimulus was progressively shortened until the S2 stimulus failed to capture. Subsequently the AERP was defined as the longest S1–S2 interval without S2 capturing the tissue. Finally, AF inducibility was tested by applying 5 identical stimulation series of burst stimulation during which the CL decreased in steps of 2 ms from (40–8 ms). Since there are no strict guidelines in literature, the threshold for AF inducibility was set at an episode of  $\geq 1$  s. AF inducibility was then defined as the percentage of inducible stimulation series out of the total number of attempts per group. Moreover, AF inducibility was quantified per stimulation series and presented in waterfall plots. Total AF duration was determined by calculating the sum of all PES-induced AF episodes over 5 consecutive stimulation series. Additionally, single episode AF duration was quantified and categorized per animal in waterfall plots. AF episodes  $< 3$  s were defined as short, while AF episodes  $\geq 3$  s were considered long.

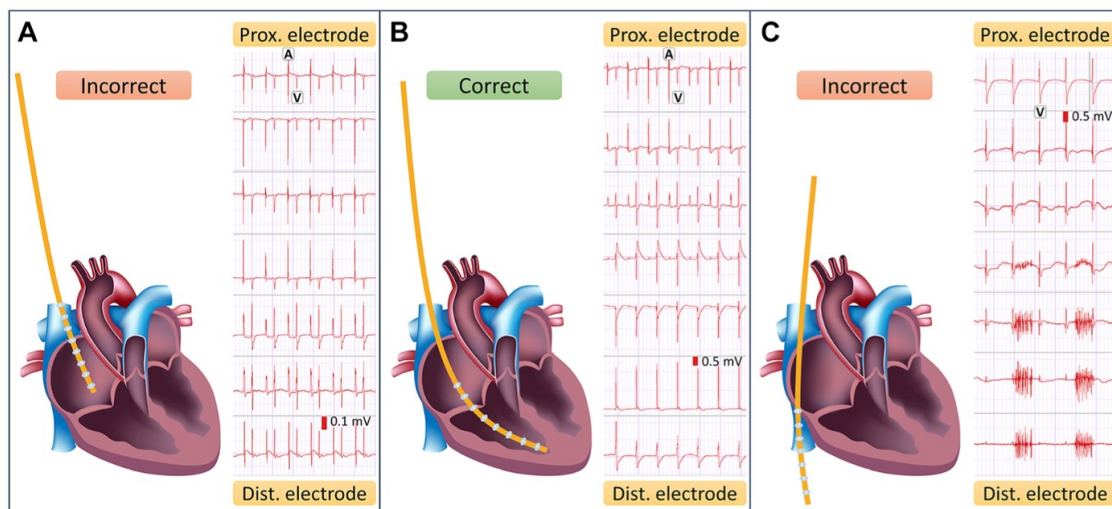


**Figure 16. Endocardial electrogram morphology according to catheter position.** Adapted from J. Van fraeyenhove *et al. AJP Heart Circ. Physiol.*, 2022 (5). Endocardial tracings go from proximal (top) to distal (bottom). **(A)** Atrial position of the catheter as evidenced by prominent atrial electrical activity in all channels. Correct positioning requires advancement of the catheter into the right ventricle. **(B)** Correct catheter position with solely ventricular signal in the most distal electrodes and predominant atrial activity in the proximal electrodes. **(C)** Catheter positioned into the inferior vena cava with diaphragmatic contraction artifacts in the distal electrodes. A indicates atrial signal; V, ventricular signal.

## **Cardiac measurements**

### **Echocardiographic measurements**

Transthoracic echocardiography (Vevo 2100 Imaging System, equipped with a MS55D probe, Visualsonics) was performed on anesthetized mice (1.5—2% v/v isoflurane, Forene<sup>®</sup>, Abbvie). The imaging area was shaved and washed. Mice were placed on a heating pad in a slight left lateral position conform with the plate electrodes to record an ECG tracing and heartrate. A 2D long-axis view of the LA was obtained in B-mode to measure the LA diameter.

### **Blood pressure measurements**

Systolic and diastolic blood pressure were recorded at the end of four weeks of Ang II minipump implantation, via the tail-cuff method as previously described (7). Briefly, mice were restrained in a plexiglas cage and positioned in a heating (37° C) chamber. A pneumatic pulse sensor was attached to the tail distal to an occluding cuff controlled by a programmed electro-sphygmomanometer (Narco Bio-systems, Austin, TX). The voltage output from the cuff and the pulse sensor were recorded and analyzed by a PowerLab signal transduction unit and associated LabChart software (ADInstruments, Colorado Springs, CO). At least three to five recordings were used and averaged from each animal to measure the systolic and diastolic blood pressure.

## **Ex vivo studies on atrial tissue samples**

### **Fibrosis assay**

To assess the anti-fibrotic effects of JK07 on atrial tissues, atrial samples were harvested from 10 weeks old male Wistar Han rats, cut into 1—2 mm<sup>2</sup> pieces and kept in 1% FBS enriched DMEM, in the presence or absence of JK07 (3.3 x 10<sup>-4</sup> mg/mL). Culture medium was daily refreshed. After 1-7 days, RNA was extracted using Nucleospin RNA XS (Machery Nagel). RT-qPCR was performed and mRNA levels of collagen type I (*Col1a1*) and collagen type III (*Col3a1*) were quantified. Data were normalized against housekeeping genes *Actb* and *Gapdh*. Expression levels were calculated using the comparative cycle method and expressed as fold change to appropriate control. The following TaqMan primers were used: (Thermofisher Scientific): *Gapdh* (Hs02758991\_g1), *Actb* (Mm02619580\_g1), *Col1a1* (Hs00164004\_m1), *Col3a1* (Hs00943809\_m1).

## **Histology**

Mice were sacrificed following longitudinal telemetry monitoring, electrophysiology studies or four weeks after osmotic minipump implantation and left and right atrial and ventricular tissue separated. To assess fibrosis and macrophage infiltration on histological level, cardiac tissue samples were first fixed in 4% buffered formalin and transferred to 60% isopropanol after 24 h until paraffin embedding. Embedded tissues were then cut into sections of 5  $\mu\text{m}$  thickness and dried overnight at 37°C. Subsequently slides were deparaffinized, rehydrated, treated with 3%  $\text{H}_2\text{O}_2$  to quench peroxidase activity, and blocked with BSA. Next, cardiac tissue samples were stained with Masson's trichrome according to the manufacturer's guidelines. To study macrophage infiltration, specific sections were stained with antibodies directed against MAC-3 (macrophage infiltration, PharMingen). Histological images were captured on light microscope and additional software (Olympus SC50, Olympus Stream Motion Software). Cardiac tissue fibrosis was quantified in a blinded fashion using ImageJ 1.53t software as a ratio of positively stained fibrotic area (blue) to total cardiac area (red). Macrophage infiltration was quantified as a ratio of positively stained MAC-3 area (red) to total cardiac area.

## **Cell culture**

### **U2OS**

PathHunter® U2OS ERBB2/3 dimerization cells (93-0535C3, Eurofins) and PathHunter® U2OS ERBB4/4 dimerization cells (93-0961C3, Eurofins) were cultured according to the manufacturer's guidelines. Briefly, cells were thawed and cultured in thawing reagent T3 (92-4103TR, Eurofins), including the first propagation. Afterwards cells were cultured using Cell culture reagent 103 (92-3103G, Eurofins) supplemented with 250  $\mu\text{g}/\text{mL}$  hygromycin B and 500  $\mu\text{g}/\text{mL}$  G418 (Eurofins) and were maintained at 37°C in humidified atmosphere of 5%  $\text{CO}_2$  in air. PathHunter® U2OS dimerization cells have been engineered to co-express one receptor subunit fused to an enzyme donor, and a second dimer partner fused to an enzyme acceptor (Figure 17). The cytoplasmic tail has been deleted from both receptors. Binding of a ligand to one receptor subunit induces it to interact with its dimer partner, forcing complementation of the two enzyme fragments. This results in the formation of a functional enzyme ( $\beta$ -galactosidase) that hydrolyzes a substrate to generate a chemiluminescent signal.

In this way, the PathHunter® dimerization assay detects ligand-induced dimerization of two subunits of a receptor-dimer pair. This assay was used to test the potency and efficacy of NRG1- and JK07-induced receptor dimerization.

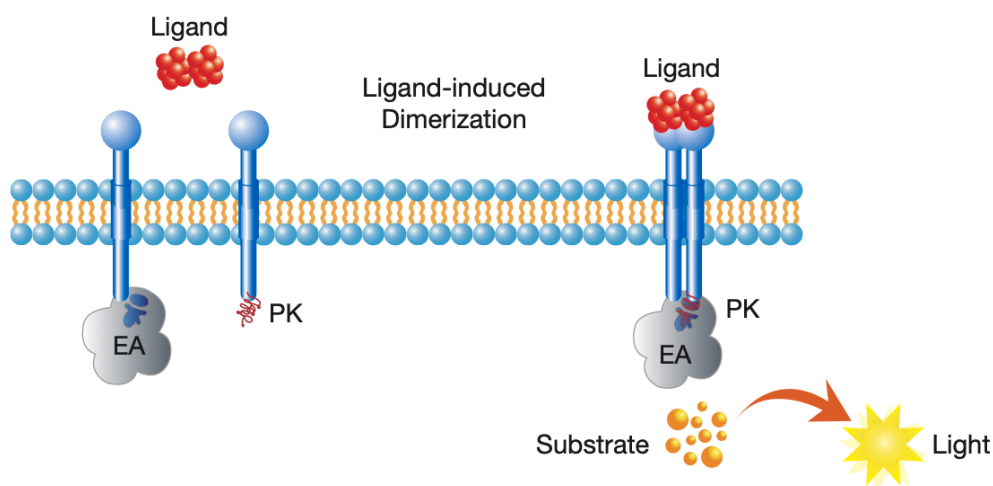


**Figure 17. PathHunter dimerization assay principle for detecting ligand-induced dimerization.** Schematic overview of the dimerization assay, based on an enzyme fragment complementation technology.  $\beta$ -galactosidase enzyme is split into two fragments, PK and EA. Independently these fragments have no  $\beta$ -galactosidase activity. Upon ligand binding, the two fragments are forced to complement through protein-protein interactions and form an active  $\beta$ -galactosidase enzyme. This functional enzyme then hydrolyzes a substrate and generates a chemiluminescent signal. PK indicates ProLink; EA, Enzyme acceptor.

## Macrophages

Murine macrophage cell line (J774A.1) was cultured according to the manufacturer's (ATCC®) guidelines. Briefly, cells were thawed and cultured in DMEM enriched with 10% heat-inactivated FBS (ThermoFisher Scientific, 10082147), penicillin/streptomycin (100 units/mL and 100  $\mu$ g/mL, ThermoFisher Scientific) and maintained at 37°C and 5% CO<sub>2</sub> in air. Two hours in advance and during experimental conditions, culture medium was changed to DMEM enriched with lower serum concentration (0.1% FBS) for basal restoration. To assess cytokine synthesis, macrophages were classically activated with LPS (100 ng/mL, PeproTech) for eight hours in the presence or absence of JK07 (3.3 x 10<sup>-4</sup> mg/mL). After stimulation, cells were collected for further analysis. mRNA levels of different inflammatory markers were determined.

### **Rat conditionally immortalized atrial myocytes**

iAMs were cultured in iAM proliferation medium (advanced DMEM/F-12, ThermoFisher Scientific, 12634010), 2% (v/v) FBS (ThermoFisher Scientific, 10082147), 1% (v/v) penicillin/streptomycin (10,000 units and 10,000 µg/mL, ThermoFisher Scientific, 15140148), 1X GlutaMAX (ThermoFisher Scientific, 35050061) and doxycycline 100 ng/mL (Tocris, 4090), and maintained at 37°C in humidified atmosphere of 5% CO<sub>2</sub> in air. For differentiation, iAMs were maintained in wells coated with 0.1 mg/mL fibronectin (R&D systems, 1030-FN-05M) and proliferation medium was changed to differentiation medium, consisting of advanced DMEM/F-12 medium supplemented with 2% (v/v) FBS and 1X GlutaMAX. After 12 days, cells were fully differentiated.

### **Human conditionally immortalized atrial myocytes**

hiAMs with preserved cardiomyogenic differentiation capacity were cultured in uncoated TC-treated CELLSTAR flasks (Greiner Bio-One, 6901755, 658175, 660175) in hiAM proliferation medium (advanced DMEM/F-12, ThermoFisher Scientific, 12634), 2 mM GlutaMAX (ThermoFisher Scientific, 35050061), 2% (v/v) FBS (Biowest, S1810), 100 U/mL penicillin and 100 µg/mL streptomycin supplemented with 100 ng/mL doxycycline hyclate (Sigma-Aldrich, D9891) (8). For differentiation, hiAMs were cultured in fibronectin-coated culture plates and proliferation medium was changed to differentiation medium, consisting of advanced DMEM/F-12, 2 mM GlutaMAX, and 2% (v/v) FBS. Starting at day 4 of differentiation, hiAM differentiation medium was supplemented with 20 ng/mL T3 hormone (Sigma-Aldrich, T6397), 400 ng/mL dexamethasone (Centrafarm, 55091), 8 µM LF3 (Selleck Chemicals, S8474) or 10 µM ICRT14 (Sigma-Aldrich, SML0203) and 10 µM phenylephrine (Sigma-Aldrich, P6126). After 12 days, cells were fully differentiated, and CV and APD reached their plateau values.

### **Optical voltage mapping**

Optical voltage mapping was performed on differentiated hiAMs (day 12-15). Action potential properties and their propagation of hiAM monolayers were assessed after a 24-h treatment with JK07 ( $3.3 \times 10^{-4}$  mg/mL, 24 h) or vehicle iAM. hiAMs were seeded in fibronectin coated 6-well culture plates at a density of  $4 \times 10^5$  cells/cm<sup>2</sup> and differentiated as described. hiAM monolayers were incubated with 8 µM of the voltage sensitive dye di-4-ANEPPS (ThermoFisher Scientific, D1119) in DMEM/F-12 (ThermoFisher Scientific, 11039) for 10 min. in a humidified 95% air and

5% CO<sub>2</sub> incubator at 37°C. di-4-ANEPPS is a fast-response voltage sensitive dye that changes its fluorescence properties in response to electrical potential changes in its environment, such as myocardial depolarization. di-4-ANEPPS displays a potential-dependent shift in excitation spectrum, and therefore allows quantification of membrane potential using excitation ratio measurements (9). Next, medium was changed to fresh DMEM/F-12 and cells were placed on a heating plate (37°C) for the completion of the experiment. During optical voltage mapping, excitation light (525 ± 25 nm) was delivered by a halogen arc-lamp through epi-illumination. Emission light passed through a dichroic mirror and a long-pass emission filter (>590 nm). Signals were acquired using a 100 × 100 pixels complementary metal oxide semiconductor camera (MiCAM05-Ultima, SciMedia) at a spatial resolution of 250 μm per pixel, and a temporal resolution of 6 ms per frame. Total acquisition lasted from 6 s up to 15 min. and during signal recording the cells were kept at 37°C. Data were analyzed using BrainVision Analyzer (v16.04.20, BrainVision). Signals were averaged with those of the 8 nearest neighboring pixels (spatial filter) and interpolated in space and time (cubic filter) to minimize noise artifacts. Mean APD<sub>80</sub> was calculated from ten distinct measurement points and CV was determined at three different vectors equally distributed throughout the culture. Electrical point stimulation during optical voltage mapping was performed using an epoxy-coated bipolar platinum electrode, delivering 8 V, 10 ms square pulses. The electrode was connected to an STG2004 stimulus generator (Multi Channel Systems) driven by MC Stimulus II software (v3.5.0, Multi Channel Systems). Baseline AP properties and propagation were calculated during 1 Hz electrical pacing (1000 ms CL). Restitution was calculated by pacing five times at a CL of 1000 ms (S1), followed by four additional stimuli (S2) at a decreasing CL. Reentry inducibility was evaluated after every S2 stimulus until 1:1 capture was lost. Reentry inducibility was defined as the percentage of hiAM monolayers per group in which reentry was induced after S2 stimulation (all stimulations per hiAM monolayer were performed in duplicates).

## **Real time-quantitative polymerase chain reaction (RT-qPCR)**

### **mRNA isolation and cDNA synthesis**

Prior to RT-qPCR, total mRNA was extracted using Nucleospin RNA XS (Machery-Nagel) according to the manufacturer's instructions. Frozen tissues were homogenized in lysis buffer containing β-

mercaptoethanol, to release mRNA and inactivate RNAses, by using a precellys<sup>®</sup> 24 (Bertin instruments) homogenizer and ceramic mix beads. Samples were stored at -20°C until further use. For cDNA synthesis, purified total RNA was added to a solution containing buffer with random hexamers and reverse transcriptase enzyme (TaqMan reverse transcription reagents, Applied Biosystems) and settings were: 10 min. at 25 °C, 30 min. at 48 °C, 5 min. at 95 °C. After PCR, cDNA samples were stored at -20°C until further use.

### **RT-qPCR**

QuantStudio 3 Real-time PCR system (Applied Biosystems) was used to perform RT-qPCR. For the reaction, Taqman Universal PCR Master Mix (Applied Biosystems) and Taqman primers were used according to the manufacturer's instructions. Settings were as follows: 2 min. at 95°C followed by 10 min. at 95°C, 40 cycles of denaturation at 95°C for 15 sec. and 1 min. at 60°C. Reactions were run two or three times in independent experiments, and data were normalized against two housekeeping genes: *Gapdh* and *Actb*. Relative expression levels of mRNA were calculated using the comparative cycle method and expressed as FC mRNA relative to control (background) values. The following TaqMan primers were used (ThermoFisher Scientific): *Gapdh* (Mm99999915\_g1), *Actb* (Mm02619580\_g1), *Collagen type 1 alpha 1 (Col1a1)* (Mm00801666\_g1), *Collagen type 3 alpha 1 (Col3a1)* (Mm01254476\_m1), *ErbB4* (Hs00955525\_m1), interleukin 6 (*Il-6*, Mm00446190\_m1), interleukin 1 $\beta$  (*Il-1 $\beta$* , Mm00434228\_m1), *TNF- $\alpha$*  (Mm00443258\_m1), and inducible nitric oxide (*iNOS*, Mm00440502\_m1).

### **RNA-sequencing**

Prior to RNA-sequencing, total mRNA was isolated (RNeasy Plus mini kit, Qiagen) from iAMs treated with or without NRG1 (0,1  $\mu$ M, 16 h), as previously described. Cultured cells were homogenized in lysis buffer, to release mRNA and inactivate RNAses. Subsequently, total RNA was purified according to the manufacturer's protocol. Total RNA was eluted in nuclease-free water and ready to use for RNA-sequencing. RNA purity, concentration, and quality was measured with Nanodrop ND-1000 spectrophotometer (ThermoFisher Scientific). Samples were stored at -80° C until further use. RNA sequencing and bioinformatics analysis was outsourced.



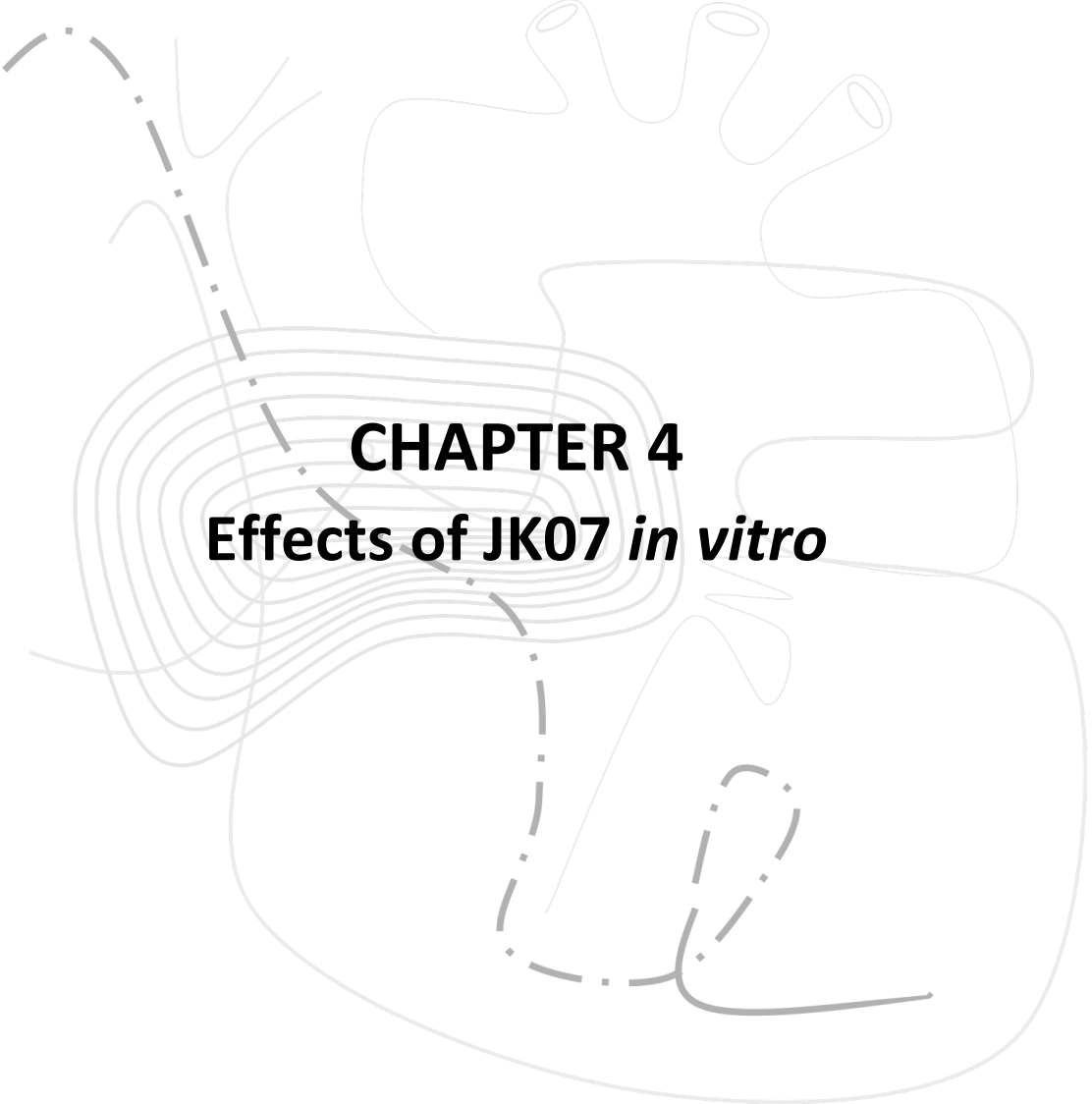
Briefly, quality and adapter trimming of the sequencing was performed prior to mapping to remove low-quality reads and adapter contaminations using FastQC (0.11.8-Java-1.8.0\_162). The reads were aligned to the rat reference genome (*Rattus\_norvegicus\_NCBI\_Rnor6*) using STAR (2.7.3a-GCCcore-6.4.0). Gene expression levels were quantified using Salmon (1.0.0-foss-2018a-Python-2.7.14). Subsequently, edgeR was used to assess whether there are statistically significant DEGs between two groups using a negative binomial model. The resulting data table assigns P-values, adjusted-P-values (calculated using the Benjamini-Hochberg false discovery rate [FDR] method to adjust for multiple hypothesis testing), and  $\log_2$  fold changes for each gene.

### **Statistical analysis**

Data are expressed as mean  $\pm$  SEM. Statistical parameters including descriptive statistics (mean and standard error of the mean), significance (p) and the number of samples (n) are reported in the text and figures. Normal distribution was tested using D' Agostino and Pearson normality test . Groups were compared using either Student's independent samples t-test or analysis of the variance (ANOVA) followed by Tukey, Bonferroni, or Tamhane's. Crosstabulation (chi-squared ( $\chi^2$ ) or Fisher exact test) was used to examine the relationship between categorical variables. All analyses were performed using SPSS software (version 28.0.1.1) or GraphPad Prism (version 9.5.1). Graphs were made using GraphPad Prism (version 9.5.1).

## References

1. John Li SL, Dixiang LUO, Yiran WU, Ming Zhou, Yang Wang, Xiaolei Zhuang, Liang Hua, Pengyi LUO inventor Human neuregulin-1 (nrg-1) recombinant fusion protein compositions and methods of use thereof. United States patent US2020/0010522 A1. 2020 9 January.
2. Saba S, Janczewski AM, Baker LC, Shusterman V, Gursoy EC, Feldman AM, et al. Atrial contractile dysfunction, fibrosis, and arrhythmias in a mouse model of cardiomyopathy secondary to cardiac-specific overexpression of tumor necrosis factor- $\alpha$ . *Am J Physiol Heart Circ Physiol*. 2005;289(4):H1456-67.
3. Vermeulen Z, Hervent AS, Dugaucquier L, Vandekerckhove L, Rombouts M, Beyens M, et al. Inhibitory actions of the NRG-1/ErbB4 pathway in macrophages during tissue fibrosis in the heart, skin, and lung. *Am J Physiol Heart Circ Physiol*. 2017;313(5):H934-h45.
4. Shi J, Hua L, Harmer D, Li P, Ren G. Cre Driver Mice Targeting Macrophages. *Methods Mol Biol*. 2018;1784:263-75.
5. Favere K, Van Fraeyenhove J, Jacobs G, Bosman M, Eens S, De Sutter J, et al. Cardiac electrophysiology studies in mice via the transjugular route: a comprehensive practical guide. *Am J Physiol Heart Circ Physiol*. 2022;323(4):H763-h73.
6. Cesarovic N, Jirkof P, Rettich A, Arras M. Implantation of radiotelemetry transmitters yielding data on ECG, heart rate, core body temperature and activity in free-moving laboratory mice. *J Vis Exp*. 2011(57).
7. Fransen P, Van Hove CE, Leloup AJA, Schrijvers DM, De Meyer GRY, De Keulenaer GW. Effect of angiotensin II-induced arterial hypertension on the voltage-dependent contractions of mouse arteries. *Pflügers Archiv - European Journal of Physiology*. 2016;468(2):257-67.
8. Harlaar N, Dekker SO, Zhang J, Snabel RR, Veldkamp MW, Verkerk AO, et al. Conditional immortalization of human atrial myocytes for the generation of in vitro models of atrial fibrillation. *Nat Biomed Eng*. 2022;6(4):389-402.
9. Knisley SB, Justice RK, Kong W, Johnson PL. Ratiometry of transmembrane voltage-sensitive fluorescent dye emission in hearts. *American Journal of Physiology-Heart and Circulatory Physiology*. 2000;279(3):H1421-H33.



**CHAPTER 4**  
**Effects of JK07 *in vitro***



## Introduction

NRG1 is important in embryonic development and in the (patho)physiology of several diseases, and may become an interesting therapeutic. However, a possible disadvantage is that NRG1 binds to both ERBB3 and ERBB4 receptors distributed over many organs, which increases the likelihood of off-target effects. Indeed, whereas ERBB4 activation has been linked to regeneration, anti-inflammatory and anti-fibrotic effects, ERBB3 activation is linked to carcinogenicity and disruption of gastrointestinal epithelial integrity, leading to gastrointestinal toxicity. The effects related to ERBB3 activation therefore may decrease the therapeutic potential of NRG1. Another shortcoming in using NRG1 as a therapeutic is its low stability with a half-life of only 10 min. (1). To overcome these hurdles, agonists specific to ERBB4 may be preferred, but the important next question is then whether selective ERBB4 activation (i.e. effects of NRG1 without ERBB3 activation) is sufficient to reproduce the therapeutic effects of NRG1. In support of a positive answer to this question, *NRG1* mRNA expression clusters more with *ERBB4* mRNA expression than with *ERBB2* and *ERBB3* expression in most tissues, including the heart. Also, ERBB4 is the most abundant ERBB receptor in the heart (in both cardiomyocytes and non-cardiomyocytes) (2). Moreover, selective overexpression of *ErbB4* in murine cardiomyocytes leads to more and smaller cardiomyocytes, equivalent to NRG1 treatment (2, 3). Additionally, a study by Schumacher *et al.* underscored the benefit of selective ERBB4 activation during inflammation. They observed that LPS-activated macrophages showed increased *ErbB4* expression *in vitro* and that LPS-activated macrophages treated with NRG4, which specifically binds to ERBB4, induced apoptosis of pro-inflammatory (M1) macrophages. Anti-inflammatory effects of NRG4 were also shown in a mouse model of colitis, where exogenous NRG4 administration reduced colonic macrophage infiltration and inflammation during colitis (4). Another argument for selective ERBB4 activation comes from observations in our lab. Vermeulen *et al.* (5) showed that the anti-inflammatory and anti-fibrotic effects of NRG1 in the heart are critically dependent on ERBB4-mediated inhibitory effects on macrophages. NRG1 suppressed the upregulation of inflammatory genes in LPS-activated cultured macrophages, which was linked to an increase in ERBB4, but not ERBB3, phosphorylation (5). Mice with a myeloid-specific *ErbB4* deletion showed an aggravated inflammatory and fibrotic response to Ang II treatment.

A final study supporting the specific role of ERBB4 has been published by Jay *et al.* (6), showing that bivalent engineered NRG1, which obligatorily signals through ERBB4 homodimers, fully reproduces NRG1's cardioprotective effects in a model of doxorubicin-induced cardiomyopathy. Accordingly, based on these studies one may hypothesize that most therapeutic effects of NRG1 are mediated by ERBB4.

In this thesis, we aimed to evaluate the potential of NRG1 as a treatment for AF. To bypass some of the drawbacks of NRG1 protein as a therapeutic agent, we collaborated with Salubris Biotherapeutics, a company that develops novel antibody and protein-based therapeutics. JK07 is one of their lead compounds, currently being tested in two phase I clinical trials (NCT04210375 and NCT05322616) in which a single-ascending dose study is being used to assess safety, tolerability, ... in HFrEF subjects ( $EF \leq 40\%$ ) aged 18-80 years old. JK07 is a recombinant fusion protein comprising a polypeptide fragment of human NRG1 fused to a fully humanized anti-ERBB3 immunoglobulin G1 mAb backbone, as shown in Figure 18A (7). The NRG1 fragment is fused to the C-terminus of the antibody heavy chain via a linker (via the first amino acid (Ser) on the N terminus) and the mAb contains a portion that is monospecific for ERBB3, which blocks the formation of ERBB3 dimers, hence inhibiting NRG1 signaling through ERBB3, and resulting in a more selective ERBB4 activation (Figure 18B, C). Consistent with the reasoning explained earlier in this chapter, the inventors of the compound postulate that JK07-induced ERBB4 signaling will suffice to recapitulate the therapeutic effects of NRG1.

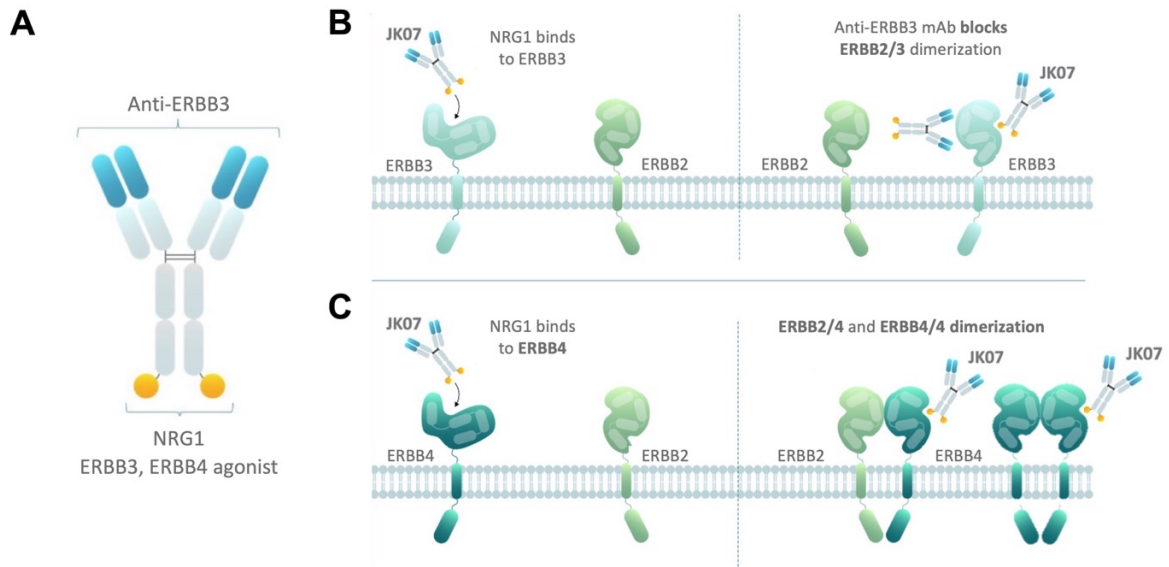


**Figure 18: Schematic representation of JK07 and receptor dimerization. (A)** JK07 is a recombinant fusion protein comprising a NRG1 fragment and a mAb specific for ERBB3. **(B)** JK07 reduces ERBB3 signaling by specifically blocking ERBB3 dimerization with its mAb against ERBB3. **(C)** JK07 induces selective ERBB4 activation without or with less ERBB3 activation, while simultaneously providing a higher stability and longer half-life compared with recombinant NRG1 protein.

The NRG1 polypeptide fragment used in JK07 originates from the human NRG1- $\beta$ 2 isoform, containing the EGF-like domain and the receptor binding domain resulting in similar binding activity as the full length NRG1 protein. Dosage, administration route and frequency were based on previously performed rodent experiments by Salubris Biotherapeutics. To test the *in vivo* efficacy, they tested JK07 treatment in a rat model of systolic heart failure. Using a twice-weekly I.V. administration of 1 mg/kg during four weeks, they observed no loss of bodyweight (which was noticed with higher dosages (3 and 10 mg/kg), a significant increase in left ventricular ejection fraction (+14.7%,  $p < 0.001$ ), and signs of a healing myocardial infarction zone (7). In this chapter, prior to initiating our studies with JK07 on AF, we aimed at validating the effects of JK07 on ERBB4 activation and signaling *in vitro*. We also tested whether JK07 induced *in vitro* anti-inflammatory and anti-fibrotic effects as previously observed with NRG1.

## Materials and methods

Materials and methods are described in chapter 3.

## Results

### JK07 preferentially induces ERBB4/4 homodimerization over ERBB2/3 heterodimerization.

We first tested the effects of JK07 and NRG1 on ERBB2/3 and ERBB4/4 dimerization assays. As shown in Figure 19A, NRG1 induced both ERBB2/3 and ERBB4/4 dimerization with a comparable potency ( $EC_{50}(\text{ERBB2/3}) 1.2 \times 10^{-9}$  RLU vs.  $EC_{50}(\text{ERBB4/4}) 4 \times 10^{-9}$  RLU) and efficacy.

Similarly, JK07 induced ERBB2/3 and ERBB4/4 dimerization with a comparable potency ( $EC_{50}(\text{ERBB2/3}) 3.3 \times 10^{-11}$  RLU vs.  $EC_{50}(\text{ERBB4/4}) 5.3 \times 10^{-10}$  RLU), but the efficacy for ERBB4/4 dimerization was significantly higher ( $14.3 \pm 1.6$  RLU vs.  $4.4 \pm 0.3$  RLU at the highest concentration point of dose-response curve;  $p < 0.0001$ , Figure 19B).

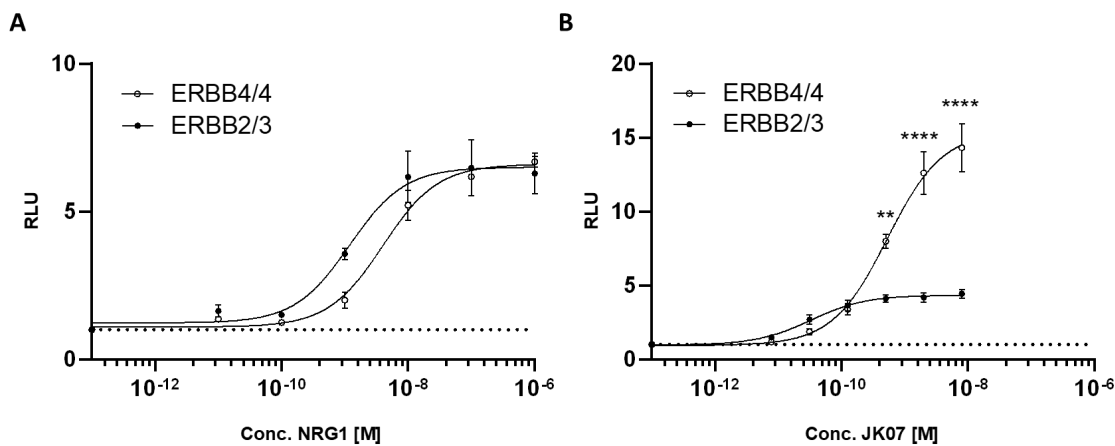


**Figure 19. NRG1 and JK07 activate ERBB dimerization.** The effect on ERBB2/ERBB3 heterodimerization and ERBB4/ERBB4 homodimerization, plotted as RLU (dotted line indicates vehicle) to the concentration of (A) NRG1 ( $n = 4 - 5$  per group from 3 independent repeats) or (B) JK07 ( $n = 6 - 9$  per group from 3 independent repeats). \*\* $p < 0.01$ , \*\*\*\* $p < 0.0001$ . Two-way Anova with Tukey's post-hoc analysis. All results are represented as mean  $\pm$  SEM. RLU indicates relative light units.

### JK07 phosphorylates ERBB4 and activates downstream signaling pathways.

We next verified the effect of JK07 on ERBB4 phosphorylation and downstream pathway signaling. For these experiments, we used cultured atrial cardiomyocytes (iAMs), since we specifically wanted to verify whether JK07 was active in atrial cells. Figure 20 shows the effects of NRG1 and JK07 on phosphorylation of ERBB4 (P-ERBB4), determined via western blot. Both NRG1 and JK07 stimulation induced phosphorylation of the ERBB4 receptor and activated downstream pathway signaling of Akt and Erk1/2.



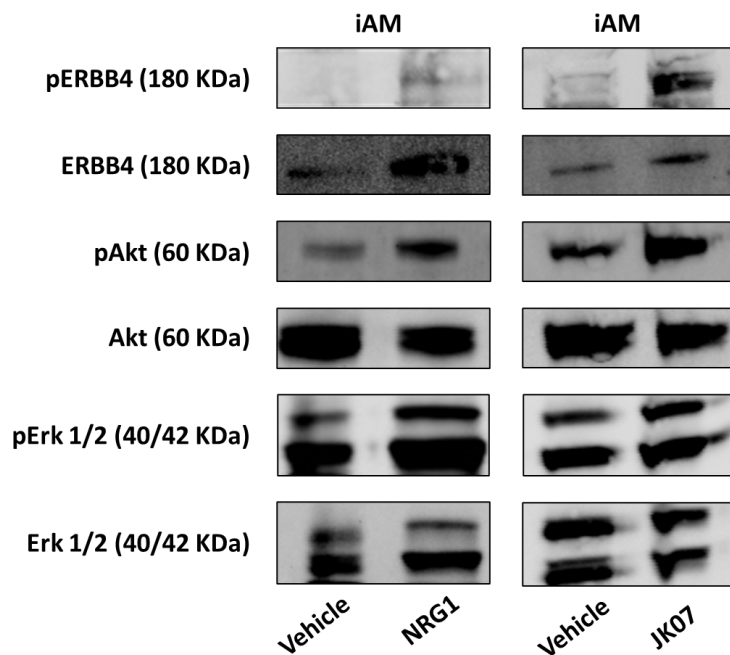


**Figure 20. JK07 increases ERBB4 phosphorylation and activates distinct downstream signaling pathways.** Protein levels of (P-)ERBB4 and downstream signaling pathways (P-)Akt and (P-)Erk1/2 were determined in atrial cardiomyocytes (iAMs) after 15 min. of NRG1 (50 ng/mL) or JK07 ( $3.3 \times 10^{-4}$  mg/mL) stimulation. GAPDH was used as a loading control and experiments were performed only once for validation purposes. iAM indicates immortalized atrial myocytes.

**JK07 attenuates mRNA level upregulation of different cytokines in cultured macrophages.**

We next tested whether JK07, similarly as NRG1, attenuated pro-inflammatory responses in activated macrophages. We previously showed that NRG1 decreases LPS-induced upregulation of cytokines in cultured macrophages (5).

Figure 21 shows that JK07 significantly attenuated LPS-induced upregulation of IL-6 and IL-1 $\beta$  mRNA levels. The induction of TNF- $\alpha$  and iNOS mRNA levels was not affected by JK07, in contrast to previous experiments with NRG1.

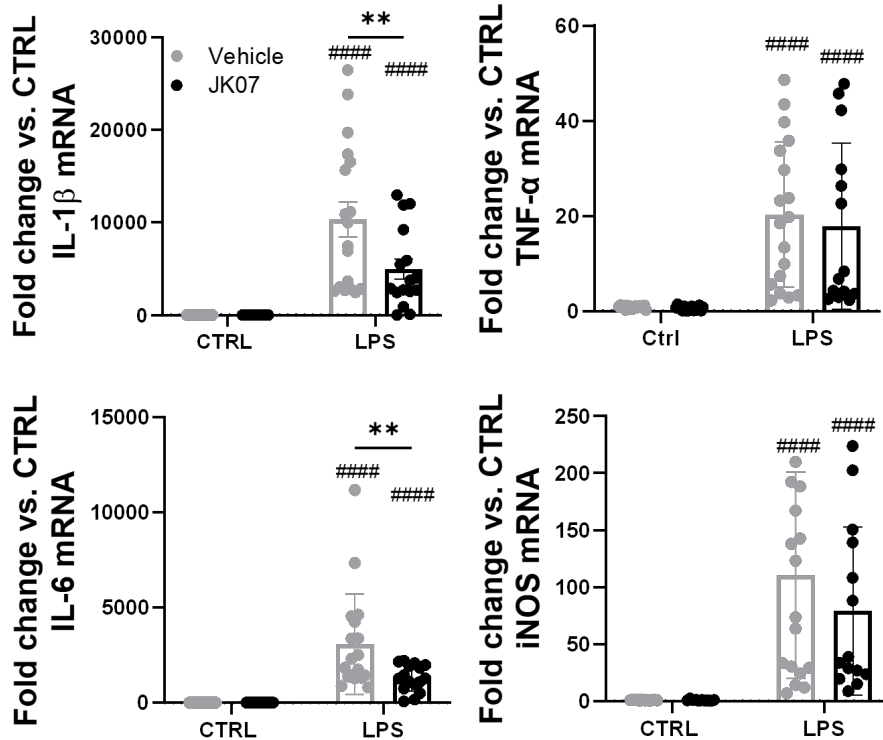


**Figure 21. JK07 attenuates cytokine mRNA expression in cultured macrophages.** IL-1 $\beta$ , IL-6, TNF $\alpha$ , iNOS mRNA expression levels in LPS-activated (100 ng/mL, 8 hours) J774A.1 macrophages with and without JK07 stimulation ( $3.3 \times 10^{-4}$  mg/mL, 8 hours;  $n = 12 - 18$  per group, from 3 independent repeats). #####  $p < 0.0001$ ; \*\* $p < 0.01$ , two-way Anova with Tukey's post-hoc analysis. All results are represented as mean  $\pm$  SEM. IL-6 indicates interleukin 6; IL-1 $\beta$ , interleukin 1 $\beta$ ; TNF- $\alpha$ , tumor necrosis factor  $\alpha$ ; iNOS, induced nitric oxygen synthase; mRNA, messenger RNA.

### JK07 mitigates mRNA level upregulation of different collagen types in atrial tissue samples.

Next, we tested whether JK07 also induced anti-fibrotic effects, since we previously showed that NRG1 has anti-fibrotic effects. For these experiments, we used an *ex vivo* fibrosis assay in which we kept atrial samples from male Wistar rats in culture medium. Figure 22A shows that collagen type I mRNA levels gradually and significantly increased during 3 days of incubation in culture medium, and similar results were observed for collagen type III. To assess the anti-fibrotic effects of JK07, atrial tissue samples were treated with JK07 ( $3.3 \times 10^{-4}$  mg/mL) or vehicle for two or three days. As shown in Figure 22B, JK07 significantly mitigated the upregulation of both collagen genes after three days.

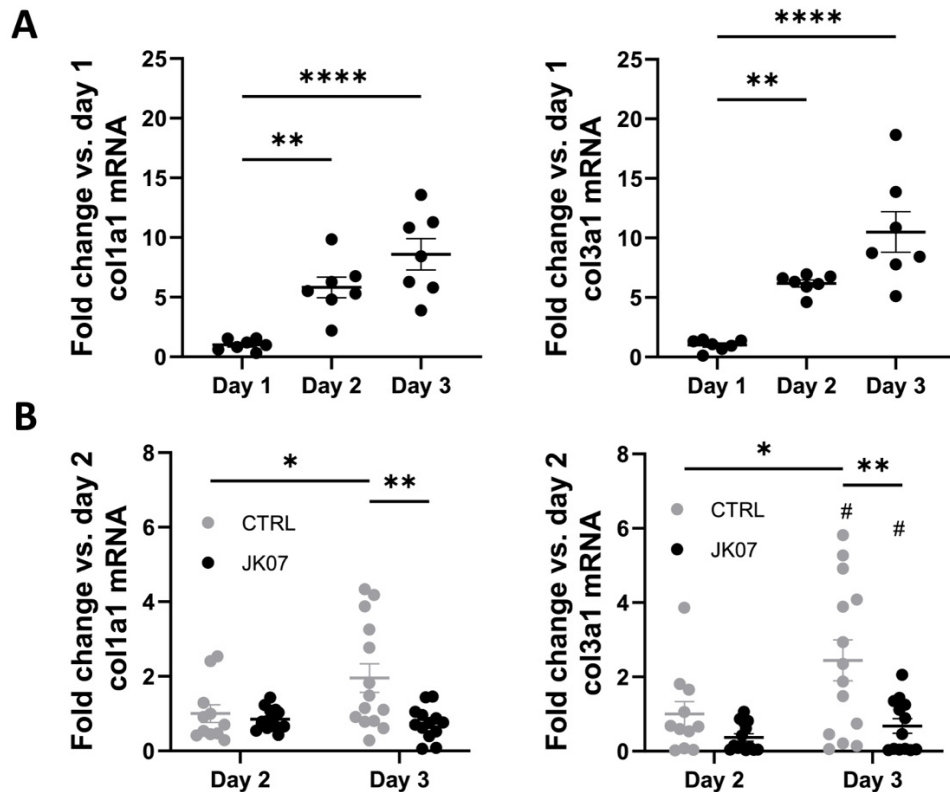


**Figure 22. JK07 mitigates collagen mRNA expression in *ex vivo* atrial tissue samples . (A)** mRNA levels of collagen type I (left) and type III (right) in atrial tissue samples after 1, 2, and 3 days of *ex vivo* culture (n = 7 per group, from 3 independent repeats). \*\*p < 0.01, \*\*\*\*p < 0.0001, one-way Anova with Dunnett’s post-hoc analysis. **(B)** mRNA levels of collagen type I (left) and type III (right) after 2 or 3 days of *ex vivo* culture, with or without JK07 treatment (n = 11 – 14 per group, from 2 independent repeats). # p < 0.05; \*p < 0.05, \*\*p < 0.01, two-way Anova with Tukey’s post-hoc analysis. All results represented as mean ± SEM.

## Discussion

In this chapter, we first confirmed that JK07 induces ERBB4/ERBB4 homodimerization. Consistent with the premise that JK07 preferentially signals through ERBB4, ERBB2/ERBB3 heterodimerization remained 3 fold lower, although activation of ERBB2/ERBB3 remained significant. We further showed that JK07 induces anti-inflammatory effects *in vitro* in LPS-activated J774A.1 macrophages and anti-fibrotic effects in *ex vivo* rat atrial tissue samples, as such recapitulating some of the biological effects previously demonstrated with NRG1 and consistent with the conjecture that ERBB4 is the dominant receptor in the therapeutic effects of NRG1.

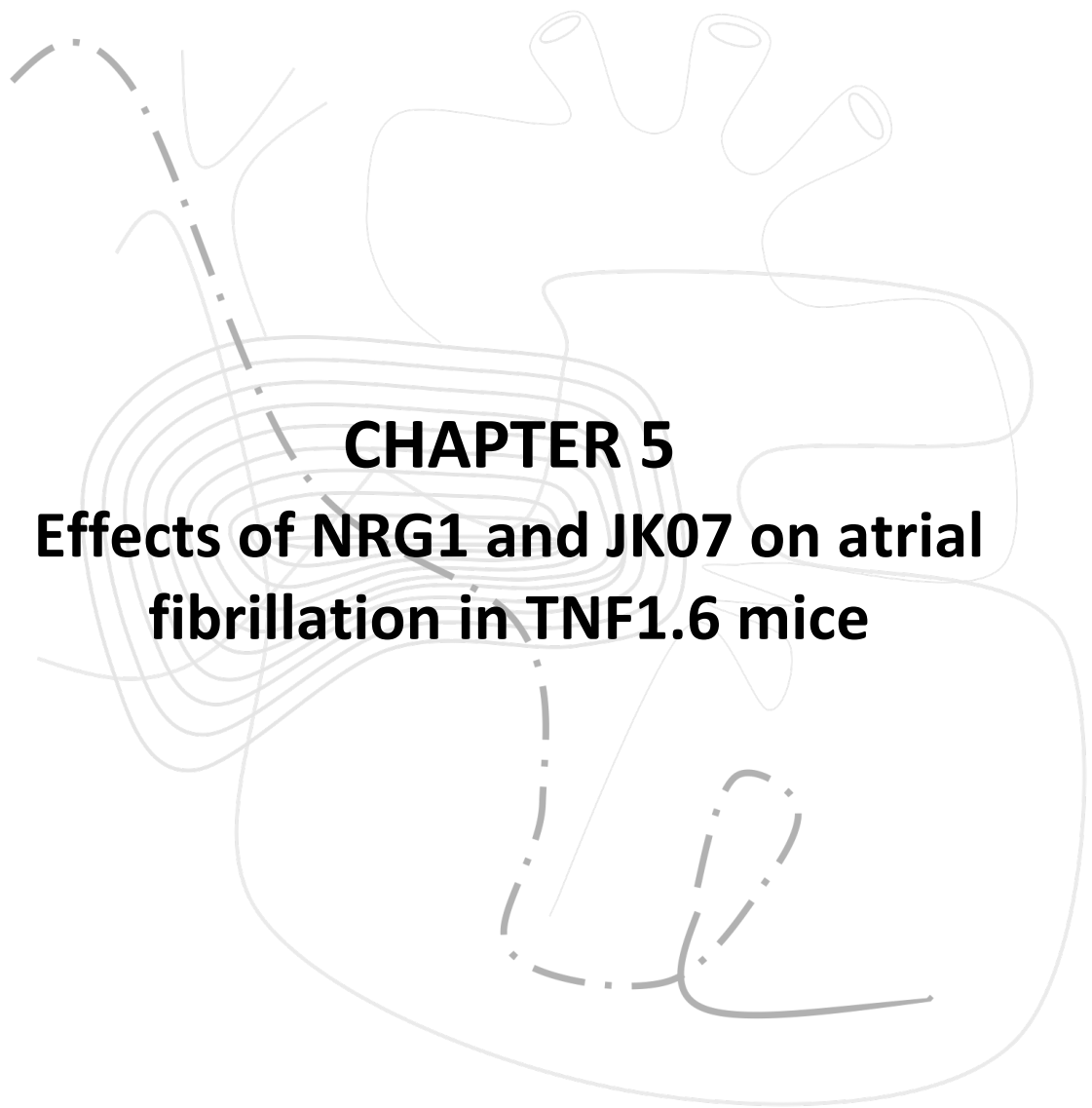
NRG1 is a paracrine protein, which is released in the heart upon cardiac injury and signals non-selectively through ERBB3 and ERBB4 (2, 8, 9). There is increasing evidence that most compensatory effects of NRG1 are mediated by ERBB4 (2, 6). The expression of ERBB3 in the heart is low and the functional role of ERBB3 in cardiac physiology is less established as transgenic mouse models with gain or loss of function have not been studied. Recent studies have demonstrated that activation of ERBB4 has anti-inflammatory and anti-fibrotic properties in various organs, including the heart (5, 10). These data suggest that selective ERBB4 activation may suffice to induce most of the beneficial effects of NRG1 during cardiac disease. This is fortunate, since ERBB3 is expressed by many cancer cells implying that NRG1 may accelerate tumor growth by promoting the formation of ERBB2/3 heterodimers (11).

JK07, a recombinant fusion protein comprising a fragment of human NRG1 fused to an anti-ERBB3 mAb backbone, is constructed as a therapeutic agent to activate ERBB signaling, with preferential signaling through the ERBB4 receptor, while keeping ERBB3 signaling low. We have used this fusion protein in this thesis to test the hypothesis that the NRG1/ERBB signaling pathway has therapeutic effects on AF. First, we validated that JK07 selectively dimerizes ERBB4/4 with a higher efficacy than ERBB2/3 compared with NRG1. We also validated the activation of different downstream signaling pathways in a similar manner as recombinant NRG1. Stimulation of iAMs by JK07 induced phosphorylation of Akt and Erk1/2 in a similar fashion compared with NRG1. A limitation in this study was that western blots were only performed once as a proof of concept and cannot be used for quantification purposes. In addition, we showed that JK07 attenuated the upregulation of different cytokines in LPS-activated cultured macrophages. This is in line with previous observations where the effect of NRG1 was tested on cytokine release in LPS-activated macrophages (5). This confirms that ERBB4 activation plays an important role during inflammation. Moreover, we showed that JK07, analogous to NRG1, has anti-fibrotic effects. Upregulation of mRNA collagen levels (*col1a1* and *col3a1*) was significantly mitigated after three days of JK07 treatment in *ex vivo* atrial tissue samples. This indicates that ERBB4 activation mediates anti-fibrotic effects through direct inhibitory actions on collagen production by (myo)fibroblasts. Based on these observations we conclude that JK07 mostly signals through ERBB4, attenuates activation of cytokine release by macrophages and reduces collagen formation

by fibroblasts. Together with its higher stability and longer half-life (1-3 days vs. 10 min.) than NRG1, JK07 is a candidate treatment for atrial inflammation, fibrosis and AF, which was further tested in this thesis.

## References

1. Xu J, Sun P, Zhao X, Meng L, Wang X, Qin X, et al. Safety, Tolerability, and Pharmacokinetics of Recombinant Human Neuregulin-1 in Healthy Chinese Subjects. *American Journal of Cardiovascular Drugs*. 2023.
2. De Keulenaer GW, Feyen E, Dugaucquier L, Shakeri H, Shchendrygina A, Belenkov YN, et al. Mechanisms of the Multitasking Endothelial Protein NRG-1 as a Compensatory Factor During Chronic Heart Failure. *Circ Heart Fail*. 2019;12(10):e006288.
3. Bersell K, Arab S, Haring B, Kühn B. Neuregulin1/ErbB4 signaling induces cardiomyocyte proliferation and repair of heart injury. *Cell*. 2009;138(2):257-70.
4. Schumacher MA, Hedl M, Abraham C, Bernard JK, Lozano PR, Hsieh JJ, et al. ErbB4 signaling stimulates pro-inflammatory macrophage apoptosis and limits colonic inflammation. *Cell Death Dis*. 2017;8(2):e2622.
5. Vermeulen Z, Hervent AS, Dugaucquier L, Vandekerckhove L, Rombouts M, Beyens M, et al. Inhibitory actions of the NRG-1/ErbB4 pathway in macrophages during tissue fibrosis in the heart, skin, and lung. *Am J Physiol Heart Circ Physiol*. 2017;313(5):H934-h45.
6. Jay SM, Murthy AC, Hawkins JF, Wortzel JR, Steinhäuser ML, Alvarez LM, et al. An engineered bivalent neuregulin protects against doxorubicin-induced cardiotoxicity with reduced proneoplastic potential. *Circulation*. 2013;128(2):152-61.
7. John Li SL, Dixiang LUO, Yiran WU, Ming Zhou, Yang Wang, Xiaolei Zhuang, Liang Hua, Pengyi LUO inventor Human neuregulin-1 (nrg-1) recombinant fusion protein compositions and methods of use thereof. United States patent US2020/0010522 A1. 2020 9 January.
8. Lemmens K, Doggen K, De Keulenaer GW. Role of neuregulin-1/ErbB signaling in cardiovascular physiology and disease: implications for therapy of heart failure. *Circulation*. 2007;116(8):954-60.
9. Gao R, Zhang J, Cheng L, Wu X, Dong W, Yang X, et al. A Phase II, Randomized, Double-Blind, Multicenter, Based on Standard Therapy, Placebo-Controlled Study of the Efficacy and Safety of Recombinant Human Neuregulin-1 in Patients With Chronic Heart Failure. *Journal of the American College of Cardiology*. 2010;55(18):1907-14.
10. Galindo CL, Ryzhov S, Sawyer DB. Neuregulin as a heart failure therapy and mediator of reverse remodeling. *Curr Heart Fail Rep*. 2014;11(1):40-9.
11. Vermeulen Z, Segers VF, De Keulenaer GW. ErbB2 signaling at the crossing between heart failure and cancer. *Basic Res Cardiol*. 2016;111(6):60.



## **CHAPTER 5**

**Effects of NRG1 and JK07 on atrial  
fibrillation in TNF1.6 mice**





## **Introduction**

The study of AF in small animals is difficult because of their small atria with low tissue mass, limiting the sustainability of AF (1, 2). This observation led to the development of Walter Garrey's "critical mass" theory (3). In compliance with the multi-wavelet theory, multiple reentrant circuits are required to sustain the fibrillatory arrhythmia. For reentrant circuits to exist, a certain wavelength is required, which is dependent on the amount of tissue mass (1). Nevertheless, a few mouse models have been developed with high and consistent rates of spontaneous AF. However, these models require genetic manipulation, resulting in severe cardiac dysfunction, atrial remodeling and a decreased lifespan (4-7).

To assess the effects of NRG1 treatment on AF, we aimed at studying the effects on spontaneous AF. Therefore, we used the TNF1.6 mouse model, which has been previously reported to spontaneously develop atrial fibrosis and recurrent AF. TNF1.6 mice have been engineered by Dr. Feldman and were genetically modified to overexpress TNF- $\alpha$  in cardiac tissue (8). TNF- $\alpha$  is an inflammatory cytokine implicated in the development and pathology of AF (9). It has been reported that up to 77% of TNF1.6 mice develop atrial dilation, inflammation and fibrosis, and thrombi by six months of age under free roaming conditions and partially mimic the pathogenesis of AF in a clinically relevant fashion (6). Atrial inflammation and fibrosis contribute to the initiation and sustainability of reentrant arrhythmias such as AF. We studied the effects of both NRG1 and JK07 on AF in TNF1.6 mice, hypothesizing that NRG1 and JK07 attenuate atrial remodeling and AF burden.

## **Materials and methods**

Materials and methods are described in chapter 3.

## Results

### TNF1.6 mice overexpress TNF- $\alpha$ in cardiac tissue resulting in increased mortality.

Overexpression of the inflammatory cytokine TNF- $\alpha$  was assessed in cardiac tissue of male transgenic mice via RT-qPCR. As shown in Figure 23A, transgenic male mice showed significantly increased mRNA levels of TNF- $\alpha$  compared with their wild type littermates ( $56.9 \pm 18.3$  vs.  $1 \pm 0.4$  FC;  $p < 0.0001$ ). Cardiac-specific overexpression of TNF- $\alpha$  (6, 8) induces premature mortality ( $p = 0.0001$ ), starting at an age of around 100 days as confirmed by our observations (Figure 23B).

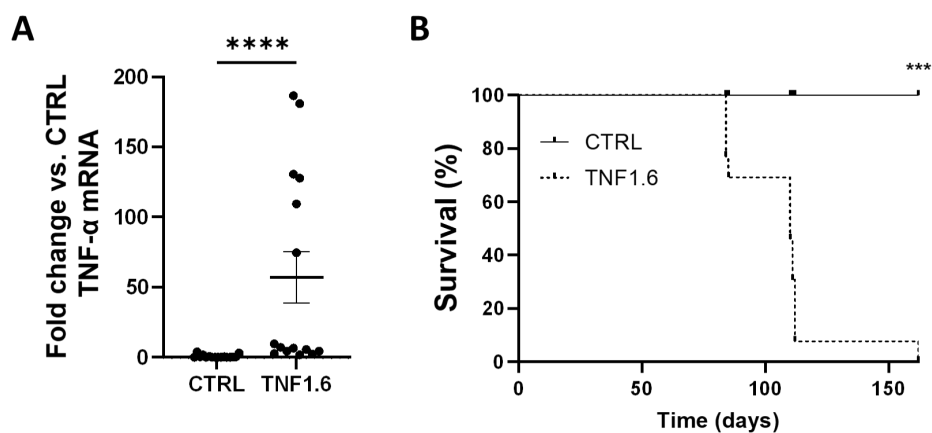


**Figure 23. Effect of cardiac-specific overexpression of TNF- $\alpha$  on survival in FVB mice. (A)** Quantification of mRNA levels of TNF- $\alpha$  in cardiac tissue of transgenic mice compared to wild type littermates ( $n = 15-16$  per group). \*\*\*\* $p < 0.0001$ , Wilcoxon signed rank test. **(B)** Effect of cardiac-specific TNF- $\alpha$  overexpression on mortality in FVB mice ( $n = 13$  per group). \*\*\* $p < 0.0001$ , Log-rank (Mantel-cox) test. All results are represented as mean  $\pm$  SEM. TNF- $\alpha$  indicates tumor necrosis factor alpha.

### Effects of NRG1 on atrial remodeling and AF burden in male TNF1.6 mice.

We first confirmed ERBB4 protein expression in the heart of TNF1.6 mice (SFigure 1). Next, we studied the effects of NRG1 on atrial remodeling and AF burden. Male TNF1.6 mice were treated for six weeks with NRG1 or vehicle. Mice were monitored via telemetry (24 h/week) for detection of spontaneous AF. TNF1.6 mice showed severe atrial myopathy, which was evaluated by assessing mRNA levels of distinct inflammatory markers, left atrial fibrosis on histological level, and by measuring left atrial diameter on echocardiography. As shown in Figure 24A, IL-10, INF- $\gamma$ , and IL-1 $\beta$  mRNA expression levels were significantly higher and TGF- $\beta$  mRNA expression levels significantly lower in transgenic mice compared with their control littermates.

NRG1 treatment did not mitigate the inflammatory response compared with vehicle-treated mice. Figure 24B shows that the magnitude of left atrial fibrosis in TNF1.6 male mice was significantly higher compared with control littermates. Again, NRG1 did not affect this. Finally, we observed that the left atrial diameter of TNF1.6 mice was significantly higher compared with their control groups, and also this was not influenced by NRG1, as shown in Figure 24C.

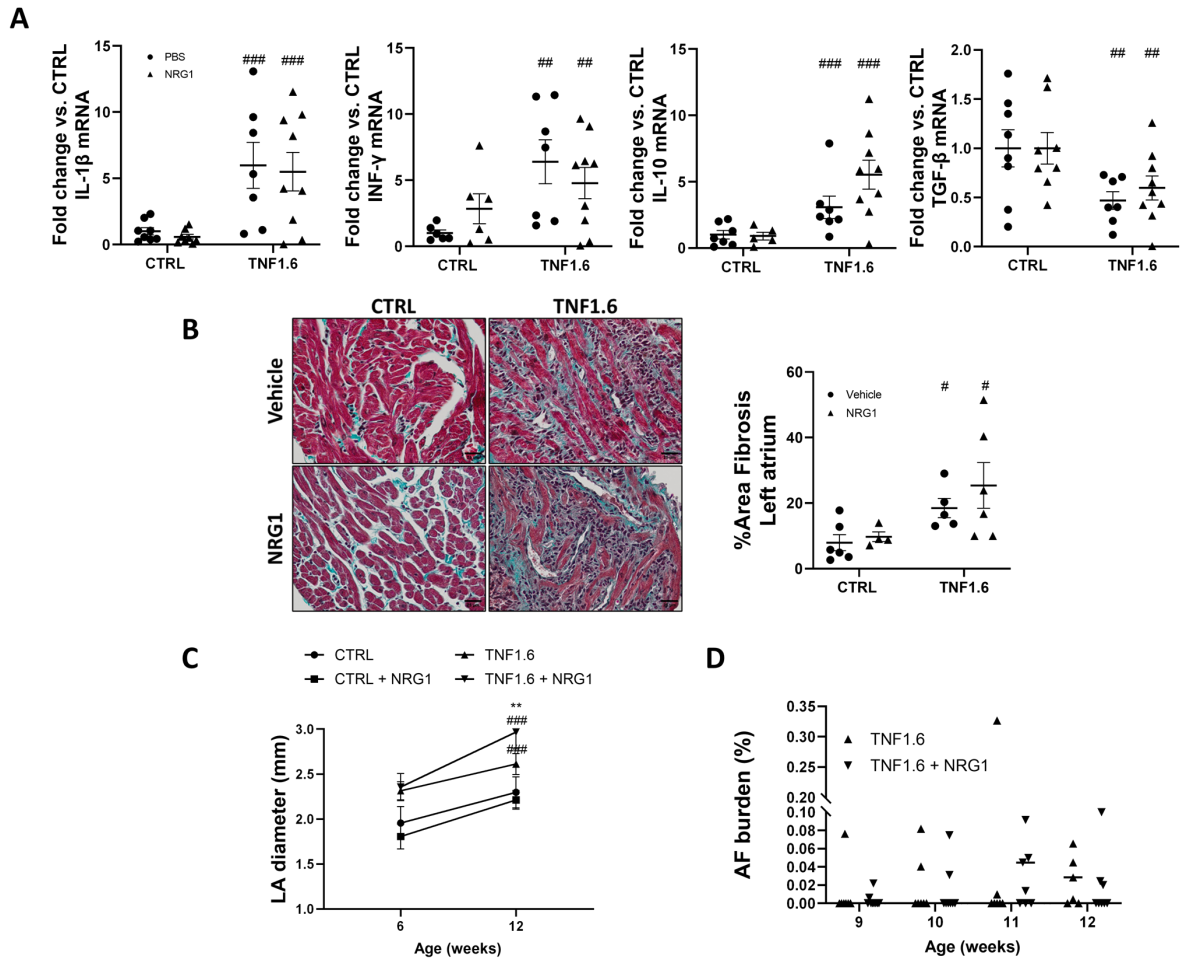


**Figure 24. Effect of NRG1 treatment on atrial remodeling and AF burden in male transgenic TNF1.6 mice. (A)** IL-1 $\beta$ , TGF- $\beta$ , IL-10, and INF- $\gamma$  mRNA expression levels in TNF1.6 mice compared with CTRL, after six weeks of either NRG1 (20  $\mu$ g/kg/day, i.p., 1x/day; 6 weeks) or PBS treatment (n = 6 - 8 per group). **(B)** Representative Masson's trichrome stained left atrial sections of transgenic and CTRL mice treated with vehicle or NRG1 (n = 4 - 6 per group; scale bars = 25  $\mu$ m; left). Quantification of the percentage fibrotic area (right) **(C)** Left atrial diameter measured at start (6 weeks old) and end of study (12 weeks old). **(D)** Mice ECGs were monitored for four weeks using implanted telemetry devices. Quantification of % spontaneous AF over 24 h/week (n = 7 - 9 per group). #p < 0.05, ###p < 0.01, ####p < 0.001; \*\*p < 0.01, two-way Anova with Tukey's post-hoc analysis. All results represented as mean  $\pm$  SEM. TNF- $\alpha$  indicates tumor necrosis factor alpha.

Spontaneous AF occurrence (% AF burden) was quantified through sustained ECG monitoring using implanted telemetry devices. We did not observe spontaneous AF episodes in the control groups (data not shown). Surprisingly, also in transgenic mice, spontaneous AF remained infrequent (< 0.5% in 24 h/week, within a monitoring period of six weeks), as shown in Figure 24D. NRG1 treatment did not change the AF burden.

#### **Effects of JK07 on atrial remodeling and AF burden in female TNF1.6 mice.**

After this study in male transgenic mice with a severe phenotype (despite a low incidence of AF and no response to NRG1 treatment, we performed a similar study in female TNF1.6 mice, showing a less severe phenotype including higher survival rates (observed by us and others) (6). In addition, we changed daily I.P. injections of NRG1 to twice weekly I.V. injections with JK07, which has a longer half-life. The effects of JK07 were tested on interstitial left atrial fibrosis in female TNF1.6. As shown in Figure 25A, left atrial fibrosis was significantly increased in female TNF1.6 mice compared with control mice, and JK07 treatment did not change this. Similarly, female TNF1.6 mice showed a larger left atrial diameter than control mice, and again JK07 treatment had no effect (Figure 25B). Likewise, as seen in male TNF1.6 mice, spontaneous AF burden was infrequent or absent in female TNF1.6 mice, and JK07 treatment did not change this (Figure 25C).

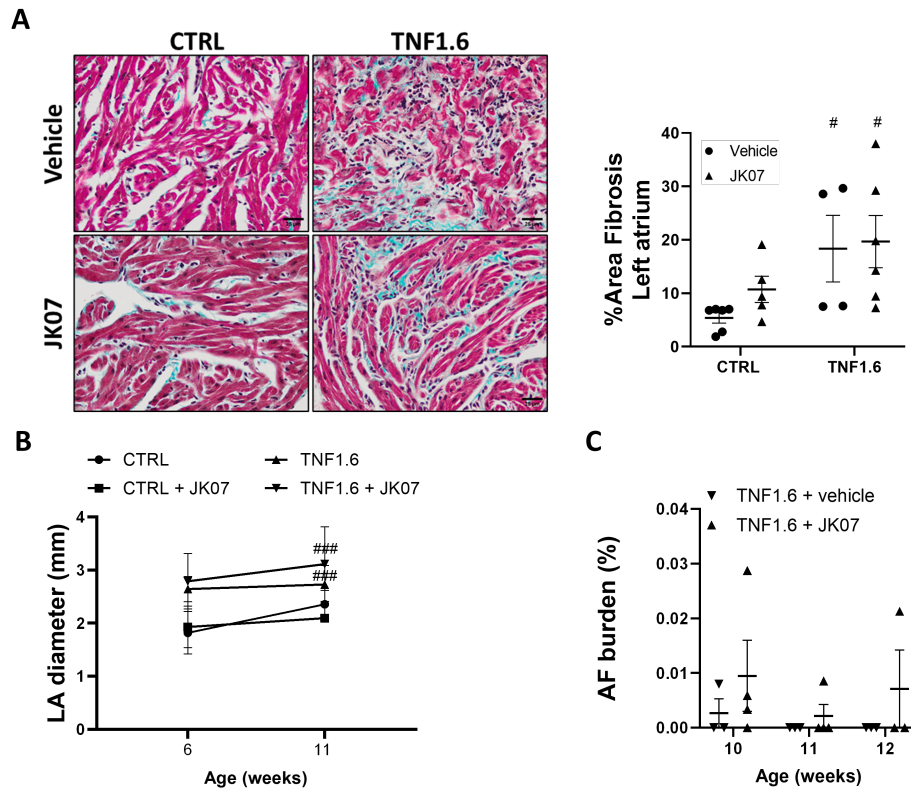


**Figure 25. Effects of JK07 treatment on atrial remodeling and AF burden in female transgenic TNF1.6 mice.**

**(A)** Representative Masson's trichrome stained left atrial sections of transgenic and control mice treated with vehicle or JK07 (1 mg/kg/day, I.V., 2x/week; 6 weeks; n = 4 - 6 per group; scale bars = 25  $\mu$ m; left). Quantification of the percentage fibrotic area (right). **(B)** Left atrial diameter measured at start (6 weeks old) and end of study (11 weeks old). **(D)** Mice ECGs were monitored for three weeks using implanted telemetry devices. Quantification of % spontaneous AF over 24 h/week (n = 3 - 4 per group). #p < 0.05, ##p < 0.01, ###p < 0.001, two-way Anova with Tukey's post-hoc analysis. Results represented as mean  $\pm$  SEM.

## Discussion

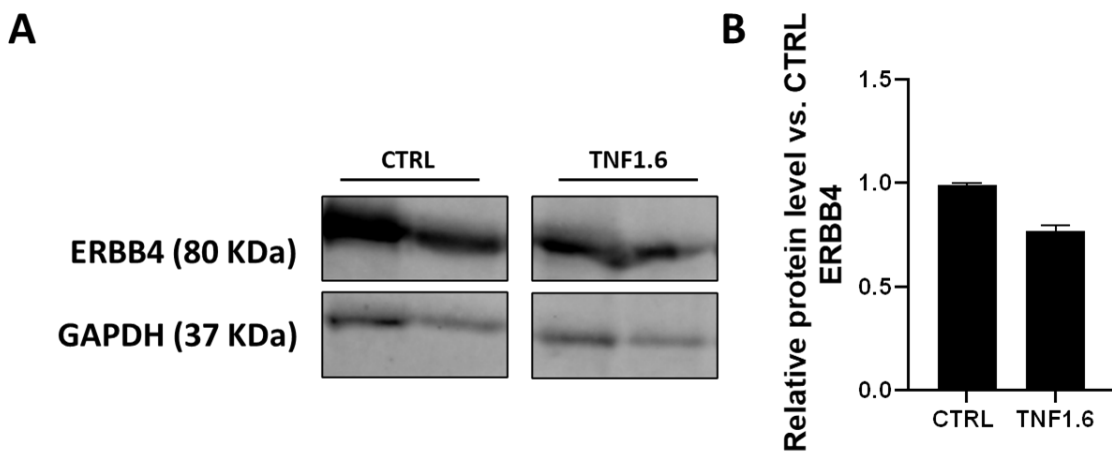
In this study, we examined the effects of NRG1 and JK07 on atrial remodeling and AF burden in male and female TNF1.6 transgenic mice with cardiac-specific overexpression of TNF- $\alpha$ . Transgenic TNF1.6 mice developed severe atrial remodeling (characterized by inflammation, fibrosis, dilation), but spontaneous episodes of AF during sustained telemetry monitoring remained absent or infrequent. Neither NRG1, nor JK07 treatment showed any significant effects on atrial inflammatory cytokine levels, atrial fibrosis, atrial dimensions and AF burden.

The inflammatory cytokine TNF- $\alpha$  is known to be implicated in the development and pathology of atrial myopathy and AF (10, 11). In support of this, previous studies performed on these TNF1.6

transgenic mouse model, showed that these mice develop atrial remodeling with spontaneous AF episodes (6). The NF- $\kappa$ B pathway, a known and important pathway that mediates TNF- $\alpha$  signaling, was also increased in TNF1.6 transgenic mice (12). This results in increased immune and inflammatory responses, and apoptosis in distinct cardiac cell types. Endothelial cells increase their expression of adhesion molecules in response to TNF- $\alpha$  signaling, resulting in increased attraction of inflammatory immune cells in local tissue. Cardiac fibroblasts become activated by TNF- $\alpha$  but also secrete this cytokine and contribute to the inflammatory cascade through the recruitment of monocytes. Cardiac fibroblasts transition into myofibroblasts, mediating oxidative stress, excessive collagen deposition and leading to cardiac remodeling. Finally, cardiomyocytes are affected by TNF- $\alpha$  signaling and undergo hypertrophy and apoptosis following chronic exposure to TNF- $\alpha$  (12, 13). Here, overexpression of the inflammatory cytokine TNF- $\alpha$  in TNF1.6 mice was confirmed via mRNA expression levels in cardiac tissue where we observed an 80-fold increase in TNF- $\alpha$  expression. mRNA levels of other inflammatory markers (IL-10, INF- $\gamma$ , IL-1 $\beta$ , TGF- $\beta$ ) were significantly altered in TNF1.6 mice compared to control mice, indicating persistent atrial inflammation. NRG1 treatment did not alter the mRNA expression levels of distinct inflammatory markers in male TNF1.6 mice. Because inflammation precedes fibrosis in chronic tissue injury, we also examined left atrial fibrosis. Male mice overexpressing TNF- $\alpha$ , showed marked atrial fibrosis which was not mitigated after NRG1 treatment. Additionally, left atrial diameter was significantly increased in transgenic mice, as consistent with previous observations by Saba *et al.* (6). Surprisingly, despite these signs of atrial myopathy, spontaneous AF in these mice remained rare, and accordingly was not affected by NRG1 treatment. Female TNF1.6 mice displayed similar left atrial remodeling compared with male TNF1.6 mice, as well as infrequent spontaneous episodes of AF during sustained monitoring. Similarly, JK07 treatment did neither alter atrial remodeling nor AF burden in female mice. Overall, we observed severe atrial inflammation and fibrosis, with scarce occurrence of spontaneous AF, and no effect of NRG1 or JK07. Several studies have shown anti-inflammatory and anti-fibrotic effects of NRG1 in different tissues, including the left ventricle (14, 15). This study, however, shows that neither recombinant NRG1 nor JK07 treatment reduced atrial fibrosis in TNF1.6 transgenic mice. NRG1 or JK07 treatments were started at age of six weeks. At this age, TNF1.6 transgenic mice might already have developed critical components of atrial myopathy, which may explain the absence of effects on atrial remodeling in our study.

A study by Li *et al.* endorses this hypothesis by showing that administration of an MMP-inhibitor to young TNF1.6 transgenic mice of only four weeks old mitigated cardiomyocyte (ventricular) hypertrophy and dilation (16). Since almost no spontaneous AF episodes were observed in our study, the question whether NRG1 and JK07 reduced AF burden could not be answered. Also, transgenic mice developed a progressive HF syndrome characterized by LV dilation, fibrosis, decreased EF and premature mortality. Therefore, we concluded that this mouse model is more a model of severe HF, rather than a model of AF, hence less appropriate for our study objectives. We therefore decided that in order to assess the effects of NRG1 or JK07 treatment on AF we needed other animal models.

## Supplemental figures



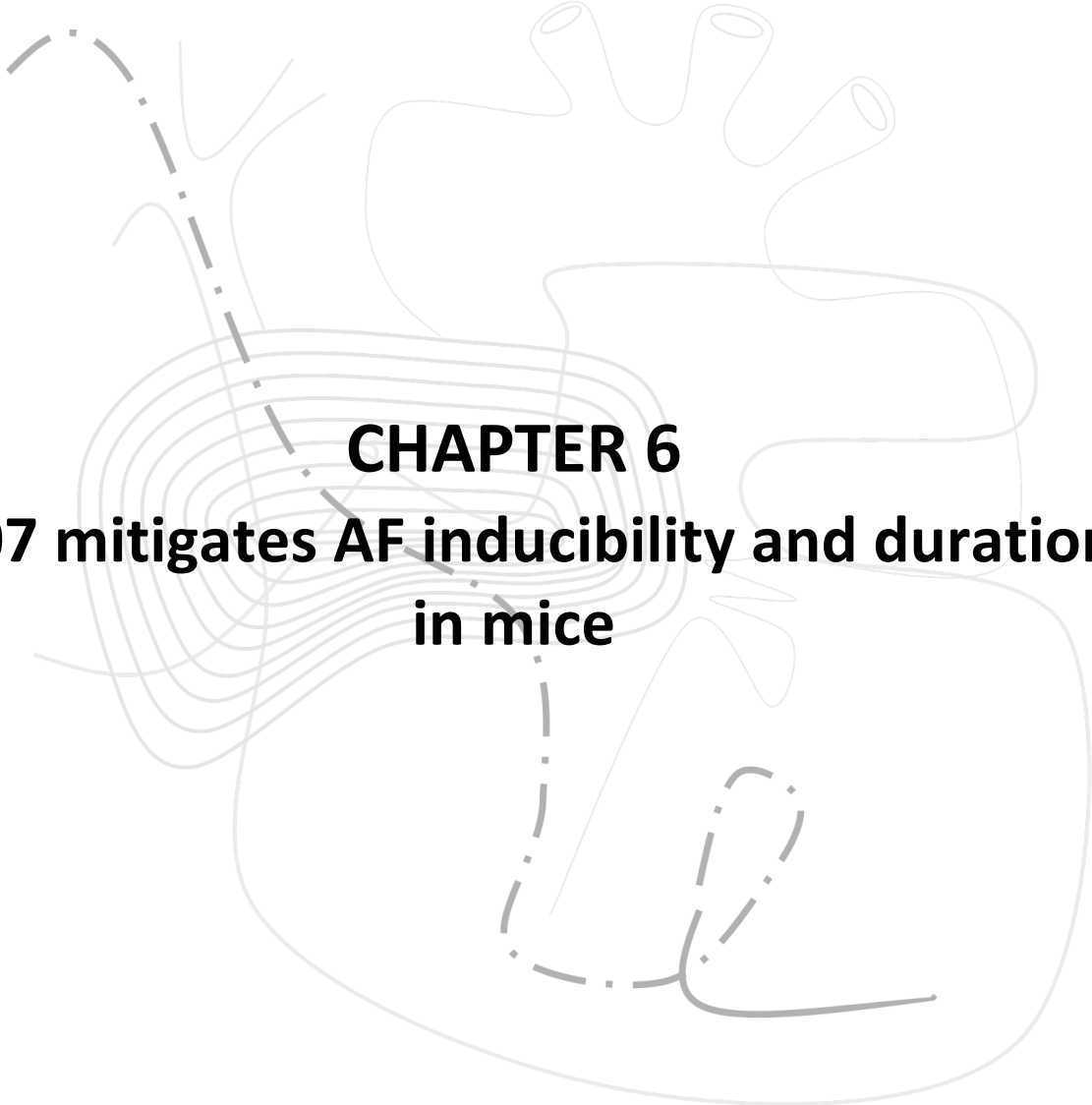
**SFigure 1. ERBB4 protein expression in cardiac tissue of TNF1.6 mice. (A)** Representative images of total protein levels of ERBB4, determined in CTRL and transgenic TNF1.6 mice, using Western blot analysis. **(B)** Protein levels (n = 2) of ERBB4 were quantified using odyssey software and confirm that ERBB4 receptor is present in atrial cardiac tissue of transgenic mice. All results are represented as mean  $\pm$  SEM.



## References

1. Kaese S, Verheule S. Cardiac electrophysiology in mice: a matter of size. *Front Physiol.* 2012;3:345.
2. Schüttler D, Bapat A, Käab S, Lee K, Tomsits P, Clauss S, et al. Animal Models of Atrial Fibrillation. *Circ Res.* 2020;127(1):91-110.
3. Garrey WE. THE NATURE OF FIBRILLARY CONTRACTION OF THE HEART.—ITS RELATION TO TISSUE MASS AND FORM. *American Journal of Physiology-Legacy Content.* 1914;33(3):397-414.
4. Verheule S, Sato T, Everett Tt, Engle SK, Otten D, Rubart-von der Lohe M, et al. Increased vulnerability to atrial fibrillation in transgenic mice with selective atrial fibrosis caused by overexpression of TGF-beta1. *Circ Res.* 2004;94(11):1458-65.
5. Ozcan C, Battaglia E, Young R, Suzuki G. LKB1 knockout mouse develops spontaneous atrial fibrillation and provides mechanistic insights into human disease process. *J Am Heart Assoc.* 2015;4(3):e001733.
6. Saba S, Janczewski AM, Baker LC, Shusterman V, Guroy EC, Feldman AM, et al. Atrial contractile dysfunction, fibrosis, and arrhythmias in a mouse model of cardiomyopathy secondary to cardiac-specific overexpression of tumor necrosis factor- $\alpha$ . *Am J Physiol Heart Circ Physiol.* 2005;289(4):H1456-67.
7. Stümpel FT, Stein J, Himmler K, Scholz B, Seidl MD, Skryabin BV, et al. Homozygous CREM- $\Delta$ C-X Overexpressing Mice Are a Reliable and Effective Disease Model for Atrial Fibrillation. *Front Pharmacol.* 2018;9:706.
8. Kubota T, McTiernan CF, Frye CS, Slawson SE, Lemster BH, Koretsky AP, et al. Dilated Cardiomyopathy in Transgenic Mice With Cardiac-Specific Overexpression of Tumor Necrosis Factor- $\alpha$ . *Circulation Research.* 1997;81(4):627-35.
9. Guo Y, Lip GYH, Apostolakis S. Inflammation in Atrial Fibrillation. *Journal of the American College of Cardiology.* 2012;60(22):2263-70.
10. Chen DY, Lin CH, Chen YM, Chen HH. Risk of Atrial Fibrillation or Flutter Associated with Periodontitis: A Nationwide, Population-Based, Cohort Study. *PLoS One.* 2016;11(10):e0165601.
11. Qu Y-C, Du Y-M, Wu S-L, Chen Q-X, Wu H-L, Zhou S-F. Activated nuclear factor- $\kappa$ B and increased tumor necrosis factor- $\alpha$  in atrial tissue of atrial fibrillation. *Scandinavian Cardiovascular Journal.* 2009;43(5):292-7.
12. Higuchi Y, Chan TO, Brown MA, Zhang J, DeGeorge BR, Jr., Funakoshi H, et al. Cardioprotection afforded by NF-kappaB ablation is associated with activation of Akt in mice overexpressing TNF-alpha. *Am J Physiol Heart Circ Physiol.* 2006;290(2):H590-8.
13. Rolski F, Błyszczuk P. Complexity of TNF- $\alpha$  Signaling in Heart Disease. *J Clin Med.* 2020;9(10).
14. Galindo CL, Ryzhov S, Sawyer DB. Neuregulin as a heart failure therapy and mediator of reverse remodeling. *Curr Heart Fail Rep.* 2014;11(1):40-9.
15. Vermeulen Z, Hervent AS, Dugaucquier L, Vandekerckhove L, Rombouts M, Beyens M, et al. Inhibitory actions of the NRG-1/ErbB4 pathway in macrophages during tissue fibrosis in the heart, skin, and lung. *Am J Physiol Heart Circ Physiol.* 2017;313(5):H934-h45.
16. Li YY, Kadokami T, Wang P, McTiernan CF, Feldman AM. MMP inhibition modulates TNF- $\alpha$  transgenic mouse phenotype early in the development of heart failure. *American Journal of Physiology-Heart and Circulatory Physiology.* 2002;282(3):H983-H9.





**CHAPTER 6**  
**JK07 mitigates AF inducibility and duration**  
**in mice**

## **ADAPTED FROM**

*Jens van fraeyenhove\**; Michiel R.L. Tubeckx\*; Bo Govaerts; Yile Fue; Juan Zhang; Arthur Bezerra; Tim De Coster; Julie Cools; Eike M. Wülfers; Siel Van den Bogaert; Bernard Thienpont; Samuel L Murphy; Antoine A.F. de Vries; Erik Fransen; Nele Vandersickel; Daniël A. Pijnappels; Guido Y. De Meyer; Hein Heidbuchel; Llewelyn H. Roderick; Vincent F.M. Segers; Gilles W. De Keulenaer. (Data reported in this chapter are submitted for publication (“ERBB4 activation as a new therapy for atrial remodeling and fibrillation”), in a manuscript that also contains studies of JK07 performed in a pig model of AF).

## **Introduction**

AF is the most diagnosed arrhythmia in clinical practice, partially due to its broad range of risk factors and co-morbidities that support the development and sustainability of AF. Common risk factors of atrial remodeling and AF include ageing, hypertension, obesity and diabetes mellitus (1). In this chapter, we used two distinct mouse models exposed to risk factors of AF: an Ang II-induced arterial hypertension model and a high fat diet-induced obesity model. Arterial hypertension is associated with activation of the renin-angiotensin system, which leads to atrial remodeling and in turn promotes AF (2, 3). The underlying mechanism by which Ang II leads to AF is not yet completely understood, but several mechanisms including atrial fibrosis, atrial dilation, tissue inflammation and oxidative stress have been implicated (4). Several studies have shown that mice treated with a high dose of Ang II (2.8—3 mg/kg/day) develop atrial remodeling and display an increased sensitivity for AF inducibility (5-8). Diet-induced obesity is another common AF risk factor, and has also been used to study AF in mice. Several studies have shown that mice fed with a HFD for a prolonged period of time (8—14 weeks) develop obesity, resulting in atrial remodeling, inflammation and decreased connexin expression in atria (9-11). Accordingly, both arterial hypertension and obesity are two important clinical risk factors for AF, for which a relation with AF has been reproduced in mice, but the underlying mechanisms are only starting to be understood (12). Importantly, neither Ang II-treated mice, nor obese mice develop spontaneous AF but only show increased inducibility of AF during EP studies. Therefore, also in our studies, we investigated the effect of JK07 on AF inducibility and sustainability during EP studies. We tested both a preventive and a therapeutic treatment strategy. JK07 treatment was initiated concomitantly with Ang II or HFD administration in the preventive strategy, whereas in the therapeutic strategy JK07 treatment was only started after three weeks of Ang II administration, a time period which suffices to initiate cardiac remodeling.

## **Materials and methods**

Materials and methods are described in chapter 3.

## Results

### JK07 prevents AF inducibility in two distinct mouse models.

First, we tested whether four weeks of preventive JK07 treatment attenuated AF inducibility in mice treated with Ang II. We first validated that mice treated with Ang II showed a significant increase in systolic blood pressure (using a small subgroup of animals,  $n = 3-4$ , Figure 26A) and in heart-to-body weight (Figure 26B, right). Ang II treatment had no significant effect on the bodyweight after 4 weeks (Figure 26B, left). We also observed Ang II-induced left ventricular fibrosis (Figure 26C), but the variation of fibrotic area in the LV induced by Ang II was large, and no significant effect was obtained. JK07 had no effect on the bodyweight and did neither attenuate heart-to-body weight, nor the fibrotic area in the LV of Ang II-treated mice.

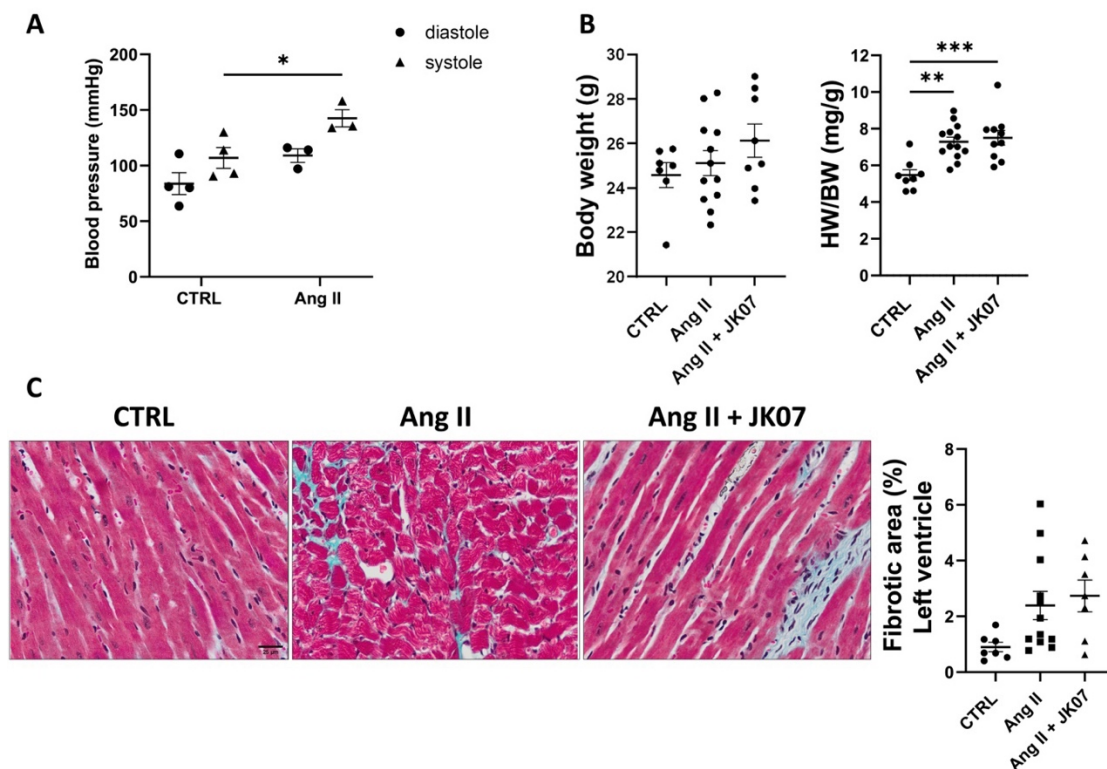


**Figure 26. Effects of Ang II and preventive JK07 treatment on blood pressure, LV hypertrophy and LV fibrosis in C57BL/6N mice.** (A) Ang II significantly increased systolic blood pressure ( $143 \pm 13$  mmHg vs.  $106 \pm 19$  mmHg in CTRL;  $n = 3-4$ ;  $p = 0.04$ ) after week four of pump implantation; effect on diastolic blood pressure was not significant.  $*p < 0.05$ , two-way Anova with Bonferroni's post-hoc analysis. (B) Ang II-treated mice showed no significant differences in body weight compared with CTRL mice (left), but did show increased levels of cardiac hypertrophy (right). JK07 (2x/week, 1 mg/kg, I.V.) had no effect on hypertrophy.  $**p < 0.01$ ,  $***p < 0.001$ , one-way Anova with Tukey's post-hoc analysis.

**(C)** Representative Masson's trichrome stained left ventricular sections (left) of C57BL/6N implanted with Ang II (4.3 mg/kg/day) osmotic minipumps for four weeks or sham operated (n = 7-12 per group; scale bar = 25  $\mu$ m). Quantification of the percentage fibrotic area (right). All results are represented as mean  $\pm$  SEM.

Next, we assessed AF inducibility and duration in Ang II-treated mice through EP studies (Figure 27A). Figure 27B, C show that Ang II induced a significant increase in AF inducibility as compared to control (from 30% to 53% per stimulation series; p = 0.046). Preventive JK07 treatment attenuated AF inducibility compared to vehicle-treated Ang II mice (from 19 to 53% per stimulation series; p = 0.003; Figure 27C and SFigure 2A). Although the mean single episode AF duration was significantly increased by Ang II treatment (from  $1.9 \pm 0.1$  to  $3.1 \pm 0.1$  s; p =  $2 \times 10^{-5}$ , Figure 27D and SFigure 3A), mean total AF duration was only slightly and not significantly increased by Ang II treatment (Figure 27E). JK07 significantly decreased mean single episode AF duration (from  $3.1 \pm 0.1$  to  $1.3 \pm 0.07$  s; p = 0.003, Figure 27D and SFigure 3A) as well as the mean total AF duration in Ang II-treated mice (from  $34.3 \pm 11.6$  to  $1.1 \pm 0.7$  s; p =  $3 \times 10^{-6}$ , Figure 27E). Interestingly, when AF-induced episodes were divided into short (< 3 s) vs. long ( $\geq$  3 s), JK07 significantly reduced the incidence of long AF episodes (from 48.6% to 0%, p =  $2.5 \times 10^{-6}$ ). Of note, AERP was not significantly different among groups (SFigure 4A).

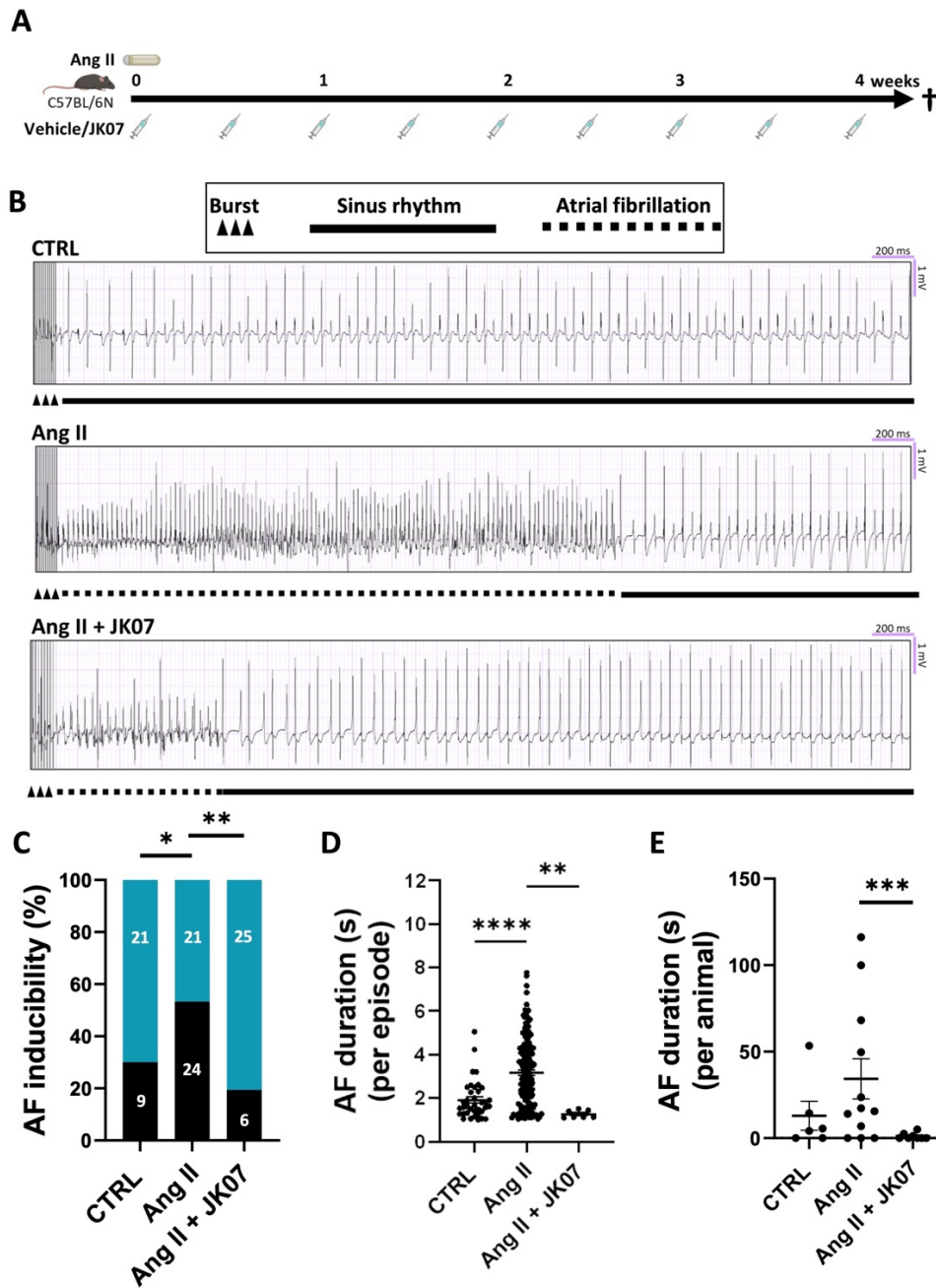


**Figure 27. JK07 prevents AF inducibility and decreases AF duration in an Ang II-induced hypertension mouse model.**

**(A)** Eight-weeks-old male C57BL/6N mice were treated with Ang II (4 weeks, osmotic mini-pumps, 4.3 mg/kg/day) and were randomized to treatment with vehicle or JK07 (2x/week, 1 mg/kg, IV). **(B)** Representative atrial intracardiac electrograms. **(C)** Ang II significantly increased AF inducibility compared to CTRL mice ( $n = 12$  per group;  $p = 0.046$ ; the total amount of AF induced (black) or sinus rhythm (blue) stimulation series are shown in the bar charts). Preventive administration of JK07 (Ang II + JK07,  $n = 8$ ) significantly reduced AF inducibility ( $p = 0.003$ , crosstabulation, Pearson chi-Square test).



(D–E) JK07 significantly reduced AF duration of (D) mean single episode and (E) mean total AF duration per animal ( $p = 3 \times 10^{-6}$ , one-way Anova with Tamhane’s post-hoc analysis). All results are represented as mean  $\pm$  SEM. AF, atrial fibrillation; Ang II, angiotensin II. \* =  $p < 0.05$ , \*\* =  $p < 0.01$ , \*\*\* =  $p < 0.001$ , \*\*\*\* =  $p < 0.0001$ .

We next evaluated whether JK07 could also prevent AF inducibility in mice with HFD-induced obesity. HFD induced severe weight gain after eight weeks compared to regular chow ( $4.8 \pm 0.7$  g vs.  $12.9 \pm 0.9$  g;  $p < 0.0001$ , Figure 28A, B). The weight gain of the HFD + JK07 group was significantly lower than vehicle-treated HFD mice ( $7.4 \pm 0.3$  vs.  $12.9 \pm 0.9$  g;  $p = 6 \times 10^{-4}$ ). However, both groups of mice that received a HFD, with or without JK07 treatment, showed impaired glucose tolerance, with an increased AUC (Figure 28C) compared with mice that received regular chow. Heart weight did not significantly differ between groups, however, heart-to-body weight ratio was significantly lower in mice that received a HFD compared with control mice due to their increased body weight ( $p = 1 \times 10^{-6}$ ; Figure 28D).

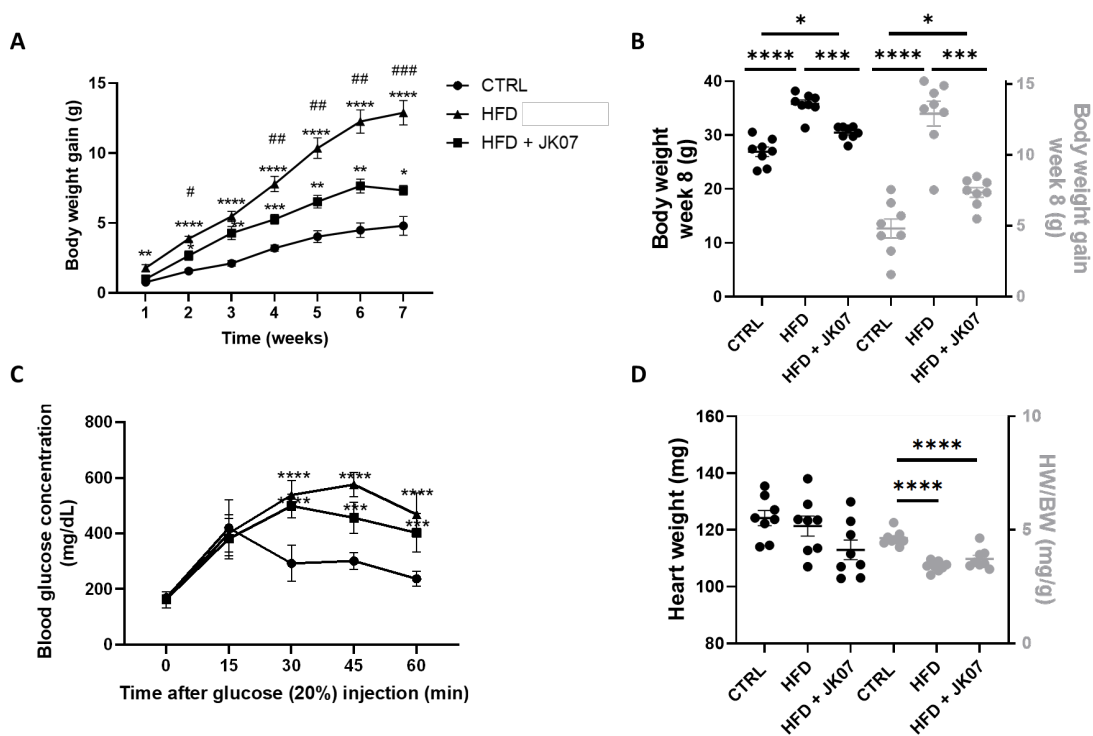


**Figure 28. Effects of HFD and preventive JK07 treatment on body weight (gain), blood glucose concentration and LV hypertrophy in C57BL/6N mice.** C57BL/6N male mice were fed with a high fat diet (HFD, 8 weeks, 60% Kcal fat) resulting in significant increase of body weight. (A) Body weight gain over 8 weeks compared to CTRL mice. \* $p < 0.05$ , \*\* $p < 0.01$ , \*\*\* $p < 0.001$ , \*\*\*\* $p < 0.0001$  indicating a significant overall effect relative to control. # $p < 0.05$ , ## $p < 0.01$ , ### $p < 0.001$ , indicating a significant overall effect of HFD + JK07 treatment relative to HFD. Two-way Anova with

Tukey's post-hoc analysis. **(B)** Body weight (black) and body weight gain (grey) on week 8 of HFD. **(C)** Blood glucose concentration over time, following I.P. injection of glucose (20% V/V) to 6 h fasting animals. \*\*\* $p < 0.001$ , \*\*\*\* $p < 0.0001$ , two-way Anova with Tukey's post-hoc analysis. **(D)** Heart weight (black) and heart-to-body weight ratio after 8 weeks of HFD. Mice fed with a HFD had significantly lower heart-to-body weight due to their increased body weight compared with CTRL mice ( $p = 1 \times 10^{-6}$ ). \*\*\*\* $p < 0.0001$ , one-way Anova with Tukey's post-hoc analysis. All results are represented as mean  $\pm$  SEM.

HFD slightly increased AF inducibility compared to control, but this was not statistically significant (from 29% to 46% per stimulation series;  $p = 0.1$ ; Figure 29C and SFigure 2B). Nevertheless, AF inducibility was significantly decreased in the HFD + JK07 group (from 46% to 11% per stimulation series;  $p = 0.002$ ; Figure 29C and SFigure 2B). With regard to AF duration, JK07 did not affect the mean single episode AF duration (Figure 29D and SFigure 3B), but significantly decreased mean total AF duration (from  $10.9 \pm 3.2$  to  $0.8 \pm 0.5$  s;  $p = 0.002$ ; Figure 3E). Of note, long AF episodes ( $\geq 3$  s) remained nearly absent in HFD mice, and JK07 had no significant effect on the incidence of these episodes. Again, AERP was not different among groups (SFigure 4B).

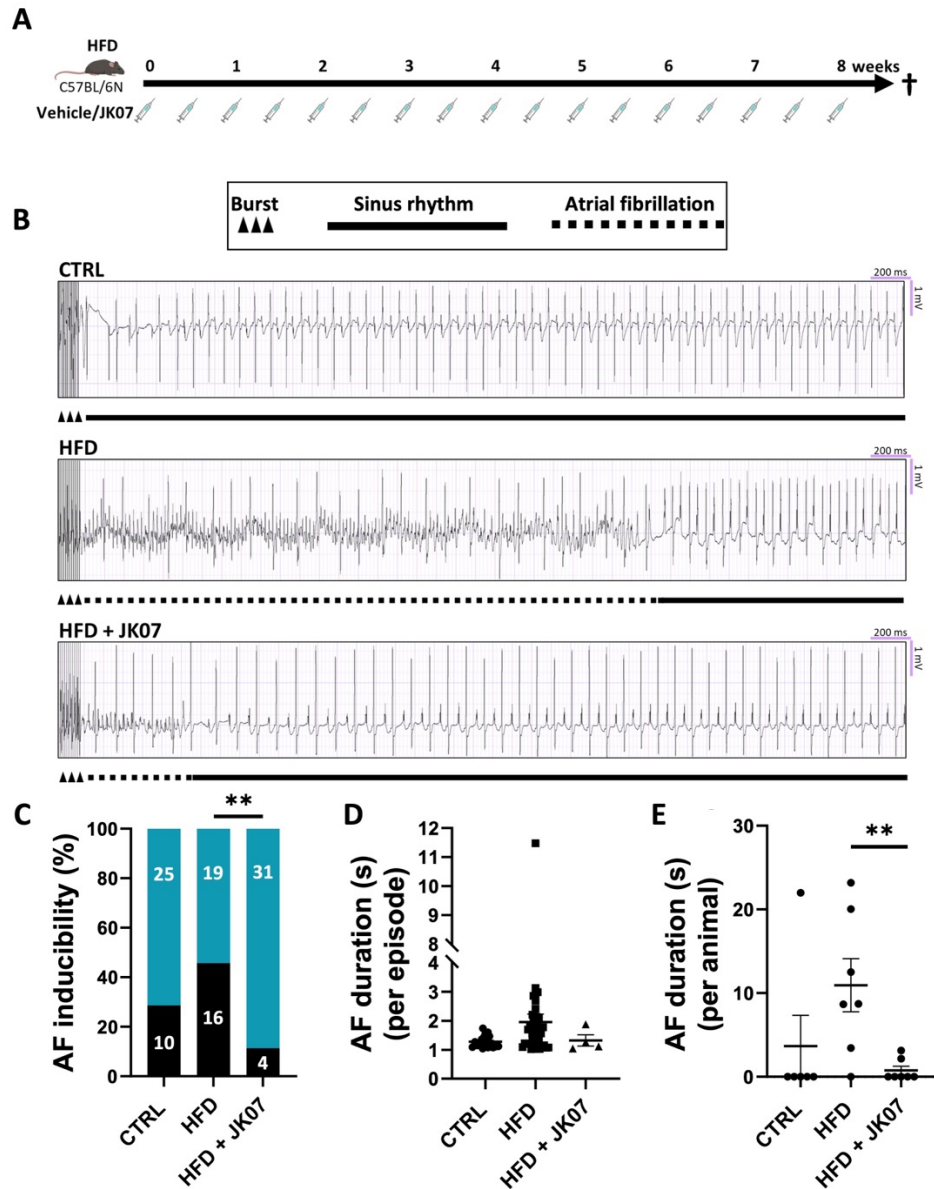


**Figure 29. JK07 prevents AF inducibility and AF duration in an HFD induced obesity mouse model.** (A) C57BL/6N male mice were fed a HFD (60% Kcal of fat, 8 weeks) and randomized to treatment with vehicle or JK07 (2x/week, 1 mg/kg, I.V.). (B) Representative atrial electrograms to detect AF after intracardiac stimulation. (C) AF inducibility was significantly reduced after 8 weeks of preventive administration of JK07 ( $n = 7$ ) compared to HFD ( $n = 7$ ;  $p = 0.002$ ; the total amount of AF induced (black) or sinus rhythm (blue) stimulation series are shown in the bar charts). (D–E) JK07 did not affect AF duration of (D) mean single episode, but significantly reduced (E) mean total AF duration compared to HFD ( $n = 7$ ;  $p = 0.002$ ; one-way Anova with Tamhane’s post-hoc analysis). All results are represented as mean  $\pm$  SEM. AF, atrial fibrillation; HFD, high fat diet. \*\* =  $p < 0.01$ .

## Effects of JK07 on atrial fibrosis

Because atrial fibrosis is important in the pathophysiology of AF, and because we showed that ERBB4 activation decreases fibrosis in *ex vivo* atrial tissue samples (chapter 4), we quantified atrial fibrosis in these models. Surprisingly, neither Ang II nor HFD increased interstitial fibrosis in left (Figure 30 A, B) or right (SFigure 5A, B) atrium compared with control mice within the timeframe of our study. In the absence of increased atrial fibrosis in these models, JK07 treatment did not influence fibrosis in the Ang II + JK07 and HFD + JK07 groups. Based on this result, we could not conclude about the preventive effects of JK07 (and the role of ERBB4) on atrial fibrosis. In a small separate study, however, we investigated the role of ERBB4 during atrial fibrosis in another way. In this experiment, we used Mye-KO mice, in which the ERBB4 receptor is deleted in macrophages and neutrophils. When exposed to Ang II (2.9 mg/kg/day), these mice, developed significantly more left atrial fibrosis than control Mye-KO mice ( $10.3 \pm 1.3$  vs.  $4.9 \pm 1$ ;  $p = 0.02$  Figure 30C), indicating that ERBB4 on macrophages plays a counterregulatory role during development of atrial fibrosis, hence recapitulating the observations by Vermeulen *et al.* in ventricular fibrosis, and showing the role of ERBB4 in atrial fibrosis. Of note, similarly as Vermeulen *et al.*, no significant differences in left atrial macrophage infiltration were observed between Mye-KO mice and their wild type littermates after four weeks of Ang II (Figure 30D).

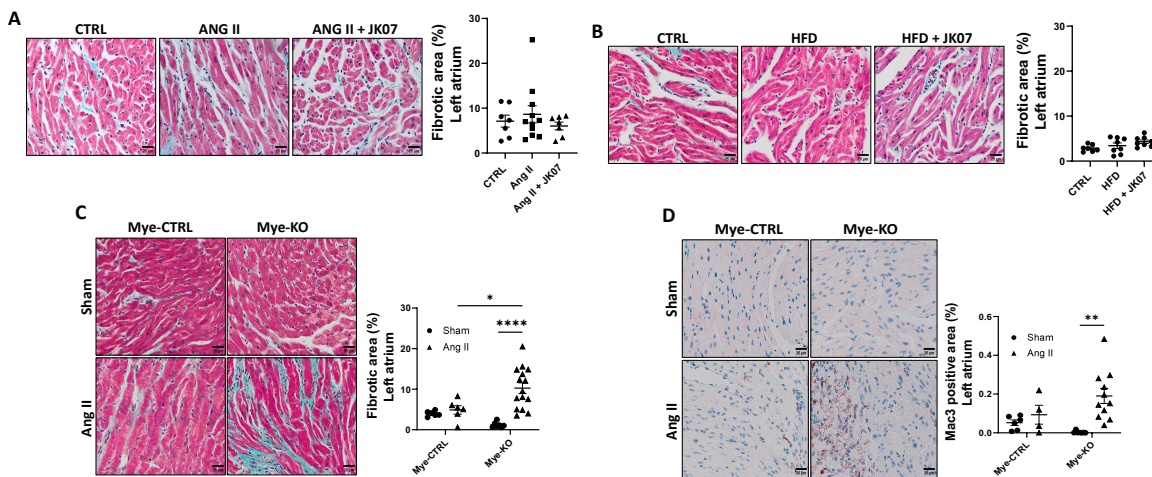


**Figure 30. Effects of Ang II, HFD and JK07 on left atrial fibrosis and macrophage infiltration. (A)** Left: representative Masson's trichrome stained left atrial sections of C57BL/6N mice implanted with Ang II (4.3 mg/kg/day) osmotic minipumps for four weeks or sham operated and treated with vehicle or JK07 (n = 7-11 per group; scale bars = 25  $\mu$ m). Right: quantification of the percentage fibrotic area. **(B)** Left: representative Masson's trichrome stained left atrial sections of C57BL/6N mice fed with a HFD or regular chow for eight weeks and treated with vehicle or JK07

(n = 7-8 per group; scale bars = 25  $\mu$ m). Right: quantification of the percentage fibrotic area. **(C)** Left: representative Masson's trichrome stained left atrial sections of *ErbB4<sup>F/F</sup>LysM-Cre<sup>+/-</sup>* (Mye-KO) and *ErbB4<sup>F/F</sup>LysM-Cre<sup>-/-</sup>* (Mye-CTRL) mice implanted with Ang II (2.9 mg/kg/day) osmotic minipumps for four weeks or sham operated (n = 6-15 per group; scale bars = 25  $\mu$ m). Right: quantification of the percentage fibrotic area. \*p < \*\*\*\*p < 0.0001, two-way Anova with Tukey's post-hoc analysis. **(D)** Left: representative Mac-3 stained left atrial sections Mye-KO and Mye-CTRL mice implanted with Ang II (2.9 mg/kg/day) osmotic minipumps for four weeks or sham operated (n = 4-11 per group; scale bars = 25  $\mu$ m). Right: quantification of the percentage macrophage infiltration. \*\* p < 0.01, two-way Anova with Tukey's post-hoc analysis. All results are represented as mean  $\pm$  SEM.

### **JK07 has therapeutic effects on AF inducibility in Ang II-treated mice.**

We next hypothesized that JK07 would also attenuate AF inducibility when given to Ang II-treated mice after development of increased AF inducibility. To test this hypothesis, we analyzed the effect of a brief, one week therapeutic JK07 treatment (two injections in one week) starting after completing a three week administration with Ang II. We opted for a short treatment with JK07 to test for rapid effects on AF. In this therapeutic strategy, JK07 significantly decreased AF inducibility compared to vehicle-treated Ang II mice (from 73% to 38% per stimulation series; p = 0.003; Figure 31C and SFigure 2C). Surprisingly, the single episode AF duration was shorter following Ang II treatment compared to CTRL ( $3.5 \pm 0.2$  vs.  $2.2 \pm 0.1$  s; p =  $6 \times 10^{-9}$ ; Figure 31D and SFigure 3C) and therapeutic JK07 treatment ( $2.2 \pm 0.1$  vs.  $3.1 \pm 0.2$  s; p =  $6 \times 10^{-5}$ ). In contrast to the mean single episode, total AF duration was not changed over the groups (Figure 31E). Again, AERP was not different among groups (SFig. 4C).

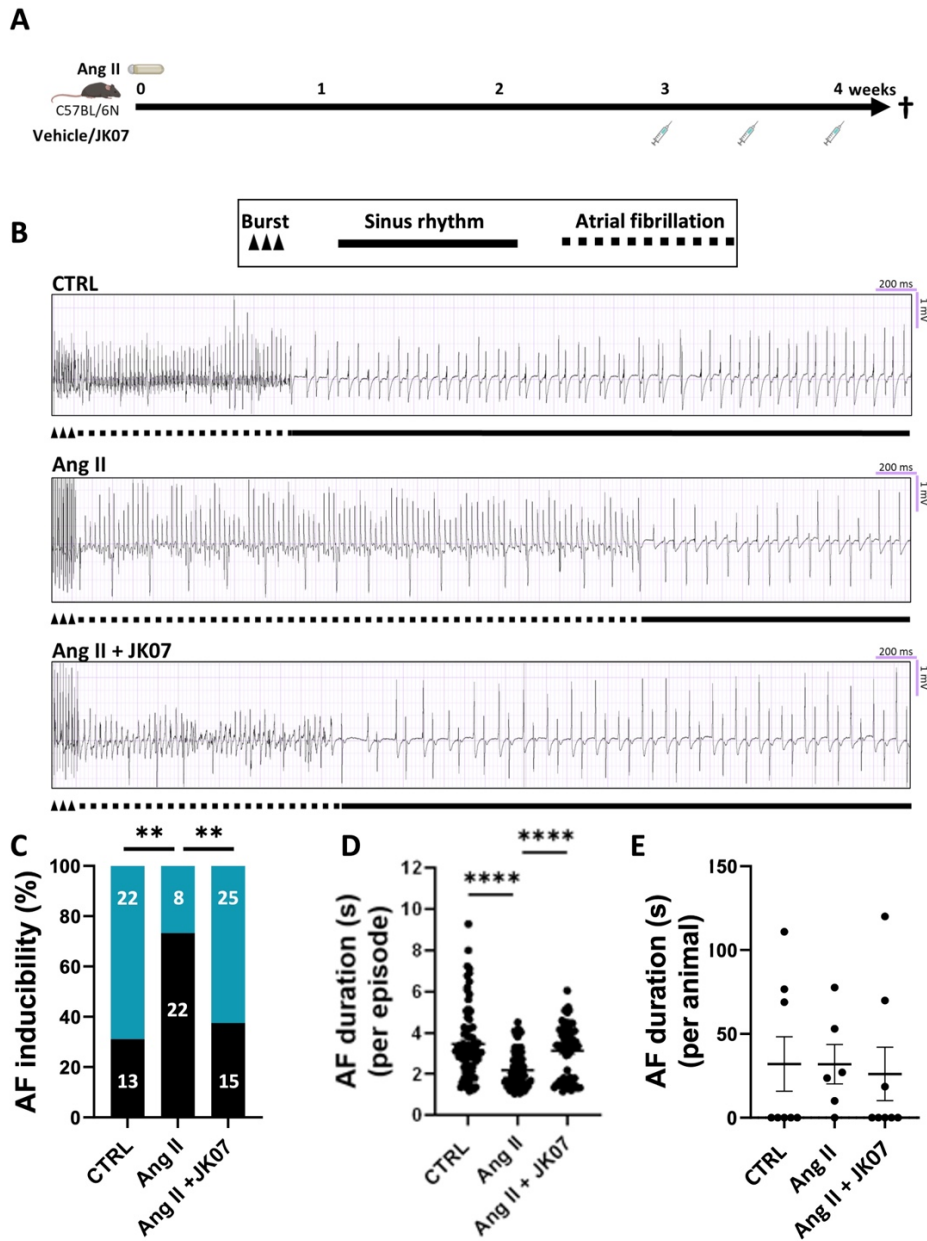


**Figure 31. JK07 treats AF inducibility but not AF duration in an Ang-II induced hypertension mouse model. (A)** C57BL/6N male mice were treated with Ang II (4 weeks, osmotic mini-pumps, 4.3 mg/kg/day) and were randomized for 1 week of treatment with vehicle or JK07 (2x/week, 1mg/kg, I.V.). **(B)** Representative atrial electrograms to detect AF after intracardiac stimulation. **(C)** AF inducibility was significantly increased after Ang II treatment (n = 6) compared to CTRL mice (n = 8) ( $p = 0.004$ ). Treatment with JK07 (Ang II + JK07, n = 8) significantly reduced AF inducibility ( $p = 0.003$ ; the total amount of AF induced (black) or sinus rhythm (blue) stimulation series are shown in the bar charts). **(D)** The mean single episode AF duration was significantly lower in the Ang II group. **(E)** No differences were seen in mean total AF duration between all groups. All results are represented as mean  $\pm$  SEM. AF, atrial fibrillation; AERP, atrial effective refractory period.

## Discussion

In the studies described in this chapter, we showed that JK07, both in a preventive and therapeutic strategy, reduced AF inducibility during EP studies in two distinct mouse models. In the preventive treatment strategy, JK07 also reduced PES-induced AF duration. By using two models with distinct pathophysiological backgrounds (based on Ang II-induced hypertension and obesity-induced cardiovascular remodeling) we extended the significance of our findings.

One could argue that the protective effects of JK07 against AF inducibility in the HFD model may be explained by a significant reduction of weight gain, but since the GTT in these JK07-treated HFD mice remained disturbed —endorsing persistence of HFD-induced metabolic disease— this explanation lacks strength, suggesting that other mechanisms are involved. Of note, in a phase Ib human clinical trial, JK07 was well-tolerated. Moreover, studies in primates, performed by Salubris Biotherapeutics, showed that JK07 did not result in clinically significant findings concerning food intake and nausea (13). Importantly, in the Ang II-induced hypertension mice, JK07 had no effect on body weight.

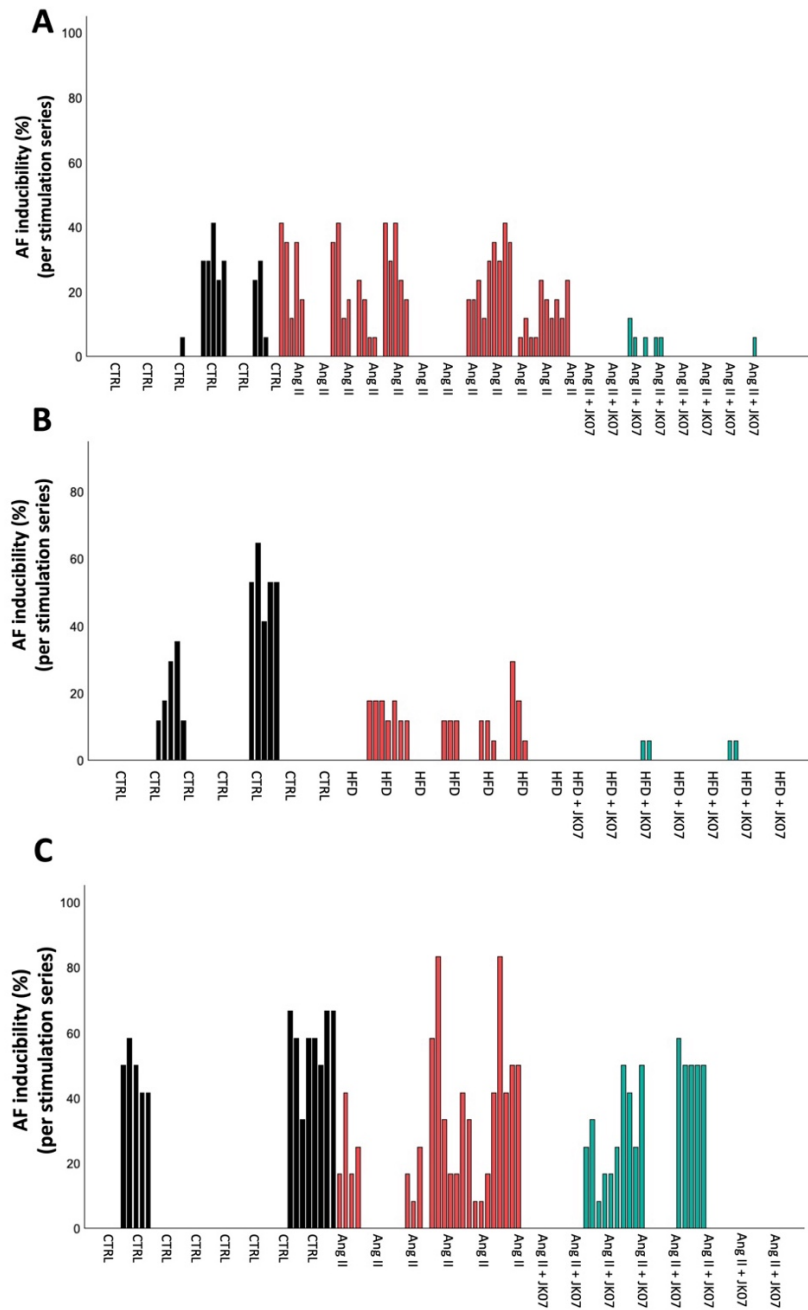
We hypothesized that JK07 attenuated AF inducibility and duration in both models by attenuating atrial fibrosis. Surprisingly, the effects of JK07 in mice were not accompanied by reduced atrial fibrosis. In fact, atrial fibrosis remained insignificant in these mice models — at least within the timespan of our experiments. Absence of increased atrial fibrosis in our mouse models contrasts with previous studies that have shown marked atrial fibrosis, both in Ang II-induced hypertension (5, 7, 8) and after a HFD (10, 11). Of note, despite the absence of atrial fibrosis, we observed increased left ventricular fibrosis after four weeks of Ang II treatment, as seen in previous studies conducted in our lab (14). The reason for this discrepancy in atrial fibrosis between our and previous studies is unclear, but differences in exposure time to Ang II and HFD, as well as the age of the mice may have played a role. We speculate that atrial fibrosis may need more time to develop than ventricular fibrosis. Of note, the lack of effect of JK07 on the extent of atrial fibrosis in our studies, did not allow to conclude on the role of ERBB4 in the control of atrial fibrosis. To address this specific question more directly, we implanted Ang II osmotic minipumps in mice with a myeloid-specific *ErbB4* deletion. Previous studies with this model showed an exaggerated fibrotic response in the left ventricle, supporting a role for ERBB4 in ventricular fibrosis (14). Mye-KO mice showed aggravated Ang II-induced atrial inflammation and fibrosis. This observation

supports the role for the NRG1/ERBB4 pathway as an endogenous counterregulatory system in atrial remodeling, at least through regulation of the function of inflammatory cells. Based on these observations we conclude that activation of the NRG1/ERBB system, and especially ERBB4 signaling, emerges as a promising pathway to target atrial fibrosis and prevent development of AF. If not by attenuating atrial fibrosis, how could JK07 attenuate AF inducibility and duration in our mouse models? Importantly, JK07 preserved its effects on AF inducibility –but not AF duration– during a therapeutic treatment strategy in which a brief JK07 treatment was started after three weeks of Ang II-induced hypertension. Since this brief therapeutic regimen is likely too short to significantly alter structural atrial changes induced by Ang II, we speculate that JK07 has effects on functional properties of atrial cardiomyocytes, e.g. electrical properties, involved in the generation of AF.

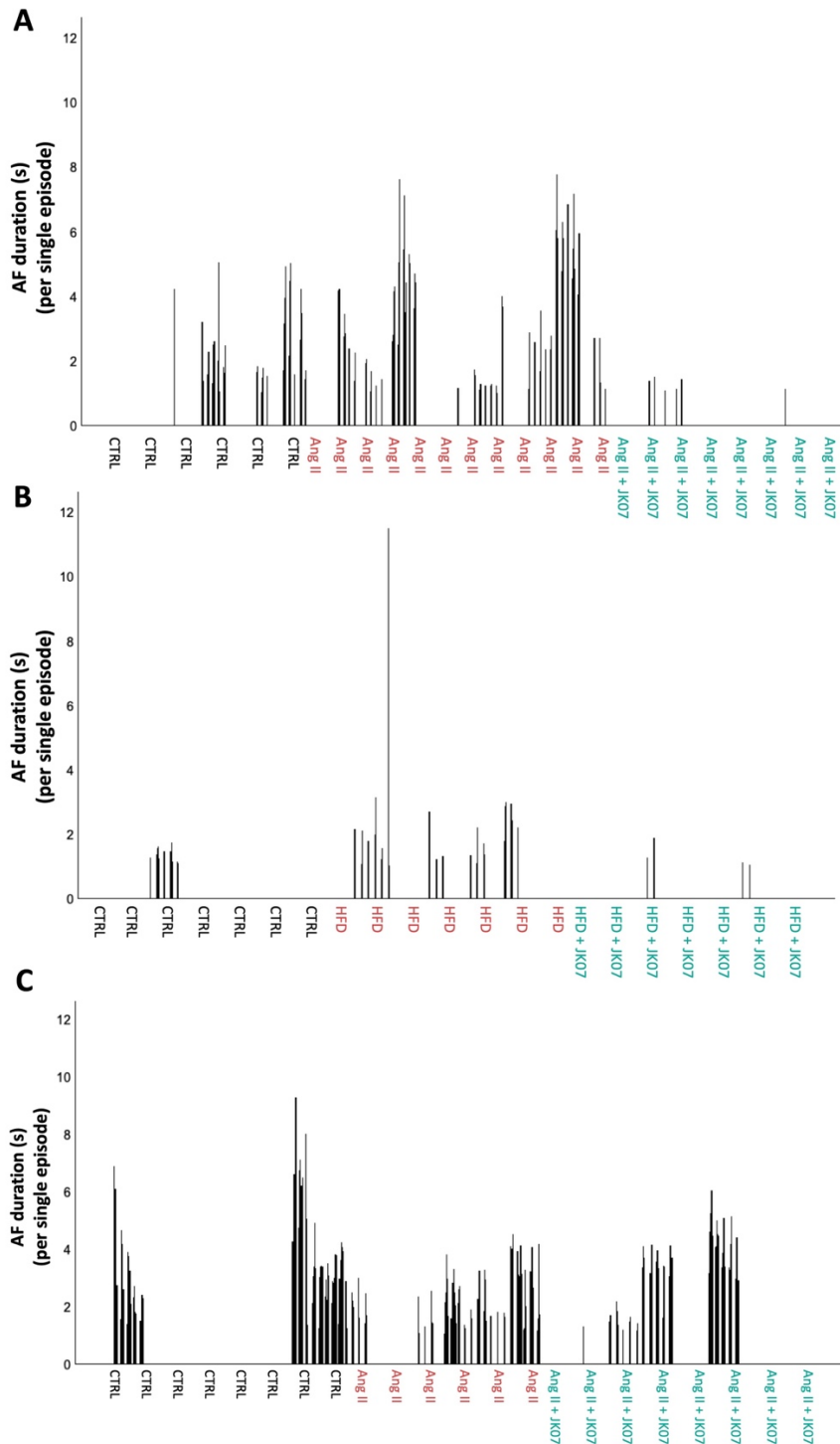
Taken together, JK07 reduced AF inducibility and duration in a preventive manner in 2 distinct mouse models with a different pathophysiological background. Furthermore, a shorter, therapeutic treatment of JK07 significantly reduced AF inducibility in Ang II-induced hypertensive mice. Since, no effects on atrial fibrosis and AERP were observed, we speculate that JK07 has direct effects on (electrophysiological) properties of atrial myocytes. To answer this question, we investigated the direct effects of JK07 on atrial cardiomyocytes in the following chapter.



## Supplemental figures



**SFigure 2. Waterfall plots of AF inducibility per stimulation series.** Graph bars represent AF inducibility (%) for each animal per stimulation series. **(A)** AF inducibility in Ang II mice (preventive regimen; black, CTRL; red, Ang II; green, Ang II + JK07). **(B)** AF inducibility in HFD mice (preventive regimen; black, CTRL; red, HFD; green, HFD + JK07). **(C)** AF inducibility in Ang II mice (therapeutic regimen; black, CTRL; red, Ang II; green, Ang II + JK07).



**Supplemental figure 3. Waterfall plots of AF duration per single episode.** Graph bars represent AF duration (s) of every single AF-induced episode per stimulation for each animal. **(A)** AF-durations in Ang II mice (preventive regimen; black, CTRL; red, Ang II; green, Ang II + JK07). **(B)** AF durations in HFD mice (preventive regimen; black, CTRL; red, HFD; green, HFD + JK07). **(C)** AF durations in minipigs (therapeutic regimen; black, CTRL; red, Ang II; green, Ang II + JK07).

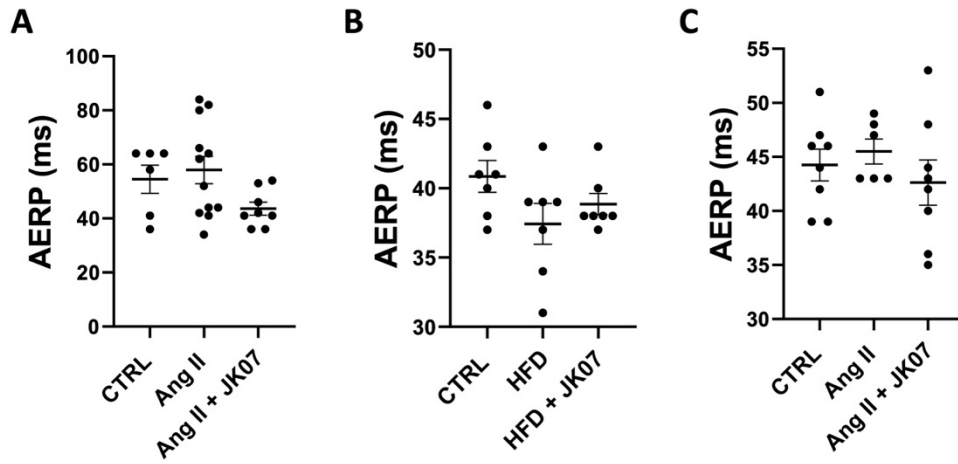


**Figure 4. Effects of JK07 on AERP in distinct mouse models of AF. (A)** AERP of Ang II-treated mice (preventive regimen), **(B)** AERP of HFD mice (preventive regimen), and **(C)** AERP of Ang II-treated mice (therapeutic regimen). AERP, atrial effective refractory period. Mean  $\pm$  SEM.

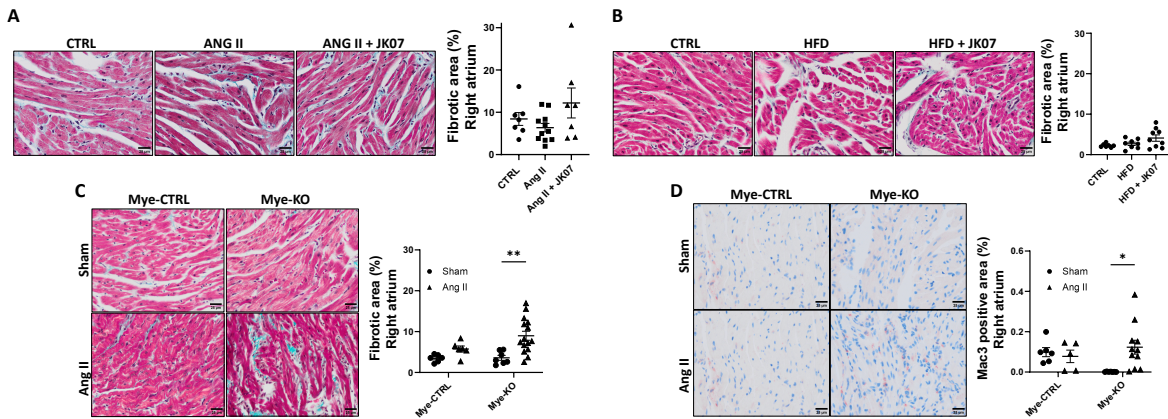
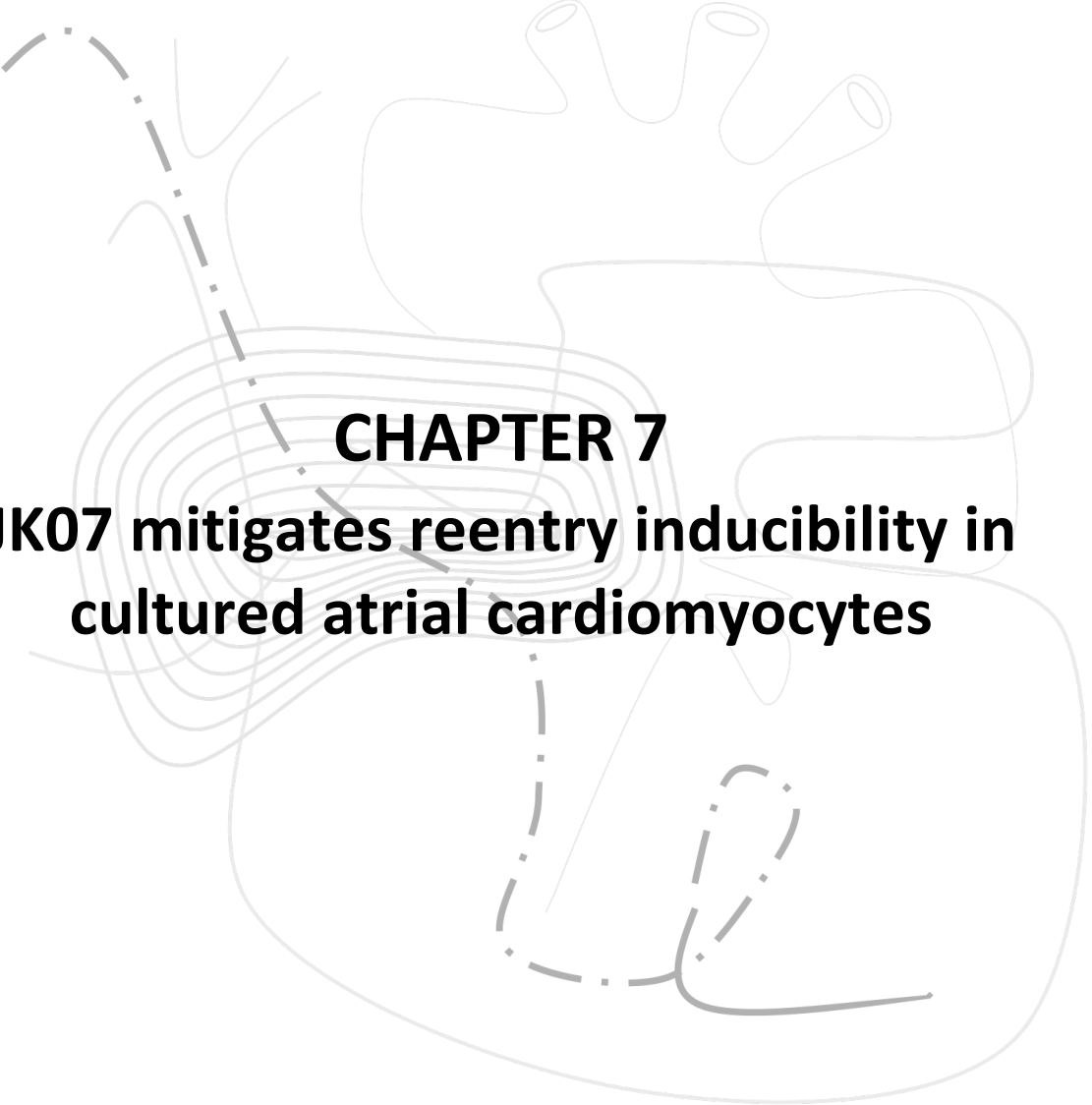


**Figure 5. Effects of Ang II, HFD and JK07 on right atrial fibrosis and macrophage infiltration. (A)** Left: representative Masson's trichrome stained right atrial sections of C57BL/6N mice implanted with Ang II (4.3 mg/kg/day) osmotic minipumps for four weeks or sham operated and treated with vehicle or JK07 (n = 7-11 per group; scale bars = 25  $\mu$ m). Right: quantification of the percentage fibrotic area. **(B)** Left: representative Masson's trichrome stained right atrial sections of C57BL/6N mice fed with a HFD or regular chow for eight weeks and treated with vehicle or JK07 (n = 7-8 per group; scale bars = 25  $\mu$ m). Right: quantification of the percentage fibrotic area. **(C)** Left: representative Masson's trichrome stained right atrial sections of *ErbB4<sup>F/F</sup>LysM-Cre<sup>+/-</sup>* (Mye-KO) and *ErbB4<sup>F/F</sup>LysM-Cre<sup>-/-</sup>* (Mye-CTRL) mice implanted with Ang II (2.9 mg/kg/day) osmotic minipumps for four weeks or sham operated (n = 6-15 per group; scale bars = 25  $\mu$ m). Right: quantification of the percentage fibrotic area. \*\*p < 0.01, two-way Anova with Tukey's post-hoc analysis. **(D)** Left: representative Mac-3 stained right atrial sections Mye-KO and Mye-CTRL mice implanted with Ang II (2.9 mg/kg/day) osmotic minipumps for four weeks or sham operated (n = 4-11 per group; scale bars = 25  $\mu$ m). Right: quantification of the percentage macrophage infiltration. \*p < 0.01, two-way Anova with Tukey's post-hoc analysis. All results are represented as mean  $\pm$  SEM.

## References

1. Hindricks G, Potpara T, Dagres N, Arbelo E, Bax JJ, Blomström-Lundqvist C, et al. 2020 ESC Guidelines for the diagnosis and management of atrial fibrillation developed in collaboration with the European Association for Cardio-Thoracic Surgery (EACTS): The Task Force for the diagnosis and management of atrial fibrillation of the European Society of Cardiology (ESC) Developed with the special contribution of the European Heart Rhythm Association (EHRA) of the ESC. *European Heart Journal*. 2020;42(5):373-498.
2. Nattel S. New ideas about atrial fibrillation 50 years on. *Nature*. 2002;415(6868):219-26.
3. Nattel S, Heijman J, Zhou L, Dobrev D. Molecular Basis of Atrial Fibrillation Pathophysiology and Therapy. *Circulation Research*. 2020;127(1):51-72.
4. Walker M, Patel P, Kwon O, Koene RJ, Duprez DA, Kwon Y. Atrial Fibrillation and Hypertension: "Quo Vadis". *Curr Hypertens Rev*. 2022;18(1):39-53.
5. Jansen HJ, Mackasey M, Moghtadaei M, Belke DD, Egom EE, Tuomi JM, et al. Distinct patterns of atrial electrical and structural remodeling in angiotensin II mediated atrial fibrillation. *Journal of Molecular and Cellular Cardiology*. 2018;124:12-25.
6. Kondo H, Abe I, Gotoh K, Fukui A, Takanari H, Ishii Y, et al. Interleukin 10 Treatment Ameliorates High-Fat Diet–Induced Inflammatory Atrial Remodeling and Fibrillation. *Circulation: Arrhythmia and Electrophysiology*. 2018;11(5):e006040.
7. Xie X, Shen T-t, Bi H-l, Su Z-l, Liao Z-q, Zhang Y, et al. Melatonin inhibits angiotensin II–induced atrial fibrillation through preventing degradation of Ang II Type I Receptor–Associated Protein (ATRAP). *Biochemical Pharmacology*. 2022;202:115146.
8. Han X, Zhang Y-L, Zhao Y-X, Guo S-B, Yin W-P, Li H-H. Adipose Triglyceride Lipase Deficiency Aggravates Angiotensin II–Induced Atrial Fibrillation by Reducing Peroxisome Proliferator–Activated Receptor  $\alpha$  Activation in Mice. *Laboratory Investigation*. 2023;103(1).
9. Takahashi K, Sasano T, Sugiyama K, Kurokawa J, Tamura N, Soejima Y, et al. High-fat diet increases vulnerability to atrial arrhythmia by conduction disturbance via miR-27b. *Journal of Molecular and Cellular Cardiology*. 2016;90:38-46.
10. McCauley MD, Hong L, Sridhar A, Menon A, Perike S, Zhang M, et al. Ion Channel and Structural Remodeling in Obesity-Mediated Atrial Fibrillation. *Circ Arrhythm Electrophysiol*. 2020;13(8):e008296.
11. Bapat A, Li G, Xiao L, Yeri A, Hulsmans M, Grune J, et al. Genetic inhibition of serum glucocorticoid kinase 1 prevents obesity-related atrial fibrillation. *JCI Insight*. 2022;7(19).
12. Huxley RR, Lopez FL, Folsom AR, Agarwal SK, Loehr LR, Soliman EZ, et al. Absolute and Attributable Risks of Atrial Fibrillation in Relation to Optimal and Borderline Risk Factors. *Circulation*. 2011;123(14):1501-8.
13. John Li SL, Dixiang LUO, Yiran WU, Ming Zhou, Yang Wang, Xiaolei Zhuang, Liang Hua, Pengyi LUO inventor Human neuregulin-1 (nrg-1) recombinant fusion protein compositions and methods of use thereof. United States patent US2020/0010522 A1. 2020 9 January.
14. Vermeulen Z, Hervent AS, Dugaucquier L, Vandekerckhove L, Rombouts M, Beyens M, et al. Inhibitory actions of the NRG-1/ErbB4 pathway in macrophages during tissue fibrosis in the heart, skin, and lung. *Am J Physiol Heart Circ Physiol*. 2017;313(5):H934-h45.





**CHAPTER 7**  
**JK07 mitigates reentry inducibility in cultured atrial cardiomyocytes**

## ADAPTED FROM

*Jens van fraeyenhove\**; Michiel R.L. Tubeeckx\*; Bo Govaerts; Yile Fue; Juan Zhang; Arthur Bezerra; Tim De Coster; Julie Cools; Eike M. Wülfers; Siel Van den Bogaert; Bernard Thienpont; Samuel L Murphy; Antoine A.F. de Vries; Erik Fransen; Nele Vandersickel; Daniël A. Pijnappels; Guido Y. De Meyer; Hein Heidbuchel; Llewelyn H. Roderick; Vincent F.M. Segers; Gilles W. De Keulenaer. (Data reported in this chapter are submitted for publication (“ERBB4 activation as a new therapy for atrial remodeling and fibrillation”), in a manuscript that also contains studies of JK07 performed in a pig model of AF).



## Introduction

In the previous chapter we showed that the ERBB4 agonist JK07 attenuated AF inducibility in two distinct mouse models, and that this effect could not be explained by concomitant effects on atrial fibrosis or on AERP. Moreover, effects of JK07 were mostly preserved when given after induction of cardiac remodeling and only for one week, which is likely too short to reverse structural remodeling. Therefore, we hypothesized that JK07 has direct, (sub-)acute effects on atrial cardiomyocytes, which may be fast and reverse functional abnormalities. To test this hypothesis and to understand more of the underlying effects of ERBB4 activation on atrial cardiomyocytes, we first analyzed atrial cardiomyocyte gene expression using RNA-sequencing technology. For this experiment, we used conditional immortalized neonatal rat atrial cardiomyocytes (iAMs), developed by the Laboratory of Experimental Cardiology in Leiden (1), because these cells display a high proliferation capacity and form a confluent monolayer, with preserved cardiomyogenic differentiation abilities. By means of a doxycycline-controlled system iAMs can either dedifferentiate (showing loss of excitability and disassembly of sarcomeres) with subsequent proliferation, or either initiate growth arrest with spontaneous cardiomyogenic differentiation in excitable and contractile cells (showing well-organized sarcomeres). This system allows access to control large numbers of functional cardiomyocytes, with electrophysiological properties superior to other existing atrial cardiomyocyte cell lines (2). Next, we tested the direct effects of ERBB4 activation on reentry (spiral wave) formation in an iAM-based AF model. For these experiments, we used human-derived iAMs that meanwhile had become available. Using human cells increases the translational value of the experiments, especially since atrial myocytes exhibit species-specific functional properties both in terms of excitability and contractility (3). Since JK07 exhibited a significant reduction on AF inducibility and duration in two distinct mouse models (chapter 6), we hypothesized that ERBB4 activation would reduce reentry inducibility in hiAM monolayers, secondary to altering electrical activity of atrial cardiomyocytes. This hypothesis was tested by treating hiAM monolayers with JK07 or its vehicle, and by evaluating reentry inducibility through electrical point stimulation during optical voltage experiments.

The hiAM monolayers have been extensively studied and compared to other *in vitro* models of AF (such as human embryonic stem cell lines and human induced pluripotent stem cell lines). As shown in a study by Harlaar *et al.*, hiAM monolayers enabled the creation of human AF models

featuring fibrillatory activity at clinically relevant frequencies, which were terminated using currently relevant antiarrhythmic drugs (3).

## Materials and methods

Materials and methods are described in chapter 3.

## Results

### ERBB4 activation changes ion channel genes expression in iAMs.

First, we performed RNA-sequencing studies to analyze the transcriptomic changes induced by ERBB4 activation (using NRG1) in differentiated (D12) iAMs. iAMs were treated with PBS (n = 4) or NRG1 (n = 4) for 16h. Principal component analysis illustrated a clear separation between NRG1 treated and control (PBS treated) iAMs. As shown in Figure 32A, grouped comparison revealed 5028 differentially expressed genes of which 2384 were downregulated and 2644 were upregulated ( $\log_2$  fold change > 1.5 and false discovery rate (FDR)-corrected p < 0.05). Hierarchical clustering of the 25 most upregulated and 25 most downregulated DEGs identified a clear distinction between iAMs by their corresponding treatment group, indicating that iAMs are highly responsive to NRG1 (Figure 32B).

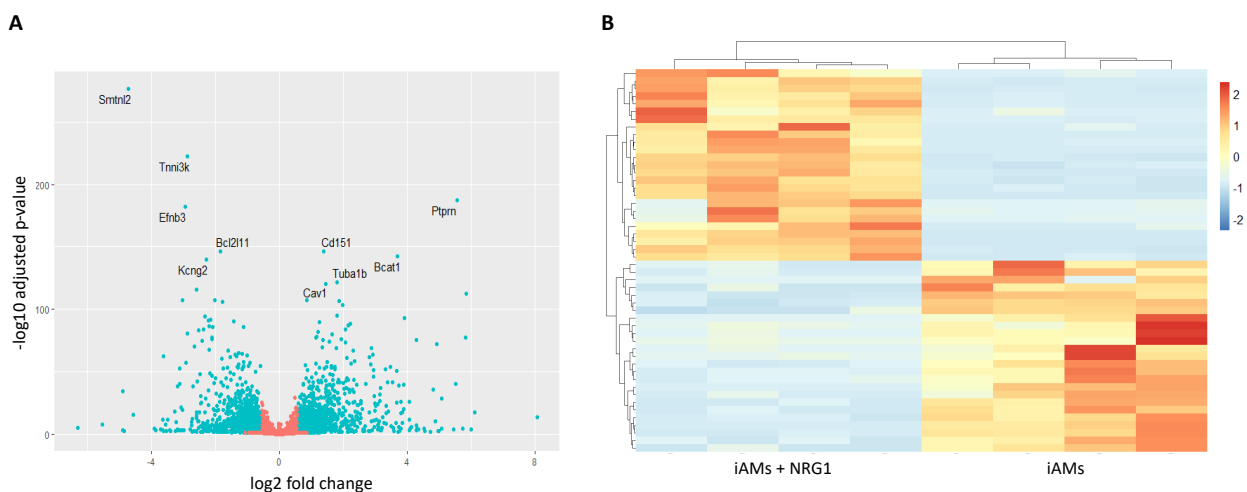


**Figure 32. Effect of ERBB4 activation on gene expression profiles of immortalized atrial cardiomyocytes (iAMs).** (A) Volcano plot of gene expression in iAMs treated with either PBS (n = 4) or NRG1 (n = 4; 0.1  $\mu$ M, 16 h). (B) Hierarchical clustering of differentially expressed genes in iAMs after PBS or NRG1 treatment in a heat map of the top 25 up and 25 down regulated genes.

All DEGs of NRG1 treated iAMs were compared with a list of 221 ion channel genes found on the IUPHAR/BPS database. Table 1 illustrates 20 differential expressed (DE) ion channel genes upregulated more than 1.5 fold, whereas Table 2 indicates 30 DE ion channel genes more than 1.5 fold downregulated compared to control samples.

NRG1 mostly downregulated ion channel genes that are associated with a gain-of-function in human patients with AF. Five of the most studied and known ion channel gene variants linked with an increase in AF susceptibility are SCN10A and SCN5A, KCNQ1, RYR2 and RYR3, and appeared to be downregulated in iAMs after NRG1 treatment.

**Table 1. Comparison of ion channel gene expression in iAMs with and without NRG1 treatment.** Upregulated ion channel genes (> 1.5 fold) in iAMs after 16 h of PBS or NRG1 treatment (n = 4 per group) were analyzed using RNA-sequencing. Data are ranked according to fold change expression. Log<sub>2</sub> fold change (log<sub>2</sub> FC) and adjusted p-value (padj) are shown relative to control (PBS) samples.

Gene	Gene name	padj	log <sub>2</sub> FC
KCNK7	potassium two pore domain channel subfamily K member 7	0.00548	4.98
TRPV2	transient receptor potential cation channel subfamily V member 2	1.39 <sup>E</sup> -11	2.36
HTR3A	5-hydroxytryptamine receptor 3A	1.58 <sup>E</sup> -08	1.97
ORAI2	ORAI calcium release-activated calcium modulator 2	1.27 <sup>E</sup> -14	1.80
KCNC1	potassium voltage-gated channel subfamily C member 1	1.33 <sup>E</sup> -06	1.68
ITPR3	inositol 1,4,5-trisphosphate receptor type 3	2.29 <sup>E</sup> -11	1.59
PIEZO1	piezo type mechanosensitive ion channel component 1	4.49 <sup>E</sup> -10	1.21
ORAI1	ORAI calcium release-activated calcium modulator 1	1.51 <sup>E</sup> -10	1.13
CLCN1	chloride voltage-gated channel 1	2.19 <sup>E</sup> -07	1.03
KCNA1	potassium voltage-gated channel subfamily A member 1	0.001014	0.90
CLCN5	chloride voltage-gated channel 5	0.001455	0.90
TRPV4	transient receptor potential cation channel subfamily V member 4	0.006243	0.85
CFTR	CF transmembrane conductance regulator	8.39 <sup>E</sup> -10	0.79
CACNA1S	calcium voltage-gated channel subunit alpha1 S	0.000182	0.77
P2RX4	purinergic receptor P2X 4	2.30 <sup>E</sup> -08	0.76
P2RX5	purinergic receptor P2X 5	9.01 <sup>E</sup> -08	0.74
PKD2	polycystin 2, transient receptor potential cation channel	0.001798	0.62
KCNH3	potassium voltage-gated channel subfamily H member 3	4.96 <sup>E</sup> -05	0.62
CLCN6	chloride voltage-gated channel 6	5.65 <sup>E</sup> -05	0.61
KCNK2	potassium two pore domain channel subfamily K member 2	0.028383	0.61

**Table 2. Comparison of ion channel gene expression in iAMs with and without NRG1 treatment.** Downregulated ion channel genes (> 1.5 fold) in iAMs after 16 h of PBS or NRG1 treatment (n = 4 per group) were analyzed using RNA sequencing. Data are ranked according to fold change expression. Log<sub>2</sub> fold change (log<sub>2</sub> FC) and adjusted p-value (padj) are shown relative to control (PBS) samples.

Gene	Gene name	padj	log <sub>2</sub> FC
KCNJ1	potassium inwardly rectifying channel subfamily J member 1	0.000163	-3.73
MCOLN2	mucolipin TRP cation channel 2	0.001253	-3.19
CACNA1G	calcium voltage-gated channel subunit alpha1 G	3.04 <sup>E</sup> -81	-2.87
KCNG4	potassium voltage-gated channel modifier subfamily G member 4	0.000197	-2.80
SCN10A	sodium voltage-gated channel alpha subunit 10	1.19 <sup>E</sup> -09	-2.39
AQP1	aquaporin 1 (Colton blood group)	5.13 <sup>E</sup> -95	-2.33
KCNG2	potassium voltage-gated channel modifier subfamily G member 2	1.99 <sup>E</sup> -140	-2.29
GRIA1	glutamate ionotropic receptor AMPA type subunit 1	2.14 <sup>E</sup> -07	-2.05
SCN5A	sodium voltage-gated channel alpha subunit 5	9.51 <sup>E</sup> -18	-1.66
AQP5	aquaporin 5	1.22 <sup>E</sup> -09	-1.52
CLCNKB	chloride voltage-gated channel Kb	0.001734	-1.43
KCNK3	potassium two pore domain channel subfamily K member 3	6.22 <sup>E</sup> -18	-1.25
KCNQ1	potassium voltage-gated channel subfamily Q member 1	3.80 <sup>E</sup> -16	-1.22
RYR2	ryanodine receptor 2	1.40 <sup>E</sup> -09	-1.15
GRIK1	glutamate ionotropic receptor kainate type subunit 1	4.82 <sup>E</sup> -07	-1.10
KCNF1	potassium voltage-gated channel modifier subfamily F member 1	0.002047	-1.06
KCNB1	potassium voltage-gated channel subfamily B member 1	8.70 <sup>E</sup> -16	-1.05
CNGA1	cyclic nucleotide gated channel subunit alpha 1	7.58 <sup>E</sup> -09	-1.00
KCNN3	potassium calcium-activated channel subfamily N member 3	3.23 <sup>E</sup> -06	-1.00
CACNA1F	calcium voltage-gated channel subunit alpha1 F	2.43 <sup>E</sup> -07	-0.99
KCNN1	potassium calcium-activated channel subfamily N member 1	1.52 <sup>E</sup> -12	-0.95
KCNH6	potassium voltage-gated channel subfamily H member 6	0.000287	-0.84
KCNJ12	potassium inwardly rectifying channel subfamily J member 12	5.35 <sup>E</sup> -05	-0.78
KCNV2	potassium voltage-gated channel modifier subfamily V member 2	5.75 <sup>E</sup> -08	-0.72
PANX2	pannexin 2	0.002329	-0.72
KCNJ3	potassium inwardly rectifying channel subfamily J member 3	0.01629	-0.72
HCN2	hyperpolarization activated cyclic nucleotide gated potassium and sodium channel 2	5.27 <sup>E</sup> -06	-0.68
ASIC1	acid sensing ion channel subunit 1	0.000782	-0.66
HCN4	hyperpolarization activated cyclic nucleotide gated potassium channel 4	5.85 <sup>E</sup> -08	-0.63
RYR3	ryanodine receptor 3	0.002017	-0.59

### JK07 abrogates reentry inducibility in cultured hiAMs.

Since ERBB4 activation by NRG1 changed the transcriptome profile of iAMs, and because ion channel genes were differentially expressed, we hypothesized that the anti-AF effect induced by JK07 in our mouse models, could be related to these changes. Generation and sustainability of AF requires disturbed AP conduction with electrical reentry activity, in which ion channels

dysregulation is involved. We therefore tested the effect of JK07 on reentry activity in a previously validated hiAM-based AF model (3). Prevention or termination of reentry-inducibility was studied through assessment of APD<sub>80</sub> and CV restitution curves, which can be described as the influence of change in CL on APD and CV. Normally, restitution curves follow a downwards slope as the CL becomes shorter, and flattening of the restitution curves generally prevents wave breaks and disorganization. The dynamic response of APD and CV to CL alteration has been shown to be an important determinant of wavefront stability. Conduction of APs in hiAM monolayers was tested by optical voltage mapping. Baseline (1000 ms CL) electrical point stimulation showed homogeneous conduction of APs and treatment with JK07 did not affect the CV ( $12.7 \pm 0.3$  cm/s for CTRL;  $12.6 \pm 0.7$  cm/s for JK07) and the APD<sub>80</sub> ( $94.5 \pm 5.7$  ms for CTRL;  $90.4 \pm 5.5$  ms for JK07). Following stimulations with a decrease in CL (S2 stimuli), reentrant activity (spontaneously terminating and permanent reentry) was induced in 36% of control hiAM monolayers (CL range 100–125 ms). Strikingly, JK07 completely abrogated reentrant activity (Figure 33A-C) although sometimes one or more extra ectopic beats were observed after point stimulation was stopped. We hypothesized that this effect could be explained by an effect of JK07 on the restitution curves of APD<sub>80</sub> and CV. However, as shown in the Figure 33D-E, APD<sub>80</sub> and CV restitution curves were not different between control and JK07 treated hiAM monolayers.

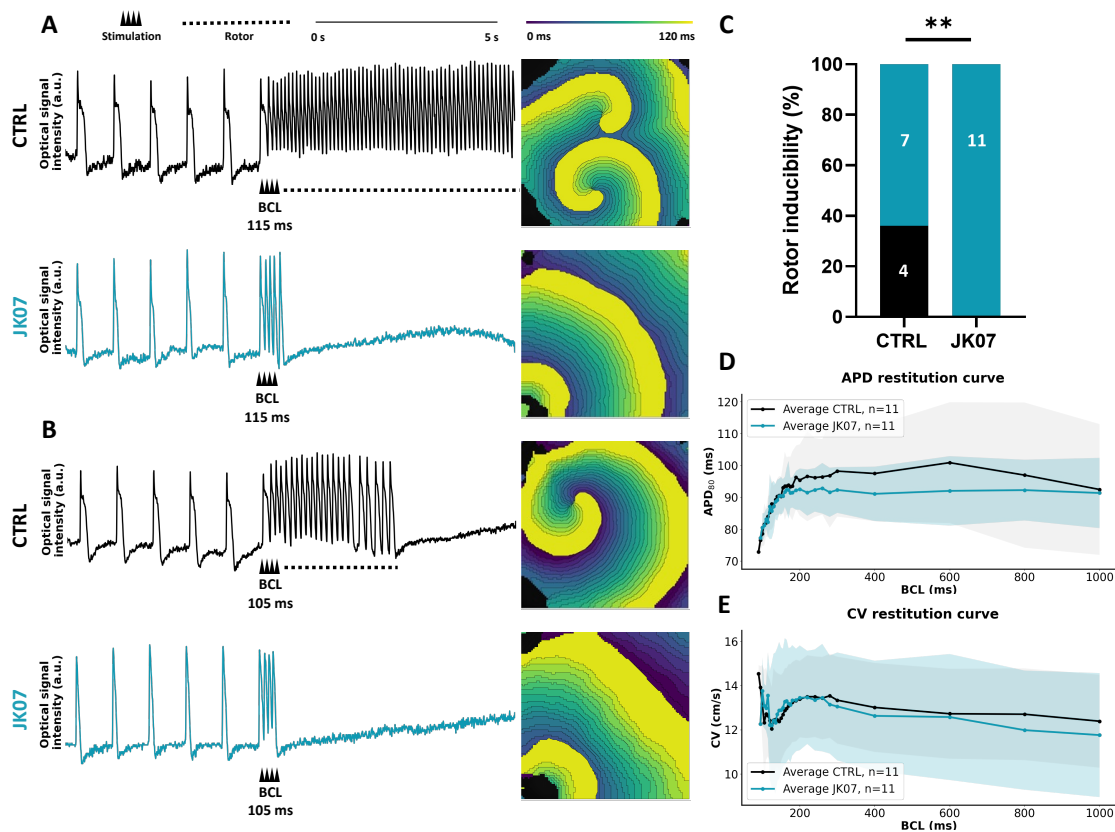


**Figure 33. JK07 prevents induction of reentry in hiAM treatment, prevents reentry inducibility in hiAMs. (A-B)** Representative AP traces and activation maps of **(A)** induced permanent reentrant activity and **(B)** induced spontaneously terminating reentrant activity in control (CTRL, black traces) hiAM monolayers ( $n = 11$  monolayers from 3 independent hiAM differentiations). No reentrant activity (but one additional beat) in JK07 (blue traces) treated hiAM monolayers ( $n = 11$  monolayers from 3 independent hiAM differentiations). **(C)** Induction of reentry was completely prevented in hiAM monolayers treated for 24 h with JK07, compared to control hiAM monolayers ( $n = 11$  per group;  $p = 0.002$ ,  $**p < 0.01$ , crosstabulation, Pearson chi-Square test; the total amount of monolayers with induced reentry activity (black) or in which high-frequency electrical stimulation failed to induce reentry (blue) are shown in the bar charts). No differences were observed between hiAM monolayers in **(D)** APD<sub>30</sub> and **(E)** CV restitution curves with JK07 or vehicle treatment (shaded area indicates  $\pm$  SD). All results are represented as mean  $\pm$  SEM. AP, action potential; hiAM, human conditionally immortalized atrial myocytes; APD, action potential duration; CV, conduction velocity.

## Discussion

In this study we showed that ERBB4 activation widely changed gene expression of iAMs, which included the expression of distinct ion channel genes. Additionally, we showed that JK07 robustly prevents rotor inducibility in a hiAM-based AF model during optical voltage mapping experiments. In chapter 6, we observed that JK07 treatment reduced PES-induced AF inducibility and sustainability, an effect unlikely explained by effects on atrial fibrosis. Here, we show direct effects of NRG1 on gene expression of ion channels by rat iAMs. Although NRG1 is less selective for ERBB4 than JK07 and also activates ERBB3, previous experiments have demonstrated that rat iAMs show a high ERBB4 but no ERBB3 expression. Therefore, the effects of NRG1 in rat iAM experiments described here can be attributed to ERBB4 activation. Treatment of iAMs with recombinant NRG1 induced more than 5000 DEGs. 1% of the total DEGs were ion channel genes, supporting our hypothesis that ERBB4 activation may have direct effects on the electrical activity of atrial cardiomyocytes. Interestingly, some ion channel genes that were downregulated possess genetic variants in humans, known to increase the likelihood of developing AF. These genetic variants of ion channel genes (e.g. SCN10A, SCN5A, and KCNQ1) are often found to have a gain-of-function phenotype, as shown in previous studies (4-6). To what extent these changes explain the effects of ERBB4 activation on AF is not clear at this stage, and deserves further investigation. For example, ion channel-specific transgenic mice of ion channels with a known gain-of-function phenotype in AF. Preferably, ion channels that were downregulated following ERBB4 activation (KCNQ1/KCNE1, SCN5A) would be of specific interest. Such models have been studied before and showed an increase in spontaneous AF KCNE1 (7, 8) or AF susceptibility (9). We subsequently evaluated the role of ERBB4 activation on reentrant inducibility in a hiAM-based AF model. This *in vitro* model has previously been validated and proven to be superior in terms of structural and electrophysiological maturation compared with permanently immortalized HL-1 cells and (i)PSC-derived atrial-like CMs (3). Therefore, the hiAM monolayers have previously been used to test pharmacological interventions on reentrant inducibility. A study by Harlaar *et al.* showed that sotalol sporadically terminated reentrant activity, whereas flecainide lead to frequent reentrant termination at high doses. Moreover, both drugs increased the APD<sub>80</sub> in a dose-dependent manner.

A main objective here was to study localized targeting of reentry in hiAM monolayers by ERBB4 activation to enhance the mechanistic understanding of ERBB4 activation on AF inducibility and sustainability. Of note, in contrast to rat iAMs, hiAMs were previously found by RNA-sequencing to express both *ERBB3* and *ERBB4* (3), albeit mRNA levels of *ERBB3* were lower. However, by using JK07 in these experiments, ERBB4 was more selectively targeted. Importantly, optical voltage mapping experiments demonstrated that JK07 completely prevented the inducibility of reentry in hiAM monolayers. The underlying mechanism by which JK07 prevented reentry formation remains poorly understood, since we did not observe any changes in APD<sub>80</sub> or CV. Additional experiments will be necessary to increase our understanding of ERBB4 mediated reentry prevention. Important control experiments of these findings would be to test the effects of JK07 in hiAMs following either ERBB3 or ERBB4 knockdown.

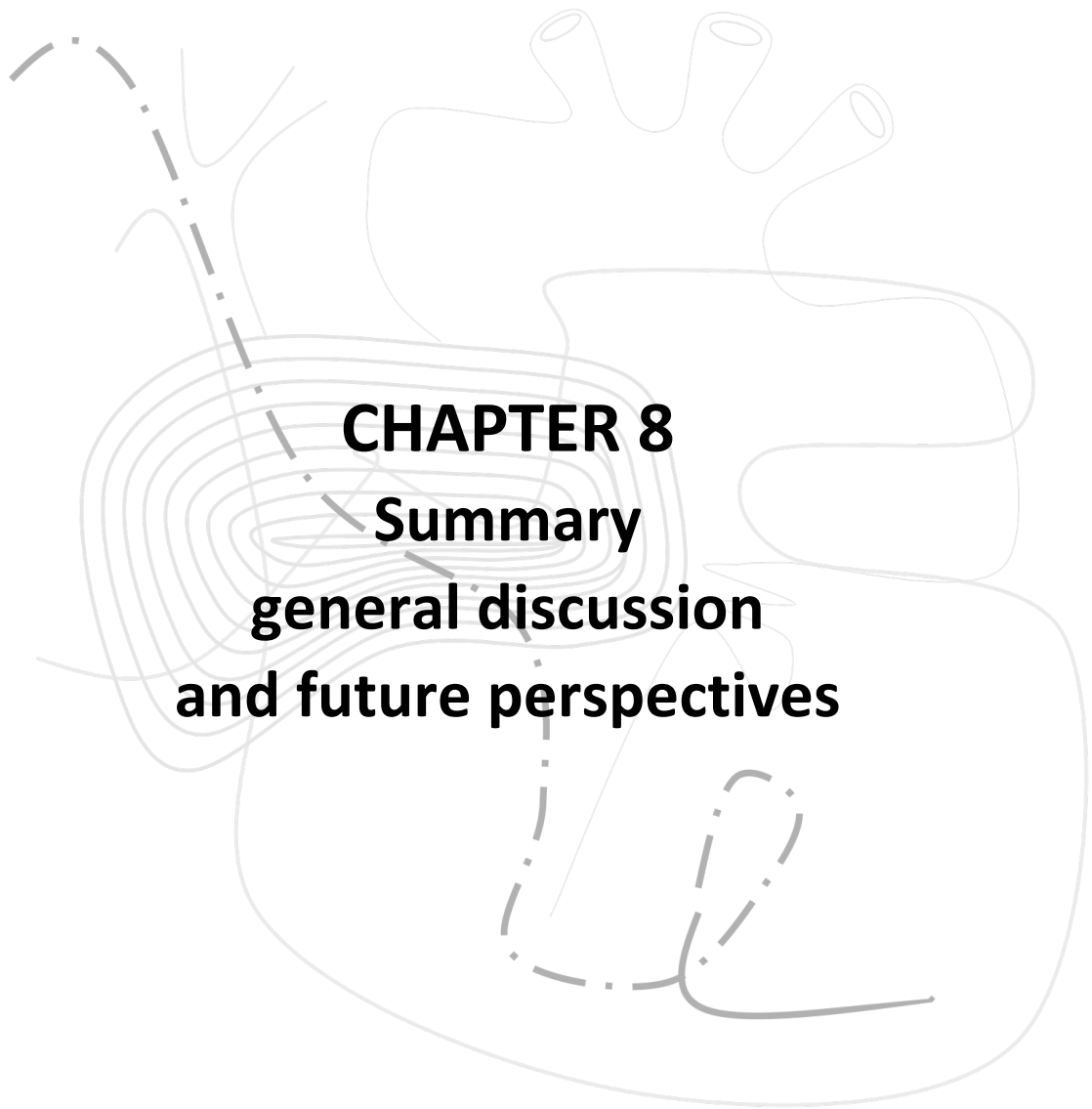
Because reentry is a driving force of both AF initiation and sustainability, these results suggest that JK07 might also reduce AF duration. Mimicking reentry termination (slow JK07 infusion) rather than preventing it would learn us more about the therapeutic and interventional characteristics of ERBB4 activation and its ability to change the reentry activation frequency. Finally, these results should be interpreted with caution as the method used herein is based on a 2D model of AF and stable induced reentry. This *in vitro* model, does not represent the structural and functional complexity found in an intact heart displaying AF. Nonetheless, we consider these findings as novel and relevant, as they are the first observation that ERBB4 activation is linked to reduced reentry activity in atrial cardiomyocytes, serving as a stepping stone to future investigations.



## References

1. Liu J, Volkens L, Jangsangthong W, Bart CI, Engels MC, Zhou G, et al. Generation and primary characterization of iAM-1, a versatile new line of conditionally immortalized atrial myocytes with preserved cardiomyogenic differentiation capacity. *Cardiovasc Res*. 2018;114(14):1848-59.
2. van Gorp PRR, Trines SA, Pijnappels DA, de Vries AAF. Multicellular In vitro Models of Cardiac Arrhythmias: Focus on Atrial Fibrillation. *Frontiers in cardiovascular medicine* [Internet]. 2020; 7:[43 p.].
3. Harlaar N, Dekker SO, Zhang J, Snabel RR, Veldkamp MW, Verkerk AO, et al. Conditional immortalization of human atrial myocytes for the generation of in vitro models of atrial fibrillation. *Nat Biomed Eng*. 2022;6(4):389-402.
4. Jabbari J, Olesen MS, Yuan L, Nielsen JB, Liang B, Macri V, et al. Common and rare variants in SCN10A modulate the risk of atrial fibrillation. *Circ Cardiovasc Genet*. 2015;8(1):64-73.
5. Wilde AAM, Amin AS. Clinical Spectrum of SCN5A Mutations: Long QT Syndrome, Brugada Syndrome, and Cardiomyopathy. *JACC Clin Electrophysiol*. 2018;4(5):569-79.
6. Yoneda ZT, Anderson KC, Quintana JA, O'Neill MJ, Sims RA, Glazer AM, et al. Early-Onset Atrial Fibrillation and the Prevalence of Rare Variants in Cardiomyopathy and Arrhythmia Genes. *JAMA Cardiol*. 2021;6(12):1371-9.
7. Temple J, Frias P, Rottman J, Yang T, Wu Y, Verheijck EE, et al. Atrial Fibrillation in KCNE1-Null Mice. *Circulation Research*. 2005;97(1):62-9.
8. Wan E, Abrams J, Weinberg RL, Katchman AN, Bayne J, Zakharov SI, et al. Aberrant sodium influx causes cardiomyopathy and atrial fibrillation in mice. *The Journal of Clinical Investigation*. 2016;126(1):112-22.
9. Blana A, Kaese S, Fortmüller L, Laakmann S, Damke D, van Bragt K, et al. Knock-in gain-of-function sodium channel mutation prolongs atrial action potentials and alters atrial vulnerability. *Heart Rhythm*. 2010;7(12):1862-9.





## **CHAPTER 8**

### **Summary**

**general discussion  
and future perspectives**



## SUMMARY

### Background and hypotheses

The NRG1/ERBB system is a paracrine system, with an indispensable role in fetal development and in the preservation of a normal structure and function of the adult heart (1, 2). NRG1 is an endothelium-released protein inducing growth and survival of target cells. Interestingly, recent studies, including studies from our laboratory, showed that NRG1 also exerts anti-fibrotic and anti-inflammatory effects in the heart, but also in other organs, and that the ERBB4 receptor is the main receptor for NRG1 in fibroblasts and macrophages (3-5). Fibrosis and inflammation in atrial tissue are two important mechanisms of AF, contributing to the electrical and contractile atrial changes in most patients with AF (6, 7). Current AF therapies merely target the electrical changes through pharmacological modulation, electrical cardioversion and invasive ablation and result often in AF recurrence and in some cases are associated with stringent side effects. Therefore, there is a high medical need for new AF treatments, and for therapies that target the structural substrate of AF. In this thesis, we investigated the effect of ERBB4 activation as a potential therapy for AF. First, we validated whether selective activation of ERBB4 by JK07 attenuated inflammatory and fibrotic response in atrial cells/samples during *in vitro* and *ex vivo* experiments. Next, we investigated if NRG1 or JK07 administration, in a transgenic mouse model of cardiac-specific overexpression of TNF- $\alpha$ , prevented spontaneous AF and/or atrial remodeling. Because we reached several experimental limitations in our study with these transgenic mice, we next evaluated JK07 therapy on AF inducibility and duration in distinct mouse models exposed to relevant clinical risk factors of AF. Finally, to further understand our *in vivo* findings, we studied the effects of ERBB4 activation on gene expression levels and electrical activity of atrial cardiomyocytes in (h)iAM monolayers.

The central hypothesis of this thesis is that **the ERBB4 signaling pathway is an inhibitory pathway in the development of atrial inflammation, fibrosis, remodeling, and hence of AF.**

- (i) **Selective ERBB4 activation by JK07 has preventive and/or therapeutic effects in AF and atrial remodeling.**
- (ii) **Selective ERBB4 activation by JK07 prevents AF inducibility and duration by modifying the electrical activity of atrial cardiomyocytes.**

## **Overview of key findings and general conclusions**

In **chapter 4** we confirmed that JK07 selectively signals through ERBB4, although some ERBB3 signaling was also observed. Nevertheless, as anticipated from how JK07 is designed, JK07 induced ERBB4/4 dimerization with similar potency but significantly higher efficacy than ERBB2/3 dimerization compared to recombinant NRG1. This confirmed that JK07 signals preferentially through ERBB4, by inducing ERBB4 phosphorylation and activation of downstream signaling pathways. Subsequently, we observed that JK07 reduced the upregulation of inflammatory cytokines in cultured macrophages, and the upregulation of collagen mRNA levels type I and III in atrial tissue samples, recapitulating the anti-inflammatory and anti-fibrotic effects previously observed with NRG1.

**In conclusion, JK07 is an agonist of ERBB4, with less ERBB3 agonistic effects than NRG1, but with similar *in vitro* anti-inflammatory and anti-fibrotic effects.**

In **chapter 5**, we observed that NRG1 and JK07 did not prevent inflammatory pathways, fibrosis, and dilation of atria in male transgenic mice with cardiac-specific overexpression of TNF- $\alpha$ . Despite the early onset of severe atrial remodeling in these male transgenic mice, we did not observe spontaneous AF (through sustained telemetry monitoring). Also female transgenic mice with cardiac-specific overexpression of TNF- $\alpha$  showed severe atrial remodeling but again spontaneous AF remained almost undetectable.

**In conclusion, NRG1 and JK07 treatment did not affect atrial remodeling (inflammation, fibrosis, and dilation) in transgenic mice overexpressing TNF- $\alpha$  in cardiac tissue. Surprisingly, spontaneous AF episodes remained undetected in both male and female transgenic mice.**

In **chapter 6**, we demonstrated that JK07 treatment, started upon induction of hypertension, prevented AF inducibility and reduced the total AF duration in an Ang II-induced hypertension model. Similar results were obtained in a diet-induced obesity model, in experiments where JK07 treatment was started together with HFD. Both mouse models are clinically relevant because arterial hypertension and obesity are important clinical risk factors of AF.

Despite developing increased inducibility of AF, these mouse models did not show increased atrial fibrosis and showed a normal AERP; JK07 did not influence these parameters.

When treatment with JK07 in the Ang II-induced hypertension model was initiated three weeks after starting Ang II infusion —i.e. after allowing time to induce atrial remodeling— and only given for one week, similar effects on AF inducibility were observed endorsing the hypothesis that JK07 exerts anti-AF effects through other mechanisms than through structural changes. Nevertheless, mice with a myeloid-specific *ErbB4* gene deletion, showed a significant increase in left atrial fibrosis after four weeks of Ang II-treatment. We conclude that JK07 treatment in mice exerts anti-AF effects through mechanisms other than anti-fibrotic effects, but that endogenous ERBB4 signaling, e.g. in macrophages, protects against development of atrial fibrosis.

**In conclusion, JK07 therapy reduces AF inducibility in two distinct models exposed to clinical risk factors of AF, and also reduces AF duration when started early. These effects could not be explained by mitigating atrial fibrosis, suggesting that other mechanisms participate. Deleting endogenous ERBB4 activation in macrophages, however, exacerbates atrial fibrotic degeneration, implying a role of the NRG1/ERBB4 pathway in the control of atrial fibrosis.**

Above findings led to our second hypothesis that JK07 has antiarrhythmic properties independently of atrial fibrosis, most likely by acting directly on electrical properties of atrial myocytes. In **chapter 7**, we showed data endorsing this hypothesis. More specifically, using RNA-sequencing experiments we observed more than 5000 DEGs in atrial cardiomyocytes after ERBB4 activation, of which 1% were distinct ion channel genes. These experiments suggest that ERBB4 activation may also regulate electrical activity of atrial cardiomyocytes. This hypothesis was further substantiated in experiments with hiAM monolayers, showing that JK07 completely prevented inducibility of reentry activity (spiral waves) during AP propagation.

**In conclusion, ERBB4 activation regulates ion channel gene expression in cardiomyocytes. Moreover, JK07 completely prevents reentry inducibility, following changes in electrical activity.**

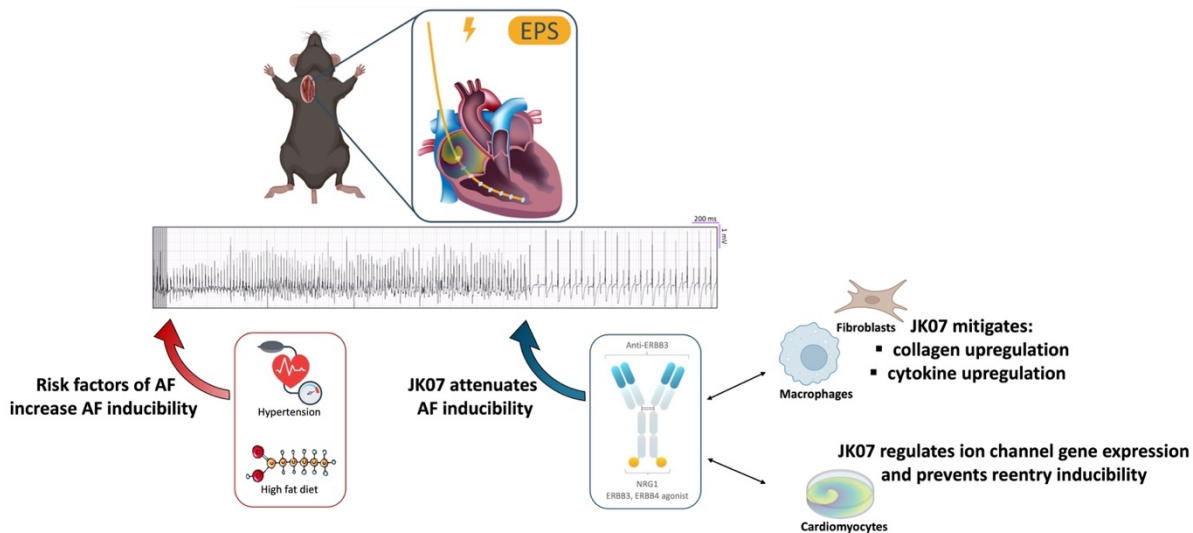


**Figure 34. Graphical overview of the key findings.** ERBB4 activation, by JK07, prevented and treated AF inducibility in distinct mouse models exposed to risk factors of AF, likely by acting directly on atrial cardiomyocytes and their electrical activity. Moreover, JK07 reduced macrophage-mediated cytokine expression *in vitro* and collagen mRNA levels expression *ex vivo*.

## General discussion

AF is the most common arrhythmia encountered in clinical practice. It is accompanied by electrical and structural remodeling of the atria, and therefore, difficult to cure. Once initiated, AF itself induces further changes, leading to a vicious circle (“AF begets AF”). There is substantial evidence that atrial fibrosis and inflammation contribute to the structural changes, and form the basis of consequent electrical and contractile dysfunction (6, 7). Recent studies, including from our laboratory, showed that NRG1 has anti-inflammatory and anti-fibrotic effects in different organs, including the heart (3-5). Moreover, ERBB4 signaling activates protective effects against cardiac remodeling, as discussed in chapter 4 (5, 8, 9). In this thesis we investigated JK07, an activator of ERBB signaling with predominant effects on ERBB4, as a drug candidate for atrial inflammation, fibrosis, and fibrillation. We found that JK07 reduced AF inducibility and duration in two distinct mouse models, with both preventive and therapeutic activity. Mechanistic studies suggest that direct effects on electrical properties of atrial cardiomyocytes, rather than structural effects on fibrosis, underlay these effects.



In order to conduct a study that mimics AF in a clinically relevant fashion, a mouse model that develops spontaneous AF was the preferred choice. However, wild type mouse models do not develop AF spontaneously, but requires genetic manipulation, which is often accompanied by severe cardiac dysfunction and a decreased lifespan. Mice exposed to clinical risk factors of AF do not spontaneously develop AF, but can be used to study AF, and require EP stimulation to evoke AF (10).

Therefore, we first tested NRG1 treatment in transgenic male mice overexpressing TNF- $\alpha$  (TNF1.6 mice), who developed severe atrial remodeling at a young age (observed from 6 weeks old) characterized by atrial inflammation, fibrosis and dilation, and resulting in increased mortality starting at 14 weeks of age. NRG1 had no effect on atrial remodeling and survival. These results deviate from the anti-fibrotic effects of NRG1 previously observed in other models, including left ventricular fibrosis in an Ang II-induced hypertensive mouse model (5). TNF1.6 mice showed clear ERBB4 receptor expression on protein level, as shown by western blot analysis. This implies that the NRG1/ERBB4 stress-response mitigating effect was not sufficient for the severe and progressive atrial remodeling in this transgenic model. Surprisingly, we did not observe substantial occurrence of spontaneous AF. TNF1.6 mice have been extensively used to study heart failure, and mostly develop spontaneous AF as a consequence of ventricular contractile dysfunction (11). The lack of observed spontaneous AF episodes in our studies remains unexplained and could originate from not monitoring frequent enough or by using a screening method which was not sensitive enough, although we consider this as unlikely. Altogether, this study did not contribute to the understanding of the role NRG1/ERBB4 signaling plays in the complex pathophysiology of AF.

We therefore switched to two distinct mouse models exposed to clinical risk factors (Ang II-induced hypertension and obesity) of AF, in which we successfully induced AF during EP studies. However, these mice did not develop an increase in atrial fibrosis, which deviated from previous studies (12-14). Ang II increases blood pressure, and activates TGF- $\beta$  signaling, facilitating a fibroproliferative process (15). Most likely, our studies were not long enough to detect atrial fibrosis. Nonetheless, Ang II-treated mice were significantly more susceptible for AF inducibility, accompanied by a significantly increased single episode and total AF duration. AF inducibility, and

both single episode and total AF duration were significantly reduced following preventive JK07 treatment. Similar to the Ang II-model, HFD-induced obese mice showed no substantial atrial fibrosis during the timeframe of our study, although this has been reported in other studies (16, 17). Obesity and its related chronic inflammation are known to play a key role in electrical remodeling but the underlying electrophysiological mechanisms are not completely understood. A recent study by McCauley *et al.* revealed that a shortened APD and decreased atrial CV in obese mice due to downregulation of sodium channels ( $I_{Na}$ ) and calcium channels ( $I_{Ca}$ ), and an increase in increase in potassium channels ( $I_{Kur}$ ) might be part of the underlying mechanism. Here, we showed that HFD-induced obesity resulted in increased AF inducibility, and single episode and total AF duration, although not significantly. Likewise, preventive JK07 treatment significantly reduced the AF inducibility and total —but not single episode— AF duration. Because JK07 significantly prevented AF inducibility and total AF duration in our studies, using two distinct models exposed to risk factors of AF, albeit without increased atrial fibrosis, we hypothesized that ERBB4 signaling has direct effects on the electrical activity of atrial cardiomyocytes. Moreover, preventive JK07 treatment significantly reduced the frequency of long ( $\geq 3$  s) AF-induced episodes in the Ang II treated mice. This was not observed in HFD mice following preventive JK07 treatment due to absence of long AF episodes.

Until now, we showed that JK07 has anti-inflammatory and anti-fibrotic effects in cultured macrophages and *ex vivo* atrial tissue samples, however, we could not determine the role of JK07 on atrial fibrosis *in vivo*. To investigate the importance of ERBB4 signaling during atrial tissue fibrosis, we evaluated the effect of specific-*ErbB4* gene deletion in myeloid cells in Ang II-treated mice. Following myeloid *ErbB4* deletion, an exaggerated response in left atrial fibrosis was observed, as well as increased macrophage infiltration, however the latter was not significant. This implies that ERBB4 signaling, mediated by myeloid cells (macrophages), is of importance during atrial inflammation and fibrosis which is in line with previous findings in left ventricular tissue (5). Additionally, a recent study by Hulsmans *et al.* showed that myeloid cells (specifically macrophages) are increased in patients with AF, leading to tissue remodeling and disruption of coordinated excitation of atrial cardiomyocytes.

Moreover, they showed in a mouse model of combined hypertension, obesity, and mitral valve regurgitation that macrophages expand more than any other cell type in atrial remodeling and that hypertension increased atrial macrophage infiltration and fibrosis in a bigger extent compared with obesity (18).

Both Ang II-induced hypertension and HFD-induced obesity in mice are established experimental models, used to investigate the pathogenesis of AF as they mimic the two most attributable risk factors of AF. Despite the absence of increased atrial fibrosis, we still observed significant increases in AF inducibility and total duration in these mouse models. These results emphasize that the underlying mechanisms of AF are multifactorial (structural and electrical remodeling). Moreover, a study by Janssen *et al.*, revealed that next to structural remodeling, Ang II causes extensive electrical remodeling associated with changes in atrial AP duration and morphology due to changes in  $I_{Na}$ ,  $I_{to}$ , and  $I_{kur}$  currents. The reduction in  $I_{to}/I_{kur}$  and resulting increase in AP duration increase the likelihood of EADs and therefore might also explain the increased AF inducibility in Ang II-treated mice (12). To study the effects of ERBB4 activation on the electrical activity of atrial cardiomyocytes, we performed RNA-sequencing on iAMs treated with NRG1. Transcriptome analysis revealed, for the first time, that NRG1 alters the expression (up and downregulation) of more than 5000 genes in atrial cardiomyocytes, of which 1% were ion channel genes known to be correlated with AF (gain- and loss-of-function). Since iAMs do not express ERBB3 (non-published observation by our lab), we can correlate the NRG1-induced changes in ion channel gene expression directly to ERBB4 signaling. We did not study the effects of ERBB4 activation on the transcriptome of iAMs exposed to Ang II (together with Ang II or after Ang II). This would be interesting as an experiment since it recapitulates the design of our *in vivo* experiment. Subsequently, we tested if these ion channel changes affected rotor inducibility in a previously validated hiAM-based AF model (19). JK07 treatment was used to target ERBB4 signaling as hiAMs express both *ERBB3* and *ERBB4*. Reentry inducibility, via electrical point stimulation, was completely prevented in hiAM monolayers, following a 24-h JK07 treatment. Together these results indicate that ERBB4 signaling holds anti-arrhythmic properties by preventing reentry inducibility through direct effects on ion channels of atrial cardiomyocytes.

Accordingly, this explains the significant reduction in AF inducibility in distinct mouse models of AF, even after a short period of JK07 treatment, as well as the reduction in AF duration.

As mentioned before, there is a clear medical need for novel treatments that target the underlying substrate of AF. Additionally, new therapies with improved efficacy and safety profiles are of high importance. JK07, a recombinant fusion protein of NRG1 and a monoclonal antibody specific for ERBB3, shows preferential selectivity for ERBB4 signaling and was extensively tested as a candidate treatment for AF. The current patient management relies on stroke prevention (anticoagulation), symptom control (rate and rhythm control), and cardiovascular risk and comorbidity optimization (lifestyle changes) based on the AF Better Care (ABC) holistic pathway of the ESC guidelines (20). While currently used treatments, work in a symptomatic manner, we showed that JK07 targets both ion channel regulation and the underlying substrate (inflammation and fibrosis). JK07 reduced macrophage-mediated cytokine expression *in vitro* and collagen levels expression *ex vivo*. Additionally, myeloid-specific *ErbB4* gene deletion resulted in increased inflammation and fibrosis in mice treated with Ang II. JK07 prevented and treated AF inducibility *in vivo*, by acting directly on atrial cardiomyocytes and their electrical activity, as confirmed by RNA-sequencing and optical voltage mapping experiments in an (h)iAM-based AF model. Compared to antiarrhythmic drugs, currently used for AF, JK07 not only targets the underlying substrate and regulates electrical activity, but moreover, does not alter the AERP, APD<sub>80</sub> and CV. Meaning that JK07 does not alter action potential duration as seen with other drugs as an adverse effect which can be severe or life-threatening (21).

Finally, the central aim of this study was to test the effects of NRG1 on atrial inflammation and fibrosis (atrial myopathy), and hence as a new drug candidate for AF. Although, the experiments performed in this thesis did not directly answer the question if the NRG1/ERBB4 system plays a role in atrial inflammation and fibrosis *in vivo*, the results obtained during this project are of high importance and lead to the discovery of novel physiologic activity of the NRG1/ERBB4 pathway in the mechanism of atrial fibrillation. More so, the lack of results on atrial myopathy in the murine studies triggered this project beyond its marks and eventually helped discovering novel functions of NRG1 on atrial cardiomyocytes and the continuing importance of NRG1 as a drug candidate for

AF. Therefore the performed research should still be considered as accomplished and moreover, the possible initiation of new projects following the discoveries herein described.

### **Future perspectives**

In this thesis, we demonstrated the importance of ERBB4 signaling, during inflammation and fibrosis, and its role in AF inducibility and sustainability. Selective activation of ERBB4 signaling resulted in preventive and therapeutic effects on AF inducibility, presumably by acting directly on the electrical activity of atrial cardiomyocytes. Despite the novelty and promising translational value of this study, several questions remain unanswered and new research questions were triggered from these findings, which would highly contribute to the fundamental understanding of the mechanistic effects of ERBB4 signaling in AF and atrial remodeling:

- (i)** As discussed in **chapter 4**, there is increasing evidence supporting the importance of ERBB4 signaling in cardiac pathophysiology. We showed that JK07 signals preferentially through ERBB4, without completely blocking ERBB3 signaling. Despite the importance of ERBB4 signaling in the heart and the predominant selectivity of JK07 for ERBB4 activation, we cannot completely exclude a potential role of ERBB3 in the pathophysiology of AF and atrial remodeling. These data indicate that selective ERBB4 signaling through macrophages, fibroblasts, and cardiomyocytes is sufficient to exert anti-inflammatory and anti-fibrotic effects, and reduce AF inducibility and duration. However, before claiming that these effects are uniquely correlated to ERBB4 signaling, it is important to examine the role of ERBB3 in more detail related to (atrial) inflammation and fibrosis, and most importantly AF. Therefore it would be of interest to breed mice with a cell-specific (fibroblast, myeloid, cardiomyocyte) gene deletion of *ErbB3* and expose them to risk factors of AF, as executed in this study.
- (ii)** Previous studies showed that NRG1 has anti-fibrotic effects in different organs and tissues in multiple animal models, ranging from rodents to large animal models (3, 5). Here, we showed that selective ERBB4 activation is sufficient to reproduce the anti-fibrotic effects. JK07 attenuated the upregulation of collagen type I and type III, the main collagen types present in the heart, in *ex vivo* atrial tissue samples. However, a limitation of this study is the absence of increased atrial fibrosis in our *in vivo* studies. We indirectly studied the role of ERBB4 signaling in atrial fibrosis, by using a myeloid-specific *ErbB4* gene deletion mouse

model. Studying additional genetically altered mouse models such as fibroblast-specific gene deletion of *ErbB4* could learn us more about the importance of ERBB4 in structural remodeling and AF.

- (iii)** The absence of atrial fibrosis was an unexpected finding, however this pushed us to pursue alternative mechanisms and explanations. In part, we discovered novel effects of ERBB4 signaling in atrial cardiomyocytes through RNA-sequencing and optical voltage mapping experiments. At the same time, these findings triggered several new questions. Because we didn't reveal the exact underlying mechanisms through which ERBB4 activation reduced AF inducibility and sustainability, it would be of great value to study this in more detail. (Single-cell) patch clamp studies would help us discover which ion channels are regulated by JK07 treatment. As well as additional RNA-sequencing experiments on the atrial tissue of the distinct mouse models used in this thesis would learn us more about the underlying mechanism.
- (iv)** Following the discovery of these promising results in small animal models, it would be a logical next step to assess the effects of JK07 on AF in a large animal model. However, as mentioned at the beginning of this thesis, similar experiments with minipigs have been executed in parallel. In these experiments, JK07 was tested in a preventive setting only, and revealed similar anti-AF results, however with the additional indication of anti-fibrotic effects in atrial tissue of minipigs. It will be of interest to further study in large animals whether anti-fibrotic effects in atria suffice to prevent AF, or whether also electrophysiological effects in atria are required.
- (v)** Following positive results of JK07 on AF inducibility and duration in small and large animal models, a reasonable next step could be to test JK07 in human studies. Several approaches could be used to test the different effects (preventive/therapeutic) of JK07 on AF. Since NRG1 and JK07 are already being tested in several human clinical trials for heart failure (NYHA Class II or III heart failure), and because patients with heart failure are frequently associated with AF, this could be an interesting set up to study the effects of JK07 on AF in humans. Moreover, patients with heart failure frequently develop the onset of new AF due to coexistence of common risk factors (hypertension, obesity, diabetes, age,...) or are already known to have pre-existing AF, allowing the assessment of both preventive and

therapeutic effects of JK07 on AF, albeit secondary to heart failure in the latter. Additionally, patients with heart failure are prone to develop atrial myopathy, which allows this study to also test the effects of JK07 on atrial remodeling, next to the anti-AF effects.

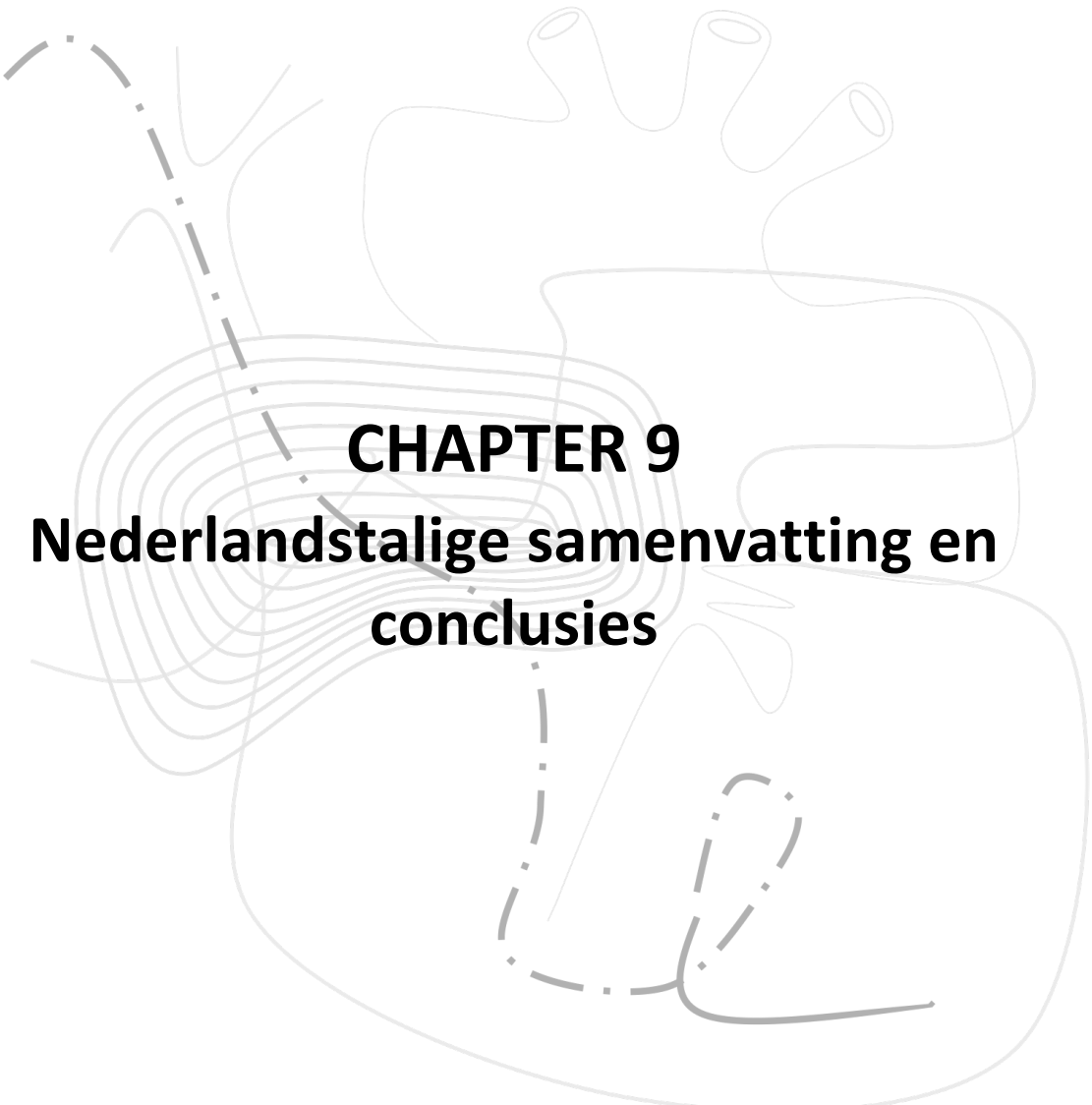
## References

1. Lemmens K, Doggen K, De Keulenaer GW. Role of neuregulin-1/ErbB signaling in cardiovascular physiology and disease: implications for therapy of heart failure. *Circulation*. 2007;116(8):954-60.
2. Mendes-Ferreira P, De Keulenaer GW, Leite-Moreira AF, Brás-Silva C. Therapeutic potential of neuregulin-1 in cardiovascular disease. *Drug Discov Today*. 2013;18(17-18):836-42.
3. Galindo CL, Ryzhov S, Sawyer DB. Neuregulin as a heart failure therapy and mediator of reverse remodeling. *Curr Heart Fail Rep*. 2014;11(1):40-9.
4. Vandekerckhove L, Vermeulen Z, Liu ZZ, Boimvaser S, Patzak A, Segers VF, et al. Neuregulin-1 attenuates development of nephropathy in a type 1 diabetes mouse model with high cardiovascular risk. *Am J Physiol Endocrinol Metab*. 2016;310(7):E495-504.
5. Vermeulen Z, Hervent AS, Dugaucquier L, Vandekerckhove L, Rombouts M, Beyens M, et al. Inhibitory actions of the NRG-1/ErbB4 pathway in macrophages during tissue fibrosis in the heart, skin, and lung. *Am J Physiol Heart Circ Physiol*. 2017;313(5):H934-h45.
6. Dzeshka MS, Lip GY, Snezhitskiy V, Shantsila E. Cardiac Fibrosis in Patients With Atrial Fibrillation: Mechanisms and Clinical Implications. *J Am Coll Cardiol*. 2015;66(8):943-59.
7. Jalife J, Kaur K. Atrial remodeling, fibrosis, and atrial fibrillation. *Trends Cardiovasc Med*. 2015;25(6):475-84.
8. Bersell K, Arab S, Haring B, Kühn B. Neuregulin1/ErbB4 signaling induces cardiomyocyte proliferation and repair of heart injury. *Cell*. 2009;138(2):257-70.
9. De Keulenaer GW, Feyen E, Dugaucquier L, Shakeri H, Shchendrygina A, Belenkov YN, et al. Mechanisms of the Multitasking Endothelial Protein NRG-1 as a Compensatory Factor During Chronic Heart Failure. *Circ Heart Fail*. 2019;12(10):e006288.
10. Schüttler D, Bapat A, Käab S, Lee K, Tomsits P, Clauss S, et al. Animal Models of Atrial Fibrillation. *Circ Res*. 2020;127(1):91-110.
11. Saba S, Janczewski AM, Baker LC, Shusterman V, Gursoy EC, Feldman AM, et al. Atrial contractile dysfunction, fibrosis, and arrhythmias in a mouse model of cardiomyopathy secondary to cardiac-specific overexpression of tumor necrosis factor- $\alpha$ . *Am J Physiol Heart Circ Physiol*. 2005;289(4):H1456-67.
12. Jansen HJ, Mackasey M, Moghtadaei M, Belke DD, Egom EE, Tuomi JM, et al. Distinct patterns of atrial electrical and structural remodeling in angiotensin II mediated atrial fibrillation. *Journal of Molecular and Cellular Cardiology*. 2018;124:12-25.
13. Xie X, Shen T-t, Bi H-l, Su Z-l, Liao Z-q, Zhang Y, et al. Melatonin inhibits angiotensin II-induced atrial fibrillation through preventing degradation of Ang II Type I Receptor-Associated Protein (ATRAP). *Biochemical Pharmacology*. 2022;202:115146.
14. Han X, Zhang Y-L, Zhao Y-X, Guo S-B, Yin W-P, Li H-H. Adipose Triglyceride Lipase Deficiency Aggravates Angiotensin II-Induced Atrial Fibrillation by Reducing Peroxisome Proliferator-Activated Receptor  $\gamma$  Activation in Mice. *Laboratory Investigation*. 2023;103(1).
15. Walker M, Patel P, Kwon O, Koene RJ, Duprez DA, Kwon Y. Atrial Fibrillation and Hypertension: "Quo Vadis". *Curr Hypertens Rev*. 2022;18(1):39-53.
16. Vyas V, Lambiase P. Obesity and Atrial Fibrillation: Epidemiology, Pathophysiology and Novel Therapeutic Opportunities. *Arrhythm Electrophysiol Rev*. 2019;8(1):28-36.



17. Kondo H, Abe I, Gotoh K, Fukui A, Takanari H, Ishii Y, et al. Interleukin 10 Treatment Ameliorates High-Fat Diet–Induced Inflammatory Atrial Remodeling and Fibrillation. *Circulation: Arrhythmia and Electrophysiology*. 2018;11(5):e006040.
18. Hulsmans M, Schloss MJ, Lee IH, Bapat A, Iwamoto Y, Vinegoni C, et al. Recruited macrophages elicit atrial fibrillation. *Science*. 2023;381(6654):231-9.
19. Harlaar N, Dekker SO, Zhang J, Snabel RR, Veldkamp MW, Verkerk AO, et al. Conditional immortalization of human atrial myocytes for the generation of in vitro models of atrial fibrillation. *Nat Biomed Eng*. 2022;6(4):389-402.
20. Hindricks G, Potpara T, Dagres N, Arbelo E, Bax JJ, Blomström-Lundqvist C, et al. 2020 ESC Guidelines for the diagnosis and management of atrial fibrillation developed in collaboration with the European Association for Cardio-Thoracic Surgery (EACTS): The Task Force for the diagnosis and management of atrial fibrillation of the European Society of Cardiology (ESC) Developed with the special contribution of the European Heart Rhythm Association (EHRA) of the ESC. *European Heart Journal*. 2020;42(5):373-498.
21. Dobrev D, Carlsson L, Nattel S. Novel molecular targets for atrial fibrillation therapy. *Nature Reviews Drug Discovery*. 2012;11(4):275-91.





**CHAPTER 9**  
**Nederlandstalige samenvatting en**  
**conclusies**

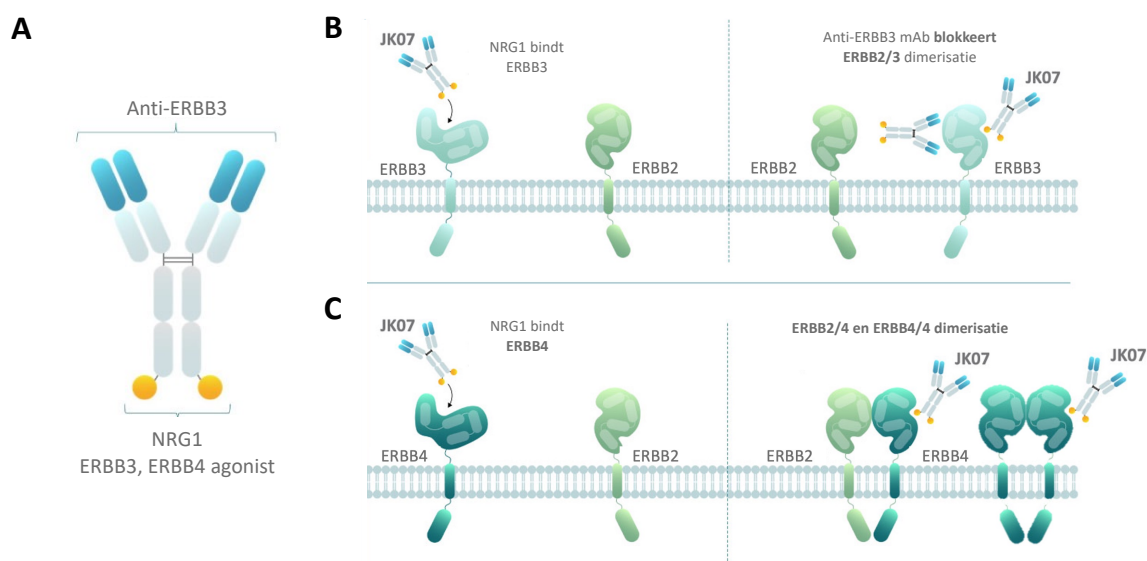


## INTRODUCTIE

Voorkamerfibrillatie (VKF) is de meest voorkomende hartritmestoornis in de klinische praktijk en tevens een van de meest voorkomende oorzaken van beroertes en hartfalen. VKF is het gevolg van elektrische, contractiele en structurele remodelering van de atria, dewelke zich frequent voordoen vaak in verschillende cardiovasculaire aandoeningen, zoals onder meer hypertensie, hartklepaandoeningen en hartfalen. Bovendien induceert VKF zelf ook veranderingen in de atria, wat leidt tot een vicieuze cirkel waarin VKF meer VKF verwekt. Atriale fibrose en inflammatie zijn belangrijke onderliggende oorzaken van de structurele veranderingen en liggen aan de basis van elektrische en contractiele atriale dysfunctie (1, 2). Gevorderde atriale fibrose wordt gelinkt aan ernstigere vormen van VKF alsook een verminderde efficiëntie van antiaritmische geneesmiddelen en ablatie therapie (1). Systemische en lokale inflammatie worden aanzien als een belangrijke factor in de pathofysiologie van atriale remodelering en is nauw gelinkt met weefsel fibrose (3, 4). Huidige therapieën van VKF zijn beperkt tot ritmecontrole, waarbij herstel en behoud van het hartritme centraal staan door cardioversie, geneesmiddelen, of door pulmonale venen isolatie (ablatie) en frequentiecontrole, waarbij er getracht wordt het hartritme te vertragen en controleren met behulp van geneesmiddelen. Aangezien een onregelmatig hartritme en hartfrequentie het risico op beroertes verhoogt, wordt er bovendien gestreefd naar een optimale preventie van beroertes door gebruik te maken van stollingstherapie ("bloedverdunding"). Tevens is het van belang om verschillende risicofactoren van VKF op te sporen en te behandelen. Veel voorkomende risicofactoren zijn: hypertensie, overgewicht, slaapapneu, overmaat aan alcohol, etc. (5, 6). Het probleem met deze eerder vermelde therapieën is, dat ze slechts enkel en alleen gericht zijn op de symptomen van VKF en niet op de onderliggende pathofysiologie, wat hun beperkte effectiviteit zou kunnen verklaren. Er is duidelijk een medische behoefte aan nieuwe therapieën die de onderliggende oorzaken zoals inflammatie en fibrose tegengaan en dus zo de structurele atriale remodelering behandelen.

Het neureguline-1/ERBB systeem is een paracrien systeem met een essentiële rol gedurende foetale ontwikkeling en in het behoud van een normale structuur en functie van het volwassen hart (7, 8). NRG1 is een eiwit dat geproduceerd wordt door de endotheel cellen en stimuleert groei en overleving van verschillende andere doelwit cellen, dewelke ERBB receptoren tot

expressie brengen. Recente studies, waaronder ook van ons labo, hebben aangetoond dat NRG1 ook anti-inflammatoire en anti-fibrotische eigenschappen bezit in de ventrikels en andere weefsels waarbij de ERBB4 receptor de hoofdreceptor is voor NRG1 in cardiomyocyten, fibroblasten en macrofagen (9-11). In deze thesis hebben we NRG1 bestudeerd als een potentiële nieuwe therapie voor VKF. Om enkele nadelen van het NRG1 eiwit als een therapeutisch middel te omzeilen, hebben we samengewerkt met Salubris Biotherapeutics. Dit Biotech bedrijf ontwikkelt innovatieve antilichamen en eiwit gebaseerde behandelingen, waaronder ook JK07, een van hun belangrijkste componenten en wordt momenteel getest in twee (fase I) klinische studies (NCT04210375 en NCT05322616). JK07 is een recombinant eiwit dat een humaan NRG1 polypeptide fragment bevat, gefuseerd aan een gehumaniseerd anti-ERBB3 monoklonaal antilichaam (Figuur 35A) (12). Het monoklonaal antilichaam bevat een deel dat specifiek is voor ERBB3 en daardoor de vorming van ERBB3 dimerisatieparen blokkeert. Dit leidt tot selectieve activatie en signalisatie van ERBB4 (Figuur 35B, C).



**Figuur 35. Schematisch overzicht van JK07 en ERBB receptor dimerisatie.** (A) JK07 is een recombinant fusie-eiwit bestaande uit een fragment NRG1 en een monoklonaal antilichaam specifiek voor de ERBB3 receptor. (B) JK07 verlaagt ERBB3 signalisatie door specifiek ERBB3 dimerisatie te blokkeren via het monoklonaal antilichaam tegen ERBB3. (C) JK07 induceert selectief ERBB4 activatie zonder of met slechts een beperkte ERBB3 activatie en tegelijkertijd biedt JK07 een verhoogde stabiliteit en een verlengde halfwaardetijd, in vergelijking met NR1.

In deze thesis hebben we de hypothese getest dat het NRG1/ERBB4 systeem een inhiberende rol speelt in de ontwikkeling van structurele remodelering in de atria en dus ook in VKF. We veronderstellen dat NRG1 een effect heeft op verschillende processen, inclusief fibrogenese en inflammatie. Deze hypothese is gebaseerd op diverse observaties, dewelke aantonen dat NRG1 anti-fibrotische en anti-inflammatoire effecten bezit in verschillende ziektemodellen, inclusief hartfalen, huid fibrose, long fibrose en diabetische nefropathie (10, 11, 13). We hebben deze hypothese onderzocht door gebruik te maken van verschillende *in vivo* muis modellen van VKF. Een eerste model was een transgeen muismodel (TNF1.6) met een overexpressie van TNF- $\alpha$  specifiek in de cardiomyocyten, wat leidde tot atriale inflammatie en fibrose. Vervolgens hebben we nog twee verschillende muis modellen bestudeerd die blootgesteld werden aan risicofactoren van VKF (hypertensie en obesitas).

**Het hoofddoel van deze thesis is dus om selectieve ERBB4 signalisatie te testen als een potentiële nieuwe manier om VKF te behandelen.**

## **RESULTATEN EN CONCLUSIES**

In **hoofdstuk 4** hebben we aangetoond dat JK07 selectief ERBB4 signalisatie tot stand brengt, hoewel beperkte ERBB3 signalisatie werd waargenomen. Zoals verwacht, op basis van de compositie van JK07, induceerde JK07 ERBB4/4 dimerisatie met een vergelijkbare potentie, maar een significant grotere effectiviteit dan ERBB2/3 dimerisatie in vergelijking met NRG1. Dit toont aan dat JK07 preferentieel functioneert via ERBB4 signalisatie en werd vervolgens ook bevestigd door het induceren van ERBB4 fosforylatie gevolgd door activatie van downstream signalisatie. Vervolgens zagen we dat JK07 de opregulatie van inflammatoire cytokines in gecultuurde macrofagen en de opregulatie van collageen type I en III in atriale weefsels significant verminderde. Deze resultaten bevestigden de anti-inflammatoire en anti-fibrotische effecten die eerder werden waargenomen met NRG1.

**In conclusie: JK07 is een ERBB4 agonist, met een duidelijk lager effect op ERBB3 in vergelijking met NRG1, maar met behoud van anti-fibrotische en anti-inflammatoire effecten zoals NRG1.**

In **hoofdstuk 5** zagen we dat NRG1 en JK07 inflammatie, fibrose en dilatatie van het linker atrium in mannelijke transgene muizen met cardiale specifieke overexpressie van TNF- $\alpha$  niet verminderde. Ondanks het vroegtijdig optreden van ernstige atriale remodelering in mannelijke TNF1.6 muizen, observeerden we geen spontane VKF (met behulp van continue telemetrie monitoring). Ook vrouwelijke TNF1.6 muizen vertoonden ernstige atriale remodelering maar desondanks weinig tot geen spontane VKF ontwikkeling.

**In conclusie: NRG1 en JK07 behandeling had geen effect op atriale remodelering (inflammatie, fibrose en dilatatie) in TNF1.6 muizen. Verrassend genoeg bleven spontane episodes van VKF onopgemerkt in zowel mannelijke als vrouwelijke transgene muizen.**

In **hoofdstuk 6** hebben we aangetoond dat JK07 behandeling, die gelijktijdig gestart is met het induceren van hypertensie, preventief werkte op VKF-induceerbaarheid en de VKF-duratie verkortte in een Ang II-geïnduceerd hypertensie muismodel. Gelijkaardige resultaten werden waargenomen in een tweede muismodel met dieet-geïnduceerde obesitas, waarbij JK07 behandeling gelijktijdig gestart was met een vetrijk dieet. Beide muismodellen zijn klinisch relevant aangezien arteriële hypertensie en obesitas veel voorkomende risicofactoren zijn van VKF. Ondanks het ontwikkelen van een verhoogde VKF-induceerbaarheid, konden we verrassend genoeg geen verhoogde atriale fibrose vaststellen in beide muismodellen en vertoonden ze een normale AERP. Daaropvolgend had preventieve JK07 behandeling ook geen invloed op beide parameters. Bovendien stelden we vast dat wanneer een verkorte JK07 behandeling van een week in het Ang II-geïnduceerde hypertensie muismodel, dat pas na drie weken Ang II toediening gestart werd (therapeutische benadering), vergelijkbare effecten opleverde in VKF-induceerbaarheid. Dit suggereert dat JK07 geen anti-VKF effecten uitoefent door het verminderen of tegengaan van structurele veranderingen, maar door een direct effect op atriale cardiomyocyten. Niettemin observeerden we bij muizen met een myeloïde-specifieke *ErbB4* gen deletie een significante toename in fibrose in het linker atrium na vier weken Ang II-behandeling. We kunnen hieruit concluderen dat hoewel JK07 zijn anti-VKF effecten niet uitoefende door middel van anti-fibrotische effecten, endogene ERBB4 activatie in macrofagen beschermt tegen de ontwikkeling van atriale fibrose.



**In conclusie: JK07 behandeling vermindert VKF-induceerbaarheid in twee verschillende muismodellen die blootgesteld werden aan klinisch relevante risicofactoren van VKF. Daarenboven verkort JK07 ook de duur van VKF episodes wanneer behandeling vroegtijdig wordt opgestart. Verrassend genoeg konden deze resultaten niet verklaard worden door het verminderen van atriale fibrose, wat insinueert dat andere mechanismen hiervoor verantwoordelijk zijn. Het verwijderen van endogene ERBB4 activatie in macrofagen verergert echter atriale fibrotische degeneratie, wat dus nog steeds een rol van betekenis impliceert voor de NRG1/ERBB4 pathway in de controle van atriale fibrose.**

Bovenstaande bevindingen leidde tot een nieuwe hypothese dat JK07 onafhankelijk van atriale fibrose anti-aritmische eigenschappen bezit, waarschijnlijk door rechtstreeks in te werken op de elektrische eigenschappen van atriale myocyten. In **hoofdstuk 7** bekrachtigden we deze hypothese. Zo observeerden we met behulp van RNA-sequencing experimenten meer dan 5000 DEG's in atriale cardiomyocyten na activatie van ERBB4. 1% van deze DEG's bleken verschillende ionkanaal genen te zijn. Deze experimenten suggereren dat ERBB4 activatie de elektrische activiteit in atriale cardiomyocyten rechtstreeks reguleert. Deze hypothese werd verder onderbouwd in '*optical voltage mapping*' experimenten met humane atriale cardiomyocyten (hiAMs), waaruit bleek dat JK07 de induceerbaarheid van elektrische rotors (spiraalvormige golven) tijdens actiepotentiaal-propagatie volledig verhinderde.

**In conclusie: ERBB4 activatie reguleert de elektrische activiteit van atriale cardiomyocyten door de genexpressie van verschillende ionenkanalen te mediëren. Bovendien voorkomt JK07 volledig de induceerbaarheid van elektrische rotors na het wijzigen van de elektrische activiteit.**

## References

1. Dzeshka MS, Lip GY, Snezhitskiy V, Shantsila E. Cardiac Fibrosis in Patients With Atrial Fibrillation: Mechanisms and Clinical Implications. *J Am Coll Cardiol*. 2015;66(8):943-59.
2. Jalife J, Kaur K. Atrial remodeling, fibrosis, and atrial fibrillation. *Trends Cardiovasc Med*. 2015;25(6):475-84.
3. Rudolph V, Andrié RP, Rudolph TK, Friedrichs K, Klinke A, Hirsch-Hoffmann B, et al. Myeloperoxidase acts as a profibrotic mediator of atrial fibrillation. *Nat Med*. 2010;16(4):470-4.
4. Hu YF, Chen YJ, Lin YJ, Chen SA. Inflammation and the pathogenesis of atrial fibrillation. *Nat Rev Cardiol*. 2015;12(4):230-43.
5. Goette A, Kalman JM, Aguinaga L, Akar J, Cabrera JA, Chen SA, et al. EHRA/HRS/APHRS/SOLAECE expert consensus on Atrial cardiomyopathies: Definition, characterisation, and clinical implication. *J Arrhythm*. 2016;32(4):247-78.
6. Hindricks G, Potpara T, Dagres N, Arbelo E, Bax JJ, Blomström-Lundqvist C, et al. 2020 ESC Guidelines for the diagnosis and management of atrial fibrillation developed in collaboration with the European Association for Cardio-Thoracic Surgery (EACTS): The Task Force for the diagnosis and management of atrial fibrillation of the European Society of Cardiology (ESC) Developed with the special contribution of the European Heart Rhythm Association (EHRA) of the ESC. *European Heart Journal*. 2020;42(5):373-498.
7. Lemmens K, Doggen K, De Keulenaer GW. Role of neuregulin-1/ErbB signaling in cardiovascular physiology and disease: implications for therapy of heart failure. *Circulation*. 2007;116(8):954-60.
8. Mendes-Ferreira P, De Keulenaer GW, Leite-Moreira AF, Brás-Silva C. Therapeutic potential of neuregulin-1 in cardiovascular disease. *Drug Discov Today*. 2013;18(17-18):836-42.
9. Galindo CL, Ryzhov S, Sawyer DB. Neuregulin as a heart failure therapy and mediator of reverse remodeling. *Curr Heart Fail Rep*. 2014;11(1):40-9.
10. Vandekerckhove L, Vermeulen Z, Liu ZZ, Boimvaser S, Patzak A, Segers VF, et al. Neuregulin-1 attenuates development of nephropathy in a type 1 diabetes mouse model with high cardiovascular risk. *Am J Physiol Endocrinol Metab*. 2016;310(7):E495-504.
11. Vermeulen Z, Hervent AS, Dugaucquier L, Vandekerckhove L, Rombouts M, Beyens M, et al. Inhibitory actions of the NRG-1/ErbB4 pathway in macrophages during tissue fibrosis in the heart, skin, and lung. *Am J Physiol Heart Circ Physiol*. 2017;313(5):H934-h45.
12. John Li SL, Dixiang LUO, Yiran WU, Ming Zhou, Yang Wang, Xiaolei Zhuang, Liang Hua, Pengyi LUO inventor Human neuregulin-1 (nrg-1) recombinant fusion protein compositions and methods of use thereof. United States patent US2020/0010522 A1. 2020 9 January.
13. De Keulenaer GW, Feyen E, Dugaucquier L, Shakeri H, Shchendrygina A, Belenkov YN, et al. Mechanisms of the Multitasking Endothelial Protein NRG-1 as a Compensatory Factor During Chronic Heart Failure. *Circ Heart Fail*. 2019;12(10):e006288.

## **Scientific curriculum vitae**



## SCIENTIFIC CURRICULUM VITAE

NAME: Jens Van fraeyenhove  
DATE OF BIRTH: July 25, 1995  
EMAIL: [jens.vanfraeyenhove@outlook.be](mailto:jens.vanfraeyenhove@outlook.be)

### EDUCATION

---

<b>PhD in Pharmaceutical Sciences</b> University of Antwerp	2019 – 2024
<b>Master of Science in Drug Development: Pharmacist</b> University of Antwerp, <i>Distinction</i>	2017 - 2019
<b>Bachelor of Pharmaceutical Sciences</b> University of Antwerp, <i>Satisfaction</i>	2013 - 2017

### Additional educational courses

<b>Spanish Level 1</b> University of Antwerp	2022
<b>Communication Skills</b> University of Antwerp	2021
<b>Connecting communication</b> University of Antwerp	2021
<b>Laboratory Animal Sciences (certificate category B)</b> KU Leuven	2019
<b>Basic Principles of Statistic</b> University of Antwerp	2019

### SCIENTIFIC ACTIVITIES

---

#### Theses

**Master in Drug Development** – Laboratory of Physiopharmacology, University of Antwerp  
“Optimization of methods to assess autophagy via transmission electron microscopy”.

### **Patent Application**

WO/2023/178086 - METHODS OF TREATING FIBROSIS AND ARRHYTHMIA WITH A NEUREGULIN-1 FUSION PROTEIN. LI, John, **VAN FRAEYENHOVE, Jens G.R**, MURPHY, Samuel L, SEGERS, Vincent F.M, DE KEULENAER, Giles W, TUBEECKX, Michiel René Lisette. 21.09.2023

### **Peer reviewed publications**

**Jens van fraeyenhove**<sup>\*</sup>; Michiel R.L. Tubebeckx<sup>\*</sup>; Bo Govaerts; Yile Fue; Juan Zhang; Arthur Bezerra; Tim De Coster; Julie Cools; Eike M. Wülfers; Siel Van den Bogaert; Bernard Thienpont; Samuel L Murphy; Antoine A.F. de Vries; Erik Fransen; Nele Vandersickel; Daniël A. Pijnappels; Guido Y. De Meyer; Hein Heidbuchel; Llewelyn H. Roderick; Vincent F.M. Segers; Gilles W. De Keulenaer. ERBB4 activation as a new therapy for atrial remodeling and fibrillation. *Manuscript submitted for publication*. This manuscript combines data from JK07 in distinct mouse models and a pig model of AF.

J.R.A. Boen, A. B. Gevaert, A. Dendooven, D. Krüger, M. Tubebeckx, **J. Van fraeyenhove**, T. Bruyns, V.F.M. Segers, E. M. Van Craenenbroeck. Divergent cardiac and renal effects of miR-181c-5p inhibition. Paper in submission

**Jens Van fraeyenhove**<sup>#</sup>, Kasper Favere<sup>#</sup>, Griet Jacobs, Matthias Bosman, Sander Eens, Johan De Sutter, Hielko Miljoen, Pieter-Jan Guns, Gilles De Keulenaer, Vincent Segers, Hein Heidbuchel. Cardiac electrophysiology studies in mice via the transjugular route: a comprehensive practical guide, *AJP-Heart and Circulatory Physiology, Innovative Methodology*, 2022 August 26. DOI: 10.1152/ajpheart.00337.2022

Michiel R.L. Tubebeckx, Steven Laga, Christel Jacobs, Marina Stroe, Steven Van Cruchten, Bo Goovaerts, **Jens Van fraeyenhove**, Hielko Miljoen, Guido R.Y. De Meyer, Gilles W. De Keulenaer, Hein Heidbuchel, Vincent F.M. Segers. Sterile Pericarditis in Aachener Minipigs As a Model for Atrial Myopathy and Atrial Fibrillation, *J Vis Exp*. 2021 Sep 24;(175). DOI: 10.3791/63094.

Eline Feyen<sup>#</sup>, Melanie Ricke-Hoch<sup>#</sup>, **Jens Van fraeyenhove**, Zarha Vermeulen, Michaela Scherr, Lindsey Dugaucquier, Janika Viereck, Tine Bruyns, Thomas Thum, Vincent Segers, Denise Hilfiker-Kleiner, and Gilles De Keulenaer. ERBB4 and multiple microRNAs that target ERBB4 participate in pregnancy-related cardiomyopathy. *Circ. Heart Fail*. 2021 Jul 12; 14(7): e0066898. DOI: 10.1161/CIRCHEARTFAILURE.120.006898

### **Abstracts for oral presentations**

**Jens Van fraeyenhove**; Michiel Tubebeckx, Eline Feyen; Tine Bruyns; Guido De Meyer; Samuel Murphy, Salubris Biotherapeutics; Hein Heidbuchel; Vincent Segers; Gilles De Keulenaer. *ERBB4-Selective And Sustained Activation By NRG1 Attenuates Atrial Fibrosis And Fibrillation*. Research Day of Pharmaceutical Sciences, University of Antwerp, 2023, May

**Jens Van fraeyenhove**; Michiel Tubebeckx, Eline Feyen; Tine Bruyns; Guido De Meyer; Samuel Murphy, Salubris Biotherapeutics; Hein Heidbuchel; Vincent Segers; Gilles De Keulenaer. *ERBB4-*

*Selective And Sustained Activation By NRG1 Attenuates Atrial Fibrosis And Fibrillation*. Belgian working group of basic research in cardiology, Brussels, 2022, December

**Jens Van fraeyenhove**; Michiel Tubeekx, Eline Feyen; Tine Bruyns; Guido De Meyer; Samuel Murphy, Salubris Biotherapeutics; Hein Heidbuchel; Vincent Segers; Gilles De Keulenaer. *ERBB4-Selective And Sustained Activation By NRG1 Attenuates Atrial Fibrosis And Fibrillation*. Belgian society of physiology and pharmacology, Brussels, 2022, November

### **Abstracts for poster presentation**

**Jens Van fraeyenhove**; Michiel Tubeekx, Eline Feyen; Tine Bruyns; Guido De Meyer; Samuel Murphy, Salubris Biotherapeutics; Hein Heidbuchel; Vincent Segers; Gilles De Keulenaer. *ERBB4-Selective And Sustained Activation By NRG1 Attenuates Atrial Fibrosis And Fibrillation*. AHA, Basic Cardiovascular Sciences Scientific Sessions, Chicago Illinois, 2022, 25-28 July

Eline Feyen, Julie Cools, **Jens Van fraeyenhove**, Michiel Tubeekx, Hans De Winter; Dominique Audenaert; Tine Bruyns, Gilles De Keulenaer; Vincent Segers. *Identification Of Selective Small-molecule ERBB4 Agonists With Cardioprotective Effects*. AHA, Basic Cardiovascular Sciences Scientific Sessions, Chicago Illinois, 2022, 25-28 July

Jente RA Boen, Dustin Krüger, Amélie Dendooven, Tine Bruyns, **Jens Van fraeyenhove**, Eline Feyen, Andreas B Gevaert; Vincent FM Segers; Emeline M Van Craenenbroeck. *Mir-181c-5p As Detrimental Player In A Mouse Model Of Cardiorenal Syndrome With Thrombotic Microangiopathy*. AHA, Basic Cardiovascular Sciences Scientific Sessions, Chicago Illinois, 2022, 25-28 July

Eline Feyen<sup>#</sup>, Melanie Ricke-Hoch<sup>#</sup>, **Jens Van fraeyenhove**, Zarha Vermeulen, Michaela Scherr, Lindsey Dugaucquier, Janika Viereck, Tine Bruyns, Thomas Thum, Vincent Segers, Denise Hilfiker-Kleiner, and Gilles De Keulenaer. *ERBB4 and multiple microRNAs that target ERBB4 participate in pregnancy-related cardiomyopathy*. ESC, Heart Failure 2021 Online & On Demand, 29 June-1 July

Eline Feyen, Julie Cools, **Jens Van fraeyenhove**, Michiel Tubeekx, Tine Bruyns, Hans De Winter, Dominique Audenaert, Gilles W. De Keulenaer, Vincent F.M. Segers. *Identification of small-molecule ERBB4 agonists to treat heart failure*. AHA, Online & On Demand, 2021 Nov.

Eline Feyen, **Jens Van fraeyenhove**, Michiel Tubeekx, Tine Bruyns, Hans De Winter, Dominique Audenaert, Gilles W. De Keulenaer, Vincent F.M. Segers. *Identification of small-molecule ERBB4 agonists*. Departmental Research Day Pharmaceutical Sciences, University of Antwerp, 2021 May.

### **Awards**

Jury prize for the best presentation in the Departmental (Pharmaceutical, Biomedical and Veterinary sciences) Research Day 2023.

